

Award Number: DAMD17-02-1-0490

TITLE: Detection of Metastatic Potential in Breast Cancer by RhoC-GTPase and WISP3 Proteins

PRINCIPAL INVESTIGATOR: Celina G. Kleer, M.D.

CONTRACTING ORGANIZATION: University of Michigan
Ann Arbor, MI 48109

REPORT DATE: May 2006

TYPE OF REPORT: Annual

PREPARED FOR: U.S. Army Medical Research and Materiel Command
Fort Detrick, Maryland 21702-5012

DISTRIBUTION STATEMENT: Approved for Public Release;
Distribution Unlimited

The views, opinions and/or findings contained in this report are those of the author(s) and should not be construed as an official Department of the Army position, policy or decision unless so designated by other documentation.

REPORT DOCUMENTATION PAGE

Form Approved
OMB No. 0704-0188

Public reporting burden for this collection of information is estimated to average 1 hour per response, including the time for reviewing instructions, searching existing data sources, gathering and maintaining the data needed, and completing and reviewing this collection of information. Send comments regarding this burden estimate or any other aspect of this collection of information, including suggestions for reducing this burden to Department of Defense, Washington Headquarters Services, Directorate for Information Operations and Reports (0704-0188), 1215 Jefferson Davis Highway, Suite 1204, Arlington, VA 22202-4302. Respondents should be aware that notwithstanding any other provision of law, no person shall be subject to any penalty for failing to comply with a collection of information if it does not display a currently valid OMB control number. **PLEASE DO NOT RETURN YOUR FORM TO THE ABOVE ADDRESS.**

1. REPORT DATE (<i>DD-MM-YYYY</i>) 01-05-2006			2. REPORT TYPE Annual			3. DATES COVERED (<i>From - To</i>) 17 Apr 2005 - 16 Apr 2006			
4. TITLE AND SUBTITLE Detection of Metastatic Potential in Breast Cancer by RhoC-GTPase and WISP3 Proteins						5a. CONTRACT NUMBER			
						5b. GRANT NUMBER DAMD17-02-1-0490			
						5c. PROGRAM ELEMENT NUMBER			
6. AUTHOR(S) Celina G. Kleer, M.D. E-Mail: kleer@umich.edu						5d. PROJECT NUMBER			
						5e. TASK NUMBER			
						5f. WORK UNIT NUMBER			
7. PERFORMING ORGANIZATION NAME(S) AND ADDRESS(ES) University of Michigan Ann Arbor, MI 48109						8. PERFORMING ORGANIZATION REPORT NUMBER			
9. SPONSORING / MONITORING AGENCY NAME(S) AND ADDRESS(ES) U.S. Army Medical Research and Materiel Command Fort Detrick, Maryland 21702-5012						10. SPONSOR/MONITOR'S ACRONYM(S)			
						11. SPONSOR/MONITOR'S REPORT NUMBER(S)			
12. DISTRIBUTION / AVAILABILITY STATEMENT Approved for Public Release; Distribution Unlimited									
13. SUPPLEMENTARY NOTES									
14. ABSTRACT: Breast cancer is the most common type of life-threatening cancer, and the second most common cause of cancer related deaths of women in the United States. Even though the larger the primary tumor, the greater the likelihood of metastases, this is not always the case. There are many small breast cancers with a highly aggressive and metastatic behavior and discouraging outcome that remain under treated because there is no marker capable of identifying them. In this proposal we will study the utility of detecting RhoC GTPase and WISP3 proteins by immunohistochemistry as biological prognostic markers capable of identifying breast cancers with high propensity to metastasize, independently of tumor size. The impact of this study is that we will develop a clinically useful test to detect which invasive cancers will metastasize, and that will allow clinicians to institute early treatment before the development of metastases. This will impact on patient outcome. We will also study the predictive power of RhoC GTPase and WISP3 expression in the response of breast cancer to farnesyl transferase inhibitors, a new gene-targeted treatment modality for advanced cancers.									
15. SUBJECT TERMS WISP3, Inflammatory Breast Cancer, RhoC-GTPase, Prognostic Factor									
16. SECURITY CLASSIFICATION OF:						17. LIMITATION OF ABSTRACT	18. NUMBER OF PAGES	19a. NAME OF RESPONSIBLE PERSON USAMRMC	
a. REPORT U	b. ABSTRACT U	c. THIS PAGE U	19b. TELEPHONE NUMBER (<i>include area code</i>)						
						UU	77		

Table of Contents

Cover.....	
SF 298.....	2
Table of Contents.....	3
Introduction.....	4
Body.....	4
Key Research Accomplishments.....	11
Reportable Outcomes.....	11
Conclusions.....	14
References.....	14
Appendices.....	16

Celina G. Kleer, M.D.

**Annual Report for Award Number: DAMD17-02-1-0490 Career Development Award
July 2006 (Reporting period 17 April 2005- 16 April 2006)**

Introduction

This is the fourth annual report for a project that aims at understanding the clinical utility of RhoC-GTPase and WISP3 proteins in breast cancer patients. These two genes were identified as key genetic determinants of inflammatory breast cancer (IBC). We believe that RhoC GTPase and WISP3 act in concert to determine a highly metastatic breast cancer phenotype, and that they may help identify which invasive breast carcinomas are aggressive from the outset and treat them more appropriately before the development of metastases. Specifically, we aim to determine whether detection of RhoC GTPase and WISP3 proteins in breast cancer tissue samples can identify aggressive tumors. A second goal of our award is to determine the effect of farnesyl transferase inhibitors (FTIs) in RhoC overexpressing xenografts. This award resulted in significant contributions to advance the knowledge of IBC and generate novel hypotheses.

Body

The major advances on this project have been to develop tissue microarrays (TMAs) using invasive breast carcinomas from 236 patients treated at our institution with over 10 years of follow up information, linked to a clinical database, and to better understand the functional significance of the WISP3 gene in Inflammatory Breast Cancer (IBC), to determine the prognostic utility of RhoC protein expression. Furthermore, we have developed and optimized key reagents to test the expression levels of WISP3 in breast cancer tissue samples. We have published several peer-reviewed publications based on these results. Below are brief descriptions of key accomplishments according to the approved statement of work (SOW):

Task 1. To determine whether the concordant alterations of RhoC-GTPase over-expression and WISP3 loss are prognostic indicators and predictors of survival in breast cancer patients. Months 1-24.

- a. Identify and retrieve the breast cancer tissue blocks and slides (489 cases total). Months 1-6.
- b. Histopathologic study of the cases and selection of adequate tumor areas to construct the tissue microarrays. Categorize the breast cancers according to stage. Months 6-9.
- c. Construction of the tissue microarrays, one containing 400 breast cancers of all anatomic stages and the other containing 89 cases of locally advanced breast cancer. Months 9-15.
- d. Immunohistochemical analysis for RhoC-GTPase and WISP3 proteins, and other markers (ER, PR, HER2/neu, Ki-67, microvessel density and apoptosis). Months 16-19.
- e. Interpretation and grading of the immunohistochemical studies and statistical analyses. Months 20-24.

Task 1

- a. Identify and retrieve the breast cancer tissue blocks and slides.
By performing a computerized search of the breast cancer database at the Department of Pathology, University of Michigan, using the words “breast” and “cancer” and “breast” and “carcinoma” from

years 1987-1991. We identified 385 consecutive invasive breast cancer patients. Of the 385 cases, 236 cases were available for study. The reasons for this were: 1. unavailability of tissue slides or blocks, and 2. primary resection performed at a referring institution.

In addition, 60 cases of locally advanced breast cancer, of which 30 are inflammatory breast cancers, and 30 are stage matched, non-inflammatory breast cancer were identified from the pathology files.

b. Histopathologic study of the cases and selection of adequate tumor areas to construct the tissue microarrays. Categorize the breast cancers according to stage.

The P.I. reviewed all the hematoxylin and eosin stained sections from all these cases and annotated the pathologic characteristics of each tumor using the following template:

Summary for Invasive Carcinomas.

Greatest dimension of invasive carcinoma (microscopic):				cm
Involvement of surgical margin:	Positive (at ink)			Close (<= 0.2 cm)
	Negative (>0.2 cm)			
If margin positive:		Single focus		Multiple foci
If margin close:		Single focus		Multiple foci
Histopathological grade (Elton and Ellis):	1	2	3	
Positive lymph nodes /total lymph nodes:		/		
Highest axillary node positive:	Yes		No	N/A
Extranodal extension:	Yes		No	N/A
Extensive DCIS:	Yes		No	N/A
DCIS > 25% of tumor:	Yes		No	
Extratumoral DCIS:	Yes		No	
Microcalcifications:	None	within inv/DCIS		within benign ducts
Hormonal receptors:	ER: POS	NEG	PR: POS	NEG
Her2neu overexpression:	POS (2+	3+)	NEG	
T	N	M		

Development of a breast cancer database

We developed a relational database in Microsoft Access to store the pathological and clinical information. The idea behind this decision was to be able to link the results of the TMA scoring with the patient pathological and clinical information. Clinical and treatment information was extracted by chart review, performed with IRB approval. The P.I. was involved in all steps of the database design and development, and learned how to perform database queries.

c. Construction of the tissue microarrays

We have now constructed six high density tissue microarrays (TMAs) to characterize WISP3 and RhoC expression in a wide range of normal breast and breast disease, and to study associations between expression of these proteins and patient outcome.

In order to construct the tissue arrays, the P.I. reviewed all cases histologically and selected the areas to array. At least three different areas of the tumors were selected and at least three tissue cores (0.6 mm in diameter) were sampled from each donor block. TMAs are assembled using the manual tissue puncher/array (Beecher Instruments). This instrument consists of thin-walled stainless steel needles

with an inner diameter of approximately 600 μm and stylet used to transfer and empty the needle contents. The assembly is held in an X-Y position guide that is manually adjusted by digital micrometers. Small biopsies are retrieved from selected regions of donor tissue and are precisely arrayed in a new paraffin block. Cores are inserted into a 45 x 20 x 12 mm recipient block and spaced at a distance of 0.8 mm apart.

d. Immunohistochemical analysis for RhoC-GTPase and WISP3 proteins, and other markers (ER, PR, HER2/neu, Ki-67, microvessel density and apoptosis).

We have optimized the conditions for immunohistochemistry for the anti-RhoC antibody and applied it to the constructed TMAs successfully. We used 1:400 dilution of antibody incubated overnight, and microwave antigen retrieval.

We have also developed a specific polyclonal antibody against WISP3 using the following peptides
 Ac-CSGAKGGKKDSDQSN-CONH2
 Ac-CPEGRPGEVSDAPQRKQ-CONH2.

After evaluating 4 different anti-WISP3 antibodies, we selected the one that worked better for Western blot and gave a specific band (shown below).

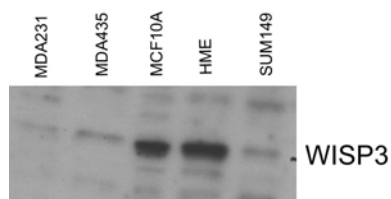
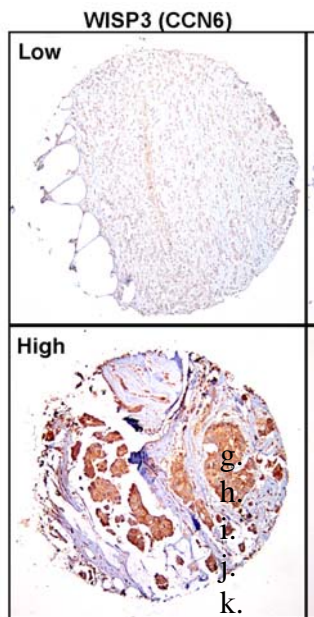


Figure 1. Western immunoblot of cell lysates of five different breast cancer cell lines (MDA231, MDA435, SUM149), and HPV immortalized human mammary epithelial cells (HME), and spontaneously immortalized human mammary epithelial cells (MCF10A). WISP3 protein is expressed in normal cells, and its expression decreases in breast cancer cells.



We have optimized the conditions for the anti-WISP3 antibody for immunohistochemistry and we have applied it to the TMAs successfully. We use the antibody at 1:100 dilution, with 60 minutes incubation and microwave antigen retrieval. Figure 2 show examples of the tissues microarray samples stained with anti-WISP3 antibody. We have also stained the TMAs for estrogen receptor, progesterone receptor and HER-2/neu.

Figure 2. TMA samples containing invasive breast carcinomas e. immunostained for WISP3 (CCN6). f.

m. Interpretation and grading of the immunohistochemical studies and statistical analyses.

I evaluated the immunohistochemistry for RhoC, ER, PR and HER-2/neu in all the TMAs, and with the assistance of Kent Griffith, the biostatistician, have analyzed the results which are shown below. I am in the process of evaluating the immunohistochemistry for WISP3, to explore its clinical relevance.

Below is the summary of our RhoC analyses, which are the subject of a manuscript that is in press in Breast Cancer Research and Treatment (see appendix).

We found that RhoC expression increases with breast cancer progression. All samples of normal breast epithelium had negative to weak staining, whereas staining intensity increased in hyperplasia, DCIS, invasive carcinoma, and metastases (Kruskal-Wallis $p < 0.001$).

RhoC expression was associated with negative ER expression and worse histologic grade. The table below show the associations between RhoC expression and clinical and pathologic features.

In patients with invasive carcinoma, high RhoC expression was an independent predictor of death from breast cancer, and of local-recurrence free survival. The hazard ratio for local recurrence for patients with high RhoC levels as compared with those with low RhoC levels was 2.37, with a 95% confidence interval of 1.18-4.77 ($p = 0.015$), Figure 3.

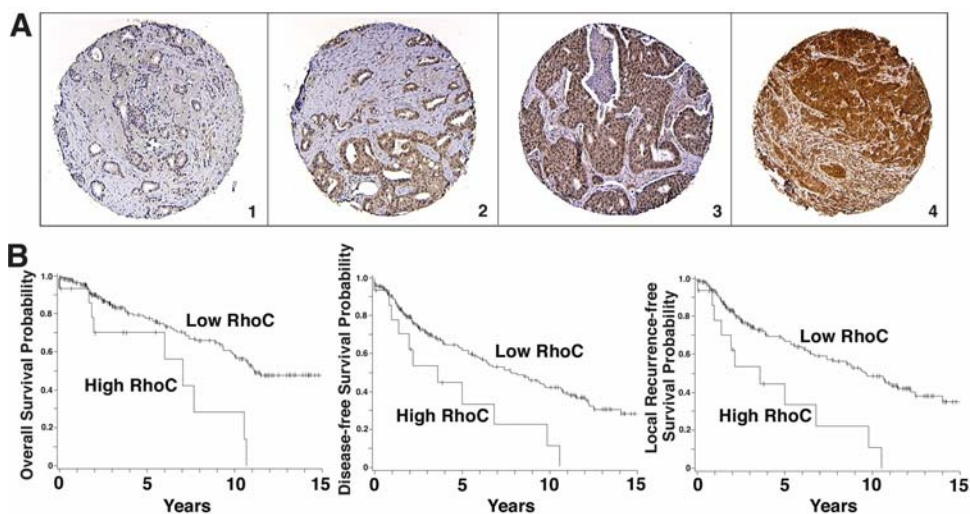


Figure 3. RhoC protein expression is associated with survival in patients with breast cancer. **A.** Tissue microarray elements containing representative invasive carcinomas with negative (1), weak (2), moderate (3), and strong (4) RhoC staining intensities. Original magnification 40x. **B.** High RhoC expression in invasive carcinomas is associated with worse overall, disease-free, and local recurrence-free survival.

Our preliminary studies show that RhoC expression increases with breast cancer progression and RhoC protein levels in tumor tissue, as measured by immunohistochemistry, are strongly associated with survival and local recurrence in patients with breast cancer. This not only extends our initial observations (Kleer et al, Am J Pathol 2002 Feb;160(2):579-84), but also suggests that RhoC may have a role in the local invasiveness and progression of breast carcinoma. Our studies suggest that RhoC protein levels may be first altered in carcinoma *in situ*, the precursor of invasive carcinoma. Clinically, our retrospective study suggests that RhoC levels may prove useful after further validation, to identify patients with breast cancer that are likely to recur locally.

These data were recently published in Breast Cancer Research and Treatment (Kleer, C.G., Griffith, K., Sabel, M.S., Van Golen, K.L., Gallagher, G., Wu, Z.F., and Merajver, S.D. RhoC-

GTPase is a Novel Tissue Biomarker Associated with Biologically Aggressive Carcinomas of the Breast. *Breast Cancer Research and Treatment* 93(2):101-10, 2005.

Task 2. To define the role of Rho-GTPase and WISP3 in the clinical setting as independent predictors of survival in patients with locally advanced breast cancer. Months 24-36.

- a. Histopathologic study of 89 cases of locally advanced breast cancer that were previously retrieved from the pathology files (first 6 months). Selection of adequate areas to construct the tissue microarray. Months 24-27.
- b. Development of the tissue microarray, and immunohistochemical analysis of RhoC-GTPase, WISP3 and other biomarkers (ER, PR, HER2/neu, Ki-67, microvessel density and apoptosis). Months 28-33.
- c. Interpretation and grading of the immunohistochemical stains and statistical analyses. Months 33- 36.

Task 2.

- a. Histopathologic study of 89 cases of locally advanced breast cancer that were previously retrieved from the pathology files (first 6 months). Selection of adequate areas to construct the tissue microarray. Months 24-27.
So far, we have identified 60 cases of locally advanced breast cancer, of which 30 are inflammatory breast cancers, and 30 are stage matched, non-inflammatory breast cancer were identified from the pathology files. We evaluated them histologically and chose the areas to construct a TMA
- d. Development of the tissue microarray, and immunohistochemical analysis of RhoC-GTPase, WISP3 and other biomarkers (ER, PR, HER2/neu, Ki-67, microvessel density and apoptosis). Months 28-33.
We have constructed a TMA with these tissues, and stained them for RhoC, ER, PR and HER-2/neu. We have stained the TMA for WISP3 as well and are in the process of evaluating the immunohistochemical results.
- e. Interpretation and grading of the immunohistochemical stains and statistical analyses. Months 33- 36.
RhoC, ER, PR and Her-2/neu stains have been evaluated and analyzed in conjunction with Task 1. We are in the process of interpreting the immunohistochemical results for WISP3 staining in this group as well. We have evaluated RhoC expression on these tissues, as well as on 5 punch biopsies from the skin from patients with a typical clinical presentation of IBC. RhoC was elevated in nearly all of these samples.

In addition, through a collaboration with my mentor on this award, Dr. Sofia D. Merajver and Dr. Amr Soliman from the School of Public Health at the University of Michigan, we have evaluated the histological features and RhoC expression of 20 samples of IBC from Egypt, where there is an increased incidence of IBC.

Preliminarily, we have found that the Egyptian IBC cases contain a significantly higher number of tumor emboli in the dermal lymphatics than the cases from US. Furthermore, RhoC was markedly

increased in the Egyptian IBC cases when compared to US cases. We will also determine WISP3 expression on these samples. We are in the process of analyzing these data and preparing a manuscript.

Task 3. To study in detail the *in vivo* effect of WISP3 loss in modulating the response of invasive breast carcinomas with RhoC-GTPase over-expression to farnesyl transferase inhibitors. Months 24-36.

- a. Prepare a panel of cell lines (SUM149 wt, SUM149/WISP3, HME/RhoC, SUM185 wt and MCF10AT wt). Since all these cell lines have been prepared in our preliminary work, getting them ready for injection will take approximately 3 weeks. Month 25-26.
- b. *In vivo* mice experiment (injection of cell lines, tumor development and treatment with farnesyl transferase inhibitor). Months 27-30.
- c. Histological and immunohistochemical study of the excised tumors stained with anti-RhoC and anti-WISP3 antibodies. Months 30-32.
- d. Analysis of the immunostains. Months 32-34.
- e. Statistical analyses. Months 34-36.

We have not yet initiated the experiments in Task 3. They will commence this year.

In addition to the Tasks, we have performed seminal work in understanding WISP3 function, and how WISP3 and RhoC may cooperate to determine a highly aggressive inflammatory breast cancer phenotype, as well as identified new breast cancer biomarkers.

1. We found that **WISP3 modulates RhoC expression** in HME cells and in the IBC cell line SUM149. This provides further evidence in support that these two genes act in concert to give rise to the highly aggressive IBC phenotype. We propose a model of this interaction as a starting point for further investigations. We have included this published manuscript in the appendix (Kleer, C.G., Zhang, Y., Pan, Q., Gallagher, G., Wu, M., Wu, Z.F., and Merajver, S.D. WISP3 and RhoC Guanosine Triphosphatase Cooperate in the Development of inflammatory Breast Cancer. *Breast Cancer Research* 6(2):R110-5, 2004.)

2. We have also made an important contribution by elucidating that **WISP3 is a secreted protein and that it modulates IGF signaling**. This work is seminal, as no other tumor suppressor gene has ever been defined specifically for Inflammatory Breast Cancer (Kleer, C.G., Zhang, Y., Pan, Q., and Merajver, S.D. WISP3 is a Secreted Tumor Suppressor Protein That Modulates IGF Signaling in inflammatory Breast Cancer. *Neoplasia* 6(2):179-85, 2004.). In this work, we found that WISP3 is secreted into the conditioned media and into the lumens of normal breast ducts. Once secreted, WISP3 was able to decrease, directly or through induction of other molecule(s), the IGF-1-induced activation of the IGF-IR, and two of its main downstream signaling molecules, IRS1 and ERK-1/2 in SUM149 IBC cells. Furthermore, WISP3 containing conditioned media decreased the growth rate of SUM149 cells. This work sheds light into the mechanism of WISP3 function by demonstrating that it is secreted, and that once in the extracellular media it induces a series of molecular events that lead to modulation of IGF-IR signaling pathways and cellular growth in IBC cells.

3. We have also established a stable siRNA inhibition of WISP3 expression in human mammary epithelial cells (HME) and characterized its functions. We found that **WISP3 inhibition resulted in epithelial to**

mesenchymal transition of HME cells and induced motility and invasion. Moreover, these cells were more sensitive to the growth and proliferative effects of IGF-1 in the medium. These experiments suggest that WISP3 may be a key a regulator of IGF-1 effects in HME cells. We have published this paper in Breast Cancer Research (Zhang, Y., Pan, Q., Zhong, H., Merajver, S.D., and Kleer, C.G. Inhibition of CCN6 (WISP3) Expression Promotes Neoplastic Transformation and Enhances the Effects of IGF-1 on Breast Epithelial Cells. *Breast Cancer Research* 7(6):R1080-9, 2005.) We were invited to write a review article on this topic in a special edition on EMT of Cells Tissues Organs journal.

4. We have also identified that EZH2 is a marker of aggressive breast cancer and that it promotes the neoplastic transformation of human mammary epithelial cells (Kleer CG, Cao Q, Varambally S, Shen R, Ota I, Tomlins SA, Ghosh D, Sewalt, RG, Otte AP, Hayes DF, Sabel MS, Livant D, Weiss SJ, Rubin MA and Chinnaiyan AM. EZH2 is a Marker of Aggressive Breast Cancer and Promotes Neoplastic Transformation of Breast Epithelial Cells. *Proceedings of the National Academy of Sciences*, 100(20): 11606-11, 2003). For this study, we used the tissue microarrays constructed and stained them using a polyclonal antibody for EZH2, a transcriptional repressor. We found that EZH2 expression was an independent factor that predicts death from breast cancer. We have included a copy reprint of this paper in the appendix section.

5. Furthermore, we found that **EZH2 overexpression impairs DNA repair in breast epithelial cells** and that this could be a mechanisms for neoplastic transformation (Zeidler, M., Varambally, S., Cao, Q., Chinnaiyan, A.M., Ferguson, D.O., Merajver, S.D., and Kleer, C.G. The Polycomb Group Protein EZH2 Impairs DNA Repair in Human Mammary Epithelial Cells. *Neoplasia* 7(11):1011-9, 2005. Featured article and Cover.)

6. Very recently we identified that **EZH2** is elevated in benign appearing breast lobules in women with increased risk of breast cancer, and **may serve as a novel molecular maker to detect neoplastic progression in the breast** before the appearance of histological atypia. This work was published in Cancer Research (Ding, L., Erdmann, C., Chinnaiyan, A.M., Merajver, S.D., and Kleer, C.G. Identification of EZH2 as a Molecular Marker for a Precancerous State in Morphologically Normal Breast Tissues. *Cancer Research* 66(8):4095-9, 2006. Selected as a Cancer Research Highlight.) In addition, we were invited to write a review article on this topic in Cancer Research that was just accepted.

7. We recently found that RhoC-GTPase protein is elevated in squamous cell carcinomas of the head and neck that develop lymph node metastasis. This work was just accepted for publication in Clinical Cancer Research (Kleer, C.G., Teknos, T.N., Islam, M., Marcus, B., Lee, J.S.J., Pan, Q., and Merajver, S.D. RhoC-GTPase Expression as a Potential Marker of Lymph Node Metastasis in Squamous Cell Carcinomas of the Head and Neck. *Clinical Cancer Research*, in Press.)

In summary, this Award helped us complete several manuscripts dealing with key aspects of WISP3 and RhoC expression in breast cancer. We have developed key reagents and resources that will enable us to move forward in testing their clinical usefulness. We have also completed a major effort in understanding the function of WISP3 gene as it contributes to the inflammatory breast cancer phenotype.

Key Research Accomplishments

- Constructed four high density tissue microarrays
- Developed a relational database with the patient information
- Generated and tested a polyclonal antibody against WISP3
- Validation of RhoC as a novel tissue biomarker that predicts local recurrence and survival in patients with breast cancer.
- Discovered that increased RhoC expression in head and neck cancer is associated with positive lymph nodes.
- Investigated the mechanisms of cooperation between RhoC and WISP3 in determining the inflammatory breast cancer phenotype.
- Elucidated that WISP3 is a secreted protein and that it modulates IGF-I signaling cascade in inflammatory breast cancer
- Discovered that WISP3 inhibition in HME cells leads to epithelial to mesenchymal transition, and triggers invasion and motility.
- Discovered that EZH2 is a marker of aggressive breast cancer and that it promotes neoplastic transformation of mammary epithelial cells.
- Discovered that increased EZH2 in normal breast epithelium is a molecular marker of increased breast cancer risk.
- Discovered that EZH2 overexpression in the mammary epithelium impairs the ability to repair DNA and causes aneuploidy.

Training component of the Award

During this year, the P.I. has had a significant learning opportunity was to direct and work closely with the statistician to perform survival analyses for RhoC and for EZH2. In the laboratory, the P.I. learned how to design hairpin siRNA and develop stable cell lines lacking WISP3 expression. She learned how to interpret the experiments conducted that revealed that loss of WISP3 results in epithelial to mesenchymal transition and down regulation of E-cadherin. The P.I. attended and presented data at the annual meeting of the United States and Canadian Academy of Pathology in Atlanta, the Era of Hope meeting in Philadelphia, PA, the International Symposium in Breast Cancer in Tianjin, China (invited speaker). She presented the findings of her research at the Beijing institute of biotechnology (invited), gave hematology/oncology grand rounds at Henry Ford Hospital, Detroit, and at the Centennial Celebration at the Mayo Clinic, Rochester, MN (invited speaker). She also presented her data at the Pathology Research Symposium and at the Breast Care Educational Forum at the University of Michigan. She also participated in the monthly meetings of the University of Michigan Breast Oncology Program to discuss research projects.

Reportable Outcomes

We are in a position to report that RhoC over expression is an early marker of aggressive breast cancers, even when they are small, and that it is a promising marker of prognosis and local recurrence in patients with breast cancer.

We can state that WISP3 is able to ameliorate the highly malignant features of inflammatory breast cancer. Specifically, WISP3 has growth and angiogenic inhibitory functions, at least in part through modulating IGF-receptor signaling pathways.

We can state that EZH2 is a marker of aggressive breast cancer, and that it can predict prognosis.

Research Manuscripts published for the period 2005- 2006:

Pu, R.T., Schott, A.F., Sturtz, D.E., Griffith, K.A., and Kleer, C.G. Pathologic Features of Breast Cancer Associated with Complete Response to Neoadjuvant Chemotherapy: Importance of Tumor Necrosis. *American Journal of Surgical Pathology* 29(3):354-58, 2005.

Witniewicz, A., Shen, R., Lnu, S., Mehra, R., Chinnaiyan, A.M., Sabel, M.S., Rubin, M.A., and Kleer, C.G. Alpha Methyl acyl-CoA Racemase (AMACR) Protein Expression is Associated with the Degree of Differentiation in Breast Cancer Using Quantitative Image Analysis. *Cancer Epidemiology, Biomarkers, and Prevention* 14(6):1418-23, 2005. Cover Article.

Khan, A., Sabel, M.S., Nees, A., Diehl, K.M., Cimmino, V.M., Kleer, C.G., Schott, A.F., Hayes, D.F., Chang, A.E., and Newman, L.A. Comprehensive Axillary Evaluation in Neoadjuvant Chemotherapy Patients with Ultrasonography and Sentinel Lymph Node Biopsy. *Annals of Surgical Oncology* 12(9):1-8, 2005.

Schott, A.F., Roubidoux, M.A., Helvie, M.A., Hayes, D.F., Kleer, C.G., Newman, L.A., Pierce, L.J., Griffith, K.A., Murray, S., Hunt, K.A., Paramagul, C., and Baker, L.H. Clinical and Radiologic Assessments to Predict Breast Cancer Pathologic Complete Response to Neoadjuvant Chemotherapy. *Breast Cancer* 92(3):231-8, 2005.

Kleer, C.G., Griffith, K., Sabel, M.S., Van Golen, K.L., Gallagher, G., Wu, Z.F., and Merajver, S.D. RhoC-GTPase is a Novel Tissue Biomarker Associated with Biologically Aggressive Carcinomas of the Breast. *Breast Cancer Research and Treatment* 93(2):101-10, 2005.

Pan, Q., Bao, L.W., Kleer, C.G., Sabel, M., and Merajver, S.D. Protein Kinase C ϵ is Elevated in High Grade Breast Cancer and a Novel Target for RNA interference Anticancer Therapy. *Cancer Research* 65(18):8366-71, 2005.

Zeidler, M., Varambally, S., Cao, Q., Chinnaiyan, A.M., Ferguson, D.O., Merajver, S.D., and Kleer, C.G. The Polycomb Group Protein EZH2 Impairs DNA Repair in Human Mammary Epithelial Cells. *Neoplasia* 7(11):1011-9, 2005. Featured article and Cover.

Zhang, Y., Pan, Q., Zhong, H., Merajver, S.D., and Kleer, C.G. Inhibition of CCN6 (WISP3) Expression Promotes Neoplastic Transformation and Enhances the Effects of IGF-1 on Breast Epithelial Cells. *Breast Cancer Research* 7(6):R1080-9, 2005.

Mehra, R., Varambally, S., Shen, R., Ding, L., Sabel, M.S., Ghosh, D., Chinnaiyan, A.M.*, and Kleer, C.G.*. Identification of GATA3 as a Breast Cancer Prognostic Marker by Global Gene Expression Meta-Analysis. *Cancer Research* 65(24):11259-64, 2005.

Krop, I., März, A., Carlsson, H., Li, X., Bloushtain-Qimron, N., Hu, M., Gelman, R., Sabel, M.S., Schnitt, S., Ramaswamy, S., Kleer, C.G., Enerbäck, C., and Polyak, K. A Putative Role for Psoriasin in Breast Tumor Progression. *Cancer Research* 65(24):11326-34, 2005.

Ben-David, M.A., Kleer, C.G., Paramagul, C., Griffith, K.A., and Pierce, L.J. Is LCIS a Component of Breast Cancer a Risk Factor for Local Failure Following Breast-Conserving Therapy? Results of a Matched Pair Analysis. *Cancer* 106(1):28-34, 2006.

O'Malley, F.P., Mohsin, S.K., Badve, S., Bose, S., Collins, L.C., Ennis, M., Kleer, C.G., Pinder, S.E., and Schnitt, S.J. interobserver Reproducibility in the Diagnosis of Flat Epithelial Atypia of the Breast. *Modern Pathology* 19(2):172-9, 2006.

Newman, E.L., Kahn, A., Diehl, K.M., Cimmino, V.M., Kleer, C.G., Chang, A.E., Newman, L.A., and Sabel, M.S. Does the Method of Biopsy Affect the Incidence of Sentinel Lymph Node Metastases? *The Breast Journal* 12(1):53-57, 2006.

Ding, L., Erdmann, C., Chinnaiyan, A.M., Merajver, S.D., and Kleer, C.G. Identification of EZH2 as a Molecular Marker for a Precancerous State in Morphologically Normal Breast Tissues. *Cancer Research* 66(8):4095-9, 2006. Selected as a Cancer Research Highlight.

Hird, R.B., Chang, A., Cimmino, V., Diehl, K., Sabel, M., Kleer, C.G., Helvie, M., Schott, A., Young, J., Hayes, D., Newman, L. Impact of estrogen receptor expression and other clinico-pathologic features on tamoxifen use in ductal carcinoma in situ. *Cancer* 15;106:2113-8, 2006.

Kuefer, R., Day, K.C., Kleer, C.G., Sabel, M.S., Hofer, M.D., Varmbally, S., Zorn, C.S., Chinnaiyan, A.M., Rubin, M.A., Day, M.L. The ADAM15 disintegrin is associated with aggressive prostate and breast cancer disease. *Neoplasia* 8(4): 319-329, 2006.

Kleer, C.G., Teknos, T.N., Islam, M., Marcus, B., Lee, J.S.J., Pan, Q., and Merajver, S.D. RhoC-GTPase Expression as a Potential Marker of Lymph Node Metastasis in Squamous Cell Carcinomas of the Head and Neck. *Clinical Cancer Research*, in Press.

Maturen, K.E., Paramagul, C.P., Roubidoux, M.A., Kleer, C.G., Weadock W.J., Abate, S.A. Interactive Computer Teaching Module for Radiologic-Pathologic Correlations in Breast Imaging. *MedEdPORTAL*, in Press.

Abstracts (2005-2006):

Zhang, Y., Monroe, S., Merajver, S.D., and Kleer, C.G. Inhibition of WISP3 (CCN6) Promotes the Neoplastic Transformation and Enhances the Effects of IGF-1 on Breast Epithelial Cells. Era of Hope Meeting, Department of Defense Breast Cancer Research Program, Poster presentation, Philadelphia, PA, June 8-11, 2005.

Zhang, Y., Pan, Q., Zhong H., Merajver, S.D., and Kleer, C.G. Inhibition of WISP3 (CCN6) Promotes a Mesenchymal Phenotype and Enhances the Effects of IGF-1 on Breast Epithelial Cells. Epithelial Mesenchymal Transition (EMT) Conference. Vancouver, BC, Canada, October 1-3, 2005. Poster Presentation.

Wei, I.*, Pu, R.*, Zhang, Y., Merajver, S.D., and Kleer, C.G. Analysis of WISP3 Promoter Methylation in Inflammatory Breast Cancer. Student Biomedical Research Forum, University of Michigan Medical School, Ann Arbor, MI, Nov. 2005.

Hayes, M.J. and Kleer, C.G. Expression of the Undifferentiated Cell Marker P63 in Primary invasive Carcinomas of the Breast and Their Nodal Metastases. *Laboratory Investigation* 86(1): 29A. Presented at USCAP meeting, Atlanta, GA, Feb. 2006.

Kunju, L.P. and Kleer, C.G. Significance of Flat Epithelial Atypia (FEA) on Mammotome Core Needle Biopsy: Should It Be Excised? *Laboratory Investigation* 86(1): 32A. Presented at USCAP meeting, Atlanta, GA, Feb. 2006.

Zeidler, M., Varambally, S., Cao, Q., Chinnaiyan, A.M., Ferguson, D.O., Merajver, S.D., and Kleer, C.G. The Polycomb Group Protein EZH2 Impairs DNA Repair in Human Mammary Epithelial Cells. AACR meeting, April 1-5, 2006, Washington DC. Poster Presentation.

Conclusion

We are encouraged by our progress. We want to move forward and test the clinical utility of WISP3 and in combination with RhoC and other markers, in detecting aggressive breast cancer phenotypes before they develop metastases. We also wish to explore the relationship between WISP3 and the IGF-receptor pathway in more depth. These are the directions we are moving on for this year.

References:

Manley, S., Mucci, N.R., De Marzo, A.M. & Rubin, M.A. Relational database structure to manage high-density tissue microarray data and images for pathology studies focusing on clinical outcome: the prostate specialized program of research excellence model. *Am J Pathol* 159, 837-43, 2001

Kleer CG, Zhang Y, Pan Q, van Golen KL, Wu Z-F, and Merajver SD. WISP3 Is a Novel Tumor Suppressor Gene of Inflammatory Breast Cancer. *Oncogene* 21, 3172-3180, 2002.

Kleer CG, van Golen KL, Zhang Y, Wu Z-F, Rubin MA, Merajver SD. Characterization of RhoC Expression in Benign and Malignant Breast Disease: A Potential New Marker for Small Breast Carcinomas with Metastatic Potential. *Am J of Pathol.* 160(2), 579-584, 2002.

Valdez R, Thorson J, Finn WG, Schnitzer B, and Kleer CG. Lymphocytic Mastitis/ Diabetic Mastopathy: A Molecular, Immunophenotypic, and Clinicopathologic Evaluation of Eleven Cases. *Modern Pathology* 16: 223-228, 2003.

Kleer CG, Cao Q, Varambally S, Shen R, Ota I, Tomlins SA, Ghosh D, Sewalt RG, Otte AP, Hayes DF, Sabel MS, Livant D, Weiss SJ, Rubin MA and Chinnaiyan AM. EZH2 is a Marker of Aggressive Breast Cancer and Promotes Neoplastic Transformation of Breast Epithelial Cells. *Proceedings of the National Academy of Sciences*, 100(20):11606-11, 2003.

Kowalski PJ, Rubin MA and Kleer CG. E-Cadherin Expression in Primary Carcinomas of the Breast and its Distant Metastases. *Breast Cancer Research*, 5:R217-R222, 2003.

Kleer CG, Zhang Y, Pan Q, Wolf J, Wu M, Wu Z-F, Merajver SD. WISP3 and RhoC-GTPase Cooperate in the Development of Inflammatory Breast Cancer. *Breast Cancer Research* 6(1): R110-5, 2004.

Ray ME, Yang ZQ, Albertson D, Kleer CG, Washburn JG, Macoska JA, Ethier SP. Genomic and Expression Analysis of the 8p11-12 Amplicon in Human Breast Cancer Cell Lines. *Cancer Research* 64(1):40-47, 2004.

Van Den Eynden GG, Van Der Auwera I, Van Laere S, Colpaert CG, Van Dam P, Merajver S, Kleer CG, Harris AL, Van Marck EA, Dirix LY, Vermeulen PB. Validation of a tissue microarray to study differential protein expression in inflammatory and non-inflammatory breast cancer. *Breast Cancer Res Treat.* 85(1):13-22, 2004.

Kleer CG, Zhang Y, Pan Q, Merajver SD. WISP3 is a Secreted Tumor Suppressor Protein that Modulates IGF Signaling in Inflammatory Breast Cancer. *Neoplasia*, 2004 Mar-Apr;6(2):179-85.

Identification of GATA3 as a Breast Cancer Prognostic Marker by Global Gene Expression Meta-analysis

Rohit Mehra,¹ Sooryanarayana Varambally,^{1,6} Lei Ding,¹ Ronglai Shen,^{1,3} Michael S. Sabel,^{4,6} Debashis Ghosh,³ Arul M. Chinnaiyan,^{1,2,5,6} and Celina G. Kleer^{1,6}

Departments of ¹Pathology, ²Urology, ³Biostatistics, and ⁴Surgery, ⁵Michigan Urology Center, and ⁶Comprehensive Cancer Center, University of Michigan Medical School, Ann Arbor, Michigan

Abstract

GATA binding protein 3 (GATA3) is a transcriptional activator highly expressed by the luminal epithelial cells in the breast. Here we did a meta-analysis of the available breast cancer cDNA data sets on a cohort of 305 patients and found that GATA3 was one of the top genes with low expression in invasive carcinomas with poor clinical outcome. To validate its prognostic utility, we did a tissue microarray analysis on a cohort of 139 consecutive invasive carcinomas ($n = 417$ tissue samples) immunostained with a monoclonal antibody against GATA3. Low GATA3 expression was associated with higher histologic grade ($P < 0.001$), positive nodes ($P = 0.002$), larger tumor size ($P = 0.03$), negative estrogen receptor and progesterone receptor ($P < 0.001$ for both), and HER2-neu overexpression ($P = 0.03$). Patients whose tumors expressed low GATA3 had significantly shorter overall and disease-free survival when compared with those whose tumors had high GATA3 levels. The hazard ratio of metastasis or recurrence according to the GATA3 status was 0.31 (95% confidence interval, 0.13-0.74; $P = 0.009$). Cox multivariate analysis showed that GATA3 had independent prognostic significance above and beyond conventional variables. Our data suggest that immunohistochemical analysis of GATA3 may be the basis for a new clinically applicable test to predict tumor recurrence early in the progression of breast cancer. (Cancer Res 2005; 65(24): 1-6)

Introduction

Adjuvant systemic therapy has contributed to the reduction in mortality observed in the Western world over the last 15 years. A major problem in clinical oncology is distinguishing those patients most likely to recur, and therefore most likely to benefit from adjuvant systemic therapy, from those with a sufficiently favorable prognosis that they might forego adjuvant systemic therapy to avoid toxicity. This highlights the need for novel molecular predictors of tumor behavior at the time of diagnosis that can be implemented in the clinic.

By applying a two-stage Bayesian mixture modeling strategy, our group was able to develop a meta-signature predictive of disease-free survival in breast cancer patients (1). GATA binding protein 3 (GATA3), a transcriptional activator, emerged as one of the top genes with low expression in the meta-signature.

Note: R. Mehra and S. Varambally contributed equally to this work. A.M. Chinnaiyan and C.G. Kleer share senior authorship.

Supplementary data for this article are available at Cancer Research Online (<http://cancerres.aacrjournals.org/>).

Requests for reprints: Celina G. Kleer, Department of Pathology, University of Michigan, 3510C MSRB1, 1150 West Medical Center Drive, Ann Arbor, MI, 48109. Phone: 734-615-3448; Fax: 734-615-3441; E-mail: kleer@umich.edu.

©2005 American Association for Cancer Research.

doi:10.1158/0008-5472.CAN-05-2495

In breast cancer, high GATA3 mRNA levels are seen in the luminal A type, associated with estrogen receptor (ER) expression and with a favorable prognosis (2–5). Recently, Usary et al. (4) identified and characterized in detail somatic mutations of GATA3 in five ER- α -positive invasive breast cancers and in the ER-positive breast cancer cell line MCF-7 and suggested that loss of GATA3 may contribute to tumorigenesis in ER-positive breast cancers. Here, we show that GATA3 protein levels are strongly associated with the degree of differentiation of breast cancer and that low GATA3 protein expression is an independent predictor of tumor recurrence after treatment in breast cancer patients.

Materials and Methods

Meta-analysis of breast cancer microarray data sets. Four published and publicly available breast cancer data sets were obtained from the authors' websites (6–9). These included 53,377 array elements from 305 breast tumor samples. A common set of 2,555 genes was identified by Unigene Cluster IDs. For each data matrix of the 2,555 genes, data preprocessing was carried out including standard normalization procedures (A and B) for different array platforms and missing data imputation by a k -nearest neighbors algorithm (10, 11). Each gene expression profile was then median centered and divided by the SD for each gene. A mixture model based data transformation was applied to each of the data matrix of the 2,555 genes. The original expression data from each study were mapped to a common probability scale and a "meta-cohort" was generated based on such data integration. The association of each gene expression profile with patient survival outcome was assessed using a univariate Cox regression model within a leave-one-out cross-validation scheme. Genes were then ranked by the significance of the effect size estimates. An essential list of 23 genes was determined based on appearance in top-ranked gene lists for each of the 305 samples from the leave-one-out analysis; GATA3 was on this list.

Western blot analysis. Nine frozen invasive carcinomas of the breast were dissected following review of an H&E section to confirm the presence and location of the carcinoma in the block by a pathologist (C.G.K.). Protein extracts for Western blot analysis were prepared from these cancer tissues. In addition, four breast cell lines (MCF-7, MDA-MB-231, HME, and MCF-10A) were used. Standard immunoblot analysis was done using an anti-GATA3 mouse monoclonal antibody (sc-269, Santa Cruz Biotechnology, Inc., Santa Cruz, CA) at 1:250 dilution (4). α -Actin and β -tubulin were used to control for equal loading.

Immunofluorescence and confocal microscopy. The breast tissue sections were deparaffinized in xylene. Slides were deparaffinized and blocked in PBS-Tween 20 with 5% normal donkey serum for 1 hour. A mixture of rabbit anti-E-cadherin antibody (LabVision Corp., Fremont, CA) and mouse anti-GATA3 antibody (Santa Cruz Biotechnology) was added to the slides at 1:50 and 1:100 dilutions, respectively, and incubated overnight at 4°C following standard immunofluorescence methods (12).

Breast sample collection and tissue microarray development. Breast tissue samples were obtained from the Surgical Pathology files at the University of Michigan with Institutional Review Board (IRB) approval. One hundred thirty-nine consecutive invasive breast carcinomas treated at our institution between 1987 and 1991 were reviewed (C.G.K.) and used to

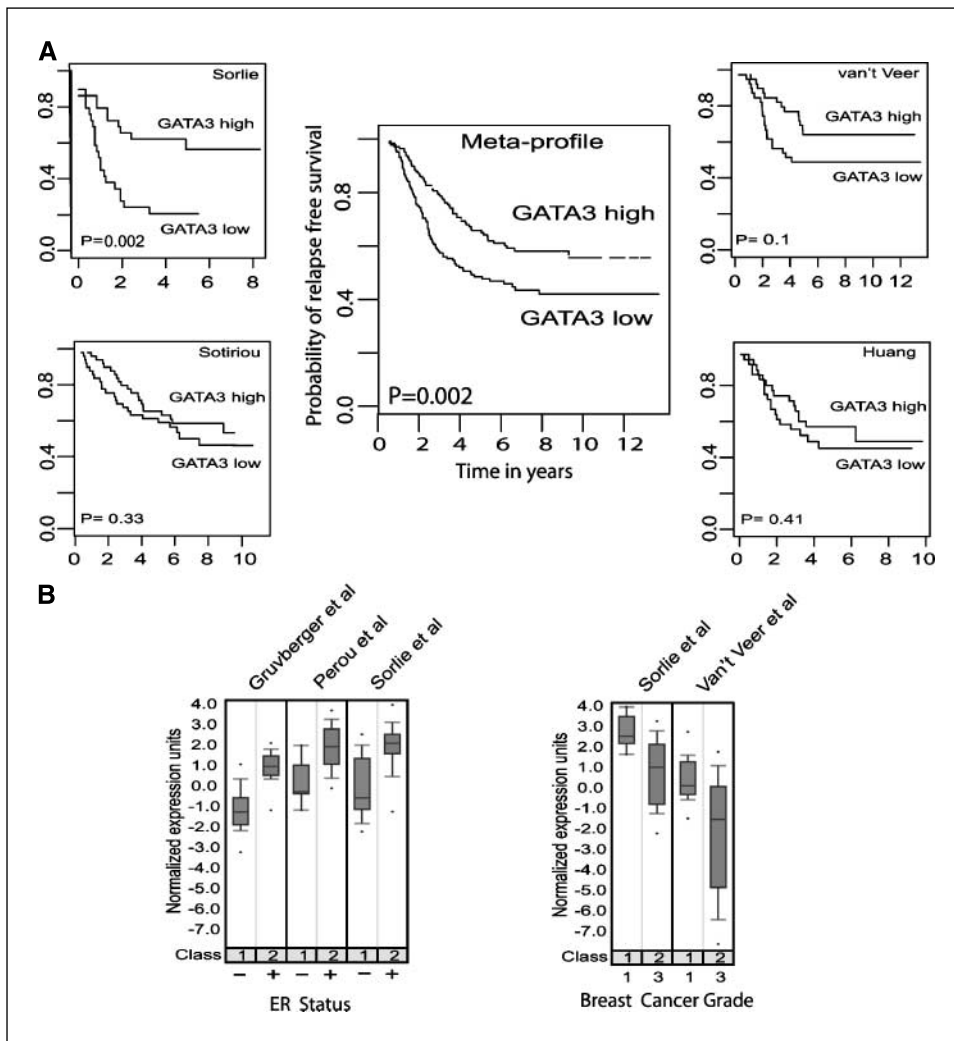


Figure 1. GATA3 transcript is associated with prognosis in breast cancer. *A*, GATA3 expression was determined in four published cDNA data sets analyzed independently and combined in a meta-analysis using a mixture modeling approach which unifies disparate gene expression data on a common probability scale and allows for a powerful tool to study the prognostic significance of single genes and gene signatures across different data sets. *B*, expression of GATA3 according to ER status and the histologic grade of the invasive carcinomas. GATA3 expression is higher in ER-positive, well-differentiated (low-grade) invasive carcinomas.

construct a TMA ($n = 417$ tissue microarray samples) using a manual arrayer as previously described (12). Each tumor was sampled in triplicate to account for tumor heterogeneity. Outcome information was obtained by chart review (M.S.S.) with IRB approval. The median duration of follow-up time was 8.9 years (range, 44 days-17 years). Clinicopathologic variables were assessed using well-established criteria (13).

Immunohistochemistry, digital image capture, and analysis. Immunohistochemistry was done on the TMA using standard biotin-avidin complex technique and a mouse monoclonal antibody against GATA3 (Santa Cruz Biotechnology) at 1:100 dilution as previously described (4). GATA3 was evaluated at least thrice for each microarray element and at least nine times for each tumor using a previously validated Web-based tool (TMA Profiler, University of Michigan, Ann Arbor, MI; ref. 14). GATA3 expression was scored blindly and independently by two surgical pathologists (C.G.K. and R.M.), as negative (score = 1), weak (2), moderate (3), and strong (4) on the basis of the intensity of staining and the percentage of tumor cells stained using a system that has been validated previously (15). The TMAs were previously stained for ER, progesterone receptor (PR), and HER-2/neu using well-described procedures (12, 15). The median value of all measurements from a patient was used for subsequent analysis. High GATA3 expression was defined as a median intensity of >2.5 and low GATA3 was defined as a median intensity of ≤ 2.5 .

Statistical analyses. Statistical analyses were done using SAS (SAS Institute, Inc., Cary, NC) software by the biostatisticians in the study (R.S. and D.G.). GATA3 expression was dichotomized into low staining (median score ≤ 2.5) and high staining (median score > 2.5). No data-based

optimization of the cut point was done. Associations between the GATA3 score and clinicopathologic features were assessed using χ^2 tests for 2×2 table analysis and Wilcoxon rank-sum test for $2 \times n$ comparisons. Overall survival time and time to breast cancer specific mortality were calculated from the date of surgery until the subjects' date of death or date of death due to breast cancer, respectively. Patients experiencing competing events were censored at the date of the competing event. Treatment failures included local recurrence and regional or distant metastases. Patients not experiencing failure events were censored on their last date of follow-up or date of death. Univariate associations were assessed using the log-rank test and the product-limit method of Kaplan and Meier. The Cox proportional hazards model was used to determine the best multivariate model of disease applied to variables including GATA3 protein expression, histologic grade, tumor size, lymph node status, angiolymphatic invasion, and ER, PR, and HER2 status. Associations with disease-free survival and overall survival were assessed for each variable. To determine the influence of multiple variables simultaneously, a multivariate Cox proportional hazards model was applied to the clinical variables and GATA3. Wald's test was used to determine statistical significance in the Cox models.

Results

Meta-analysis of breast cancer data sets identifies GATA3 as a prognostic marker. GATA3 mRNA expression was analyzed independently and by doing a meta-analysis of the four available data sets comprising a cohort of 305 patients containing data on

F1 the expression levels of 2,555 genes. GATA3 expression was associated with survival in one of the four cDNA data sets when analyzed independently; however, a strong association was found when all the data sets were combined in the meta-analysis (log-rank $P = 0.002$; Fig. 1A). The levels of GATA3 transcript were significantly lower in invasive carcinomas that metastasized when compared with invasive carcinomas that did not metastasize. These results are in line with published data showing that the mixture modeling approach we used unifies disparate gene expression data on a common probability scale and allows for robust, interstudy-validated prognostic signatures (1). Furthermore, GATA3 levels were significantly lower in the subset of ER-negative invasive carcinomas ($P < 0.0001$) and in invasive carcinomas of high histologic grade ($P < 0.0001$; Fig. 1B).

F2 **GATA3 protein expression in breast cancer tissues.** To validate the mRNA results, we did Western blots using a monoclonal antibody specific for GATA3 on nine randomly selected invasive carcinomas of the breast. We found that four had moderate to high GATA3 levels whereas five had low GATA3. As seen in Fig. 2A, in invasive carcinomas, low GATA3 protein was associated with negative ER status and high GATA3 was associated with positive ER. Furthermore, we determined the GATA3 expression of four breast cell lines with known ER status: ER-positive MCF-7 and ER-negative MDA-MB-231, HME, and MCF-10A cells. In the cell lines, GATA3 levels were also associated with the ER expression. Immunofluorescence showed crisp GATA3 expression exclusively in the nucleus of cancer cells, consistent with its function (Fig. 2B). Using TMAs, we next evaluated the expression of

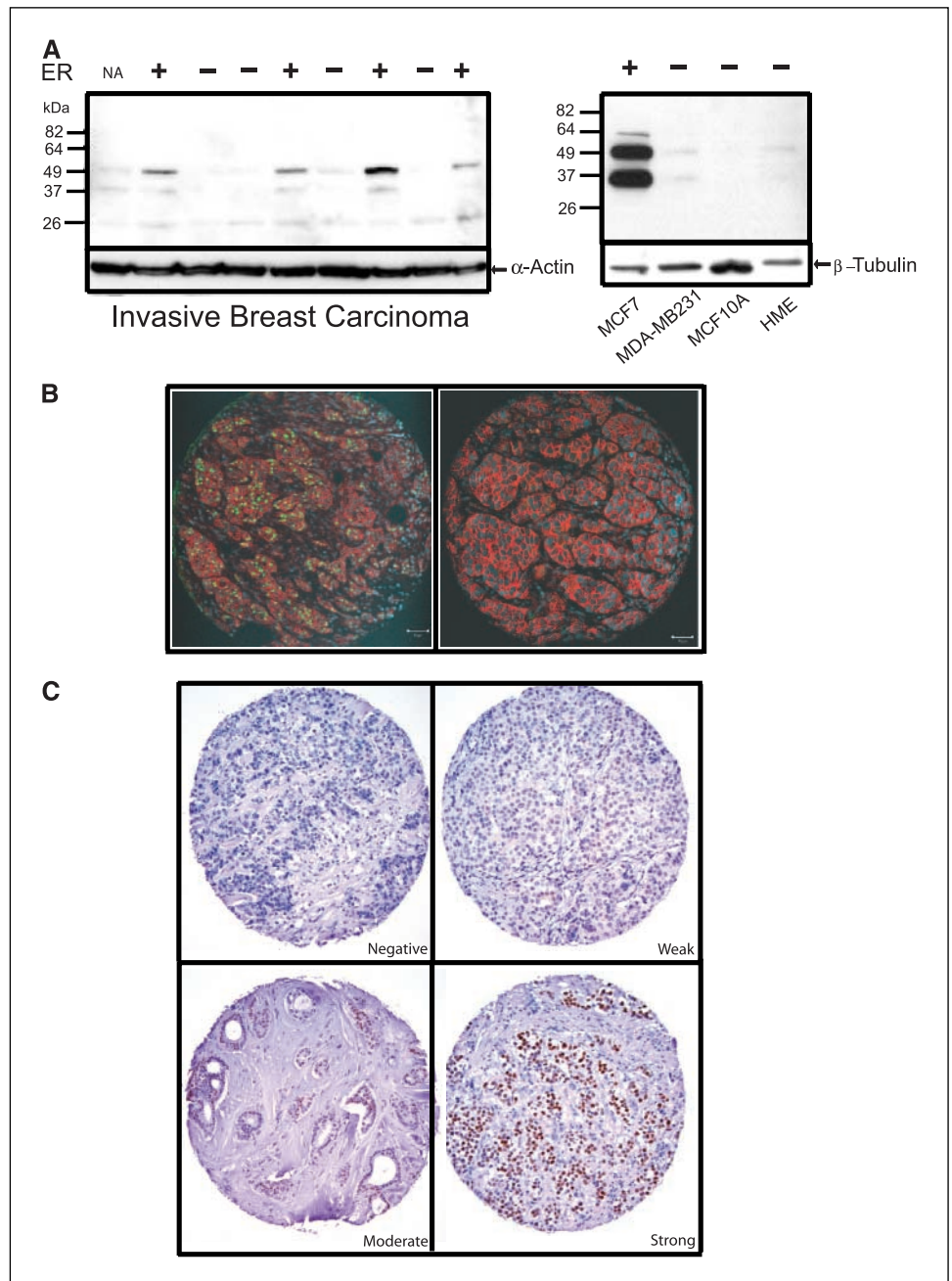


Figure 2. GATA3 protein expression in breast cancer. **A**, using a monoclonal antibody for GATA3 (sc-269), immunoblot analysis showed expression of GATA3 in nine invasive carcinomas of the breast. Two previously described bands (4, 19) at ~49 and 23 kDa are seen. GATA3 expression was associated with the ER status of the invasive carcinomas. **Right**, GATA3 expression in breast cell lines. Note the association with ER status. α -Actin and β -tubulin were used to control for equal loading. **B**, immunofluorescence and confocal microscopy revealed that GATA3 protein is localized to the nucleus of cancer cells. *Green*, GATA3; *red*, E-cadherin; *blue*, 4',6-diamidino-2-phenylindole. **Left**, invasive carcinoma positive for GATA3; **right**, invasive carcinoma negative for GATA3. **C**, GATA3 protein expression was evaluated using a high-density tissue microarray. GATA3 protein expression was readily identified in cancer cell nuclei and ranged from negative to strong in different cases of invasive breast cancer ($\times 100$).

GATA3 protein in a wide range of breast tissues (139 patients, $n = 417$ samples) to characterize its expression *in situ* by immunohistochemistry. GATA3 protein expression was observed in the nucleus (Fig. 2C) as previously reported (4).

Using our breast cancer TMA and a specific anti-GATA3 antibody, we were in the position to evaluate clinical and pathology associations of GATA3 protein levels in breast cancer. In patient cohort ($n = 139$), 129 had complete follow-up information. Clinical and pathologic characteristics are shown in Supplementary Table S1. The median age of the patients was 58.5 years (range, 29-93 years). The 3-, 5-, and 10-year disease-specific survival rates were 74%, 68%, and 64%, respectively. Low GATA3 expression was associated with larger tumor size (Wilcoxon test, $P = 0.03$) and the presence of axillary lymph node metastasis (Kruskal-Wallis test, $P = 0.002$). Low GATA3 levels were also associated with higher histologic grade (Kruskal-Wallis test, $P < 0.001$), negative ER and PR (Wilcoxon test, $P < 0.001$ for both), and HER-2/neu overexpression (Wilcoxon test, $P = 0.03$; Supplementary Table S2). The TMA analyses confirmed the breast cancer cDNA expression data showing a significant reduction of GATA3 expression levels in patients with worse outcome.

As expected, at the univariate level, lymph node status, tumor size, and histologic tumor grade were associated with disease-specific and overall survival (Table 1). PR was inversely associated with outcome. We found a strong association between GATA3 and survival. Low GATA3 protein levels were associated with a shorter disease-free interval and a high probability of death (Fig. 3A and B). The 10-year disease-free survival for patients with invasive cancers expressing low GATA3 levels was 55% and, by contrast, for high levels of GATA3, 84% (log-rank $P = 0.005$). The hazard ratio of metastasis or recurrence according to the GATA3 status was 0.31 [95% confidence interval (95% CI), 0.13-0.74; $P = 0.009$]. Furthermore, low GATA3 expression was associated with disease-specific

survival in patients with lymph node-negative disease (log-rank $P = 0.02$; Fig. 3C).

Despite the strong association between GATA3 and ER expression in breast carcinomas, we noted that there is a group of ER-positive tumors expressing low GATA3. We hypothesized that GATA3 levels may have prognostic value in patients with ER-positive tumors. Of the 83 ER-positive invasive carcinomas in our consecutive patient cohort, 38 (45.8%) had high and 45 (54.2%) had low GATA3 expression. Patients with high GATA3 had uniformly good prognosis. However, low GATA3 characterized a subset of ER-positive invasive carcinomas with a higher rate of recurrence and/or metastasis (log-rank $P = 0.04$; Fig. 3D). The prognostic value of GATA3 was independent of hormonal treatment as it was significantly associated with outcome in ER-positive patients treated with tamoxifen and those that did not receive tamoxifen (Supplementary Fig. S1).

The best multivariable model predictive of disease-specific survival showed that low GATA3 was a strong independent predictor of outcome providing survival information above other prognostic features, with a hazard ratio of 0.12 (95% CI, 0.01-1.01; $P = 0.05$; Table 1). The risk of recurrence for GATA3 low cases was eight times higher than that of the risk for GATA3 high cases.

Discussion

We validated the expression of GATA3 independently in the four previously published available cDNA databases and characterized its expression in a cohort of consecutive invasive carcinomas, with the aim of defining its role as a novel breast cancer prognostic biomarker. At the univariate level, GATA3 protein, tumor size, the presence of axillary lymph node metastases, histologic tumor grade, and PR status were associated with survival. Multivariable Cox regression analysis showed that low GATA3 expression was an independent predictor of outcome. These findings support the potential clinical utility of incorporating GATA3 into clinical nomograms to help determine the risk of cancer progression.

The promising prognostic utility of GATA3 in breast cancer patients has been suggested by analyses of published breast tumor microarray data (4, 16, 17). We provide a validation of those results derived from individual data sets. By doing a meta-analysis, we unified disparate gene expression data on a common probability scale, thus providing a robust interstudy validation of GATA3 expression as a prognostic marker. Our results further strengthen the value of the mixture model based data transformation in the identification and cross-validation of biomarkers across cDNA data sets which are based on different experimental platforms.

We found that GATA3 expression was strongly associated with ER expression and with the histologic grade of the carcinomas, a measure of differentiation. In DNA microarray analyses, GATA3 was associated with the expression of ER and of a subset of genes important for breast luminal cell differentiation including LIV-1, RERG, and TFF3 (2-4). Our data support these observations and suggest a role for GATA3 in maintaining a differentiated state in breast cells. We found a strong association between GATA3 and ER expression at the mRNA and protein levels. Recently, Usary et al. (4) reported a strong association between GATA3 and ER in normal breast luminal epithelial cells and discovered mutations of GATA3 near the highly conserved second zinc-finger domain required for DNA binding in breast cancers and in the MCF-7 breast cancer cell line, which suggested that GATA3 is expressed in normal

Table 1.

Factor	Hazard ratio (95% CI)	<i>P</i>
<i>(A)</i> Univariate analysis of disease-free survival		
GATA3	0.31 (0.13-0.74)	0.009
Histologic grade	2.28 (1.28-4.05)	0.005
ER	0.55 (0.30-1.02)	0.06
PR	0.45 (0.24-0.84)	0.01
HER-2/neu	1.12 (0.50-2.53)	0.78
ALI	3.67 (1.98-6.82)	<0.0001
Lymph node (0, 1-3, 4+)	2.29 (1.52-3.46)	<0.0001
Size (>2 vs ≤2 cm)	2.84 (1.37-5.85)	0.005
<i>(B)</i> Multivariate Cox model of disease-free survival		
GATA3	0.12 (0.01-1.01)	0.05
Histologic grade	1.56 (0.59-4.15)	0.37
ER	1.10 (0.33-3.65)	0.88
PR	0.62 (0.18-2.08)	0.44
HER-2/neu	1.36 (0.42-4.38)	0.61
ALI	2.28 (0.94-5.54)	0.07
Lymph node (0, 1-3, 4+)	1.39 (0.44-4.37)	0.57
Size (>2 vs ≤2 cm)	1.99 (0.76-5.21)	0.16

Abbreviations: PR, progesterone receptor; ALI, angiolymphatic invasion.

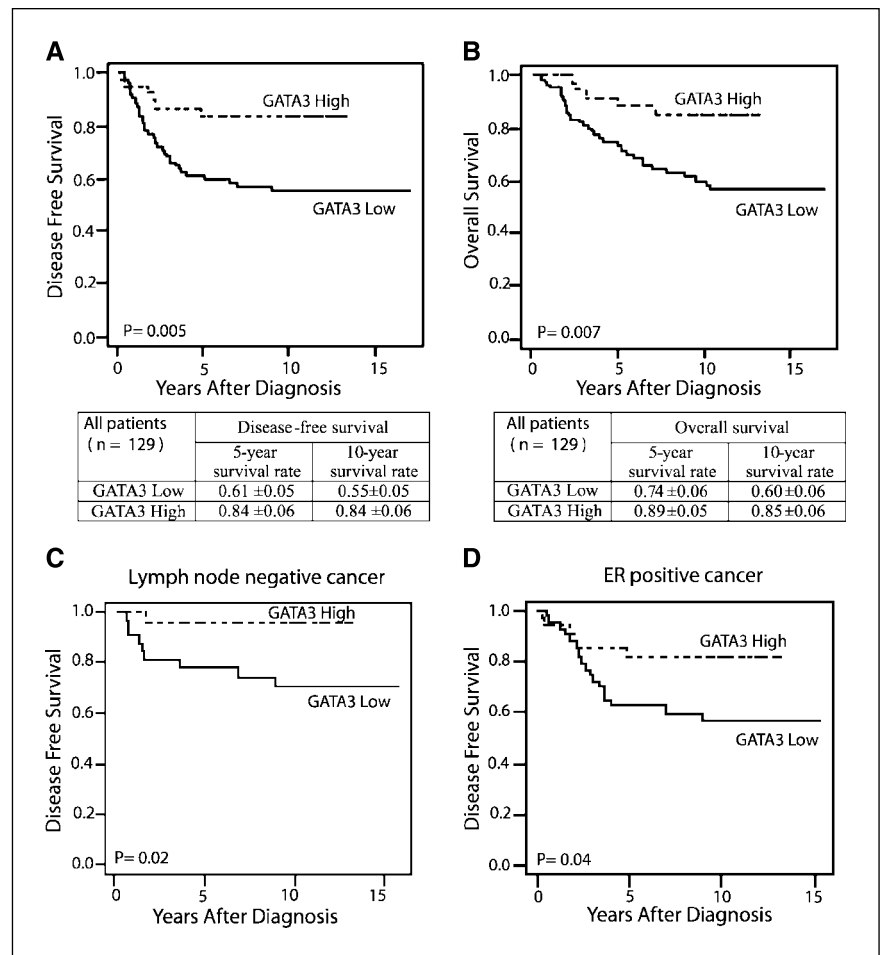


Figure 3. Low GATA3 levels are associated with aggressive breast cancer. Kaplan-Meier analysis of disease-specific (A) and overall (B) survivals according to GATA3 protein expression evaluated by immunohistochemical analysis. Patients with tumors expressing low GATA3 had worse disease-free survival and overall survival. C and D, Kaplan-Meier curves of disease-free survival according to GATA3 levels in lymph node-negative and ER-positive breast cancers.

mammary epithelium and that decreased expression due to mutation or deletion may contribute to breast cancer development.

Despite genomic coexpression of ER and GATA3 transcription factors in breast cancer, estrogens do not regulate GATA3 (3). Although the gene for ER is not induced by GATA3, it has been suggested that GATA3 variants may contribute to tumorigenesis in ER-positive tumors (4). In our study, we identified a group of ER-positive invasive carcinomas that have low GATA3 protein levels. Furthermore, GATA3 was able to uncover a group of ER-positive invasive carcinomas with worse clinical outcome who developed tumor recurrence and/or metastases independently of hormonal treatment. GATA3 was able to predict outcome in patients with ER-positive tumors regardless of whether or not they received hormone treatment, which may have clinical implications. Future studies will test the model developed in this study to confirm these initial observations.

Furthermore, GATA3 protein levels were able to discern which node-negative patients develop tumor recurrence or metastases from those who do not. These results suggest that detection of GATA3 protein may be useful in supplying additional power to delineate prognosis in node-negative breast cancer patients. In the future, this may pave the way to tailor the aggressiveness of therapies to molecular profiles that include GATA3.

By interrogating 29 cancer microarray data sets for evidence of differential expression of GATA3 transcript in benign and malignant tissues using OncoPrint 2.0 (18), GATA3 was elevated

in several carcinomas including lung ($P = 0.002$), prostate ($P = 0.003$), pancreas ($P = 0.046$), liver ($P < 0.0001$), endometrium ($P = 0.004$), adenoid cystic carcinoma of salivary gland ($P < 0.0001$), and diffuse large B-cell lymphomas ($P = 0.007$). These microarray studies suggest a role of GATA3 in several human tumor types.

In summary, we show that GATA3 is a promising novel prognostic biomarker in breast cancer. Our retrospective studies suggest that GATA3 levels may be used to identify patients with ER-positive and lymph node-negative breast cancer with a more aggressive phenotype, thereby enhancing our prognostic knowledge. Although our results are promising, they need to be validated in relationship to outcome in the context of controlled clinical trials. If confirmed, application of GATA3 immunohistochemical analysis will be technically straightforward and clinically useful.

Acknowledgments

Received 7/20/2005; revised 9/20/2005; accepted 10/3/2005.

Grant support: National Cancer Institute grants K08CA090876 and R01CA10746 (C.G. Kleer), Department of Defense grants PC040517 (R. Mehra), DAMD17-01-1-490 (C.G. Kleer), and DAMD17-01-1-491 (C.G. Kleer), and a John and Suzanne Munn Award from the University of Michigan (C.G. Kleer).

The costs of publication of this article were defrayed in part by the payment of page charges. This article must therefore be hereby marked *advertisement* in accordance with 18 U.S.C. Section 1734 solely to indicate this fact.

We thank Dr. Daniel Hayes (University of Michigan, Ann Arbor, MI) for review of this manuscript and helpful suggestions, Srilakshmi Bhagavathula for assistance in preparation of data, Nancy McAnsh and Michele LeBlanc for immunohistochemical support, and Scott A. Tomlins for critical review of figures.

References

1. Shen R, Ghosh D, Chinnaiyan AM. Prognostic meta-signature of breast cancer developed by two-stage mixture modeling of microarray data. *BMC Genomics* 2004;5:94.
2. van de Rijn M, Perou CM, Tibshirani R, et al. Expression of cytokeratins 17 and 5 identifies a group of breast carcinomas with poor clinical outcome. *Am J Pathol* 2002;161:1991–6.
3. Hoch RV, Thompson DA, Baker RJ, Weigel RJ. GATA-3 is expressed in association with estrogen receptor in breast cancer. *Int J Cancer* 1999;84:122–8.
4. Usary J, Llaca V, Karaca G, et al. Mutation of GATA3 in human breast tumors. *Oncogene* 2004;23:7669–78.
5. Sorlie T, Tibshirani R, Parker J, et al. Repeated observation of breast tumor subtypes in independent gene expression data sets. *Proc Natl Acad Sci U S A* 2003;100:8418–23.
6. van de Vijver MJ, HeYD, van't Veer LJ, et al. A gene-expression signature as a predictor of survival in breast cancer. *N Engl J Med* 2002;347:1999–2009.
7. Sotiriou C, Neo SY, McShane LM, et al. Breast cancer classification and prognosis based on gene expression profiles from a population-based study. *Proc Natl Acad Sci U S A* 2003;100:10393–8.
8. Huang E, Cheng SH, Dressman H, et al. Gene expression predictors of breast cancer outcomes. *Lancet* 2003;361:1590–6.
9. Lonning PE, Sorlie T, Perou CM, Brown PO, Botstein D, Borresen-Dale AL. Microarrays in primary breast cancer—lessons from chemotherapy studies. *Endocr Relat Cancer* 2001;8:259–63.
10. Irizarry RA, Hobbs B, Collin F, et al. Exploration, normalization, and summaries of high density oligonucleotide array probe level data. *Biostatistics* 2003;4:249–64.
11. Yang YH, Dudoit S, Luu P, et al. Normalization for cDNA microarray data: a robust composite method addressing single and multiple slide systematic variation. *Nucleic Acids Res* 2002;30:e15.
12. Witkiewicz AK, Varambally S, Shen R, et al. α -methylacyl-CoA racemase protein expression is associated with the degree of differentiation in breast cancer using quantitative image analysis. *Cancer Epidemiol Biomarkers Prev* 2005;14:1418–23.
13. Elston CW, Ellis IO. Pathology and breast screening. *Histopathology* 1990;16:109–18.
14. Manley S, Mucci NR, De Marzo AM, Rubin MA. Relational database structure to manage high-density tissue microarray data and images for pathology studies focusing on clinical outcome: the prostate specialized program of research excellence model. *Am J Pathol* 2001;159:837–43.
15. Kleer CG, Cao Q, Varambally S, et al. EZH2 is a marker of aggressive breast cancer and promotes neoplastic transformation of breast epithelial cells. *Proc Natl Acad Sci U S A* 2003;100:11606–11.
16. Perou CM, Sorlie T, Eisen MB, et al. Molecular portraits of human breast tumours. *Nature* 2000;406:747–52.
17. van't Veer LJ, Dai H, van de Vijver MJ, et al. Gene expression profiling predicts clinical outcome of breast cancer. *Nature* 2002;415:530–6.
18. Rhodes DR, Yu J, Shanker K, et al. ONCOMINE: a cancer microarray database and integrated data-mining platform. *Neoplasia* 2004;6:1–6.
19. Nesbit MA, Bowl MR, Harding B, et al. Characterization of GATA3 mutations in the hypoparathyroidism, deafness, and renal dysplasia (HDR) syndrome. *J Biol Chem* 2004;279:22624–2263.

WISP3 (CCN6) Is a Secreted Tumor-Suppressor Protein that Modulates IGF Signaling in Inflammatory Breast Cancer¹

Celina G. Kleer*, Yanhong Zhang*, Quintin Pan[†] and Sofia D. Merajver[†]

Departments of *Pathology and [†]Internal Medicine, Division of Hematology and Oncology, University of Michigan Medical Center, Ann Arbor, MI, USA

Abstract

Inflammatory breast cancer (IBC) is the most lethal form of locally advanced breast cancer. We have found that WISP3 is lost in 80% of human IBC tumors and that it has growth- and angiogenesis-inhibitory functions in breast cancer *in vitro* and *in vivo*. WISP3 is a cysteine-rich, putatively secreted protein that belongs to the CCN family. It contains a signal peptide at the N-terminus and four highly conserved motifs. Here, for the first time, we investigate the function of WISP3 protein in relationship to its structural features. We found that WISP3 is secreted into the conditioned media and into the lumens of normal breast ducts. Once secreted, WISP3 was able to decrease, directly or through induction of other molecule(s), the IGF-1–induced activation of the IGF-IR, and two of its main downstream signaling molecules, IRS1 and ERK-1/2, in SUM149 IBC cells. Furthermore, WISP3 containing conditioned media decreased the growth rate of SUM149 cells. This work sheds light into the mechanism of WISP3 function by demonstrating that it is secreted and that, once in the extracellular media, it induces a series of molecular events that leads to modulation of IGF-IR signaling pathways and cellular growth in IBC cells.

Neoplasia (2004) 6, 179–185

Keywords: IGF-binding proteins, MAPK signaling, cell proliferation, cell cycle control, ERK-1/2 phosphorylation.

Introduction

Inflammatory breast cancer (IBC) is the most lethal form of locally advanced breast cancer [1,2]. It is also a very distinct clinical and pathological type of carcinoma. Clinically, patients present with what has been classically termed “peau d’orange,” characterized by skin thickening and dimpling, also with nodularity, erythema, and, often, nipple retraction [1–4]. IBC is highly angiogenic and angioinvasive. Clusters of malignant cells invade the dermal lymphatics, forming tumor emboli that likely cause the clinical symptoms, and disseminate to distant sites [1].

In our previous work, we found that WISP3 is lost in 80% of human IBC tumors and is a key genetic determinant of the IBC phenotype [5]. WISP3 has growth-, invasion-, and

angiogenesis-inhibitory functions in IBC *in vitro* and *in vivo* [6]. WISP3 is a member of the CCN family of proteins, which also includes connective tissue growth factor (CTGF), Cyr61, Nov, WISP1, and WISP2 [7,8]. A putatively secreted protein with a secretory signal peptide at the NH₂ terminus, WISP3 contains 36 conserved cysteine residues that are organized into four highly conserved modules: 1) a motif associated with insulin-like growth factor binding protein (IGFBP) (GCGCCXXC); 2) a von Willebrand type C–like motif; 3) a thrombospondin 1 module; and 4) a carboxyl-terminal domain putatively involved in dimerization [8,9]. The role of each of these conserved domains in the function of the CCN proteins, in general, and of WISP3, in particular, remains to be elucidated.

IGF-I and its major receptor, IGF-IR, play an important role in normal breast biology and in the development of breast cancer [10–13]. A large body of work implicates the IGF family in breast cancer progression. High concentrations of IGF-I in serum are associated with increased mammographic density (one of the strongest predictors of breast cancer risk), and also reliably predict increased breast cancer risk specifically in premenopausal women [14]. *In vitro*, IGF-I is a strong mitogen for human breast cancer cells and has been found in the epithelial and stromal component of breast cancers [13]. High expression of IGF-IR has been demonstrated in most primary human breast cancers when compared to normal or benign breast tissues, and hyperactivation of IGF-IR in breast cancer has been linked to increased radioresistance and cancer recurrence at the primary site [13,15,16]. High levels of IRS-1, a major signaling molecule downstream of the IGF-IR, correlate with tumor size and shorter disease-free survival in ER⁺ breast cancer patients [17,18]. Based on the protein sequence of WISP3 and the important role of IGF signaling in breast cancer, we hypothesized that WISP3 is secreted into the extracellular medium and that the growth-inhibitory effect of

Address all correspondence to: Sofia D. Merajver, MD, PhD, and Celina G. Kleer, MD, Department of Internal Medicine, 7217 CCGC, 1500 East Medical Center Drive, Ann Arbor, MI 48108-0948, USA. E-mail: smerajve@umich.edu

[†]This work was supported, in part, by Army grants DAMD17-02-1-0490 (C.G.K.), DAMD17-02-1-491 (C.G.K.), and DAMD-17-00-1-0345 (S.D.M.); National Institutes of Health grants K08CA090876 (C.G.K.), RO1CA77612 (S.D.M.) and 1 P50-CADE97258 (S.D.M.); and a grant from the John and Suzanne Munn Endowed Research Fund of the University of Michigan Comprehensive Cancer Center (C.G.K.).

Received 5 September 2003; Revised 2 December 2003; Accepted 3 December 2003.

WISP3 in IBC may be dependent, at least in part, on modulation of IGF-I signaling. To test this hypothesis, we investigated the downstream effects of WISP3 starting at the IGF-IR receptor and signaling pathway. Here, we demonstrate that WISP3 is a secreted protein and that, once in the conditioned media, it can effectively modulate IGF-IR activation and its signaling cascade and the cellular growth of IBC cells.

Materials and Methods

Cell Culture and Transfections

SUM149 cells derive from a primary IBC that has lost WISP3 expression [6,19]. SUM149 cells and their transfectants were cultured in Ham's F-12 media supplemented with 5% fetal bovine serum (FBS), hydrocortisone (1 µg/ml), insulin (5 µg/ml), fungizone (2.5 µg/ml), gentamycin (5 µg/ml), and penicillin/streptomycin (100 µ/ml each), at 37°C under 10% CO₂. HEK-293 cells derived from human embryonic kidney epithelial cells were grown in Dulbecco's modified Eagle's medium (DMEM) containing 10% FBS. SUM149 and HEK-293 cells were transfected with HIS⁻ tagged (pcDNA 3.1/V5-HIS TOPO TA expression vector; Invitrogen, Carlsbad, CA) and Flag⁻ tagged (pFlag-CMV vector; Sigma, St. Louis, MO) full-length WISP3 cDNA, and clonal cell lines were established as described previously [6]. Control cell lines were generated by transfecting the SUM149 and HEK-293 cell lines with the empty vectors. The inserts were confirmed by sequencing. Cells were incubated in serum-free medium. WISP3 and control conditioned media were collected 3 days later. The conditioned media were cleared of cell debris by centrifugation, and concentrated 10-fold through a Centrplus YM-10 column (Millipore, Bedford, MA) before use.

IGF-I Stimulation

Seventy percent confluent SUM149 cells were shifted to serum-free medium. After 24 hours of starvation, the cells were cultured in WISP3 and control conditioned media for 24 hours. Subsequently, SUM149 cells were stimulated with 20 ng/ml human recombinant IGF-I (Upstate Biotechnology Inc., Lake Placid, NY) for 15 minutes.

Immunoprecipitation and Western Blotting

Cells were lysed in lysis buffer composed of 50 mM Tris-HCl (pH 7.4), 150 mM NaCl, 1% NP-40, 0.25% sodium deoxycholate, 1 mM EGTA, 1 mM Na₃VO₄, 1 mM PMSF, and 1 µg/ml aprotinin. The lysates were clarified by centrifugation at 14,000g for 10 minutes. A total of 500 µg of cell lysates was incubated with 1 µg/ml anti-IGF-IR mAb (Calbiochem, San Diego, CA) overnight at 4°C. Immune complexes were precipitated by adding 50 µl of protein A/G plus agarose bead slurry for 2 hours. The agarose beads were collected and washed three times with ice-cold lysis buffer, and resuspended in 25 µl of 2 × Laemmli sample buffer for sodium dodecyl sulfate polyacrylamide gel electrophoresis (SDS-PAGE). Fifty micrograms of protein extract was separated by SDS-PAGE and transferred onto a PVDF

membrane (Amersham Pharmacia Biotech). The precipitated IGF-IR was detected with anti-IGF-IR β subunit polyclonal Ab (Santa Cruz Biotechnology, Santa Cruz, CA). Tyrosine phosphorylation of immunoprecipitated IGF-IR was assessed with anti-phosphotyrosine mAb PY20 (Transduction Laboratories, Lexington, KY). Total IGF-IR, phosphorylated and total IRS1, and ERK-1/2 were measured with appropriate antibodies (Transduction Laboratories; Upstate Biotechnology Inc.). WISP3 expression was confirmed by Western blot using a polyclonal anti-WISP3 antibody (gift from Dr. Warman) and an antibody against the HIS tag (Invitrogen). The protein bands were visualized using enhanced chemiluminescence (Amersham Pharmacia Biotech, Piscataway, NJ). All experiments were repeated at least three times and the optical density of the bands was quantified by densitometry (Scio Image software for Win 95/98, version 0.4). Statistical analysis was performed using 95% confidence intervals for the estimates of the means. A *P* value of < .05 was considered statistically significant.

Effect of WISP3 in the Proliferation of SUM149 cells

SUM149 cells were plated in 96-well tissue culture plates at a density of 5 × 10⁴ cells/ml in Ham's F-12 media with 5% FBS. One hundred microliters of serum-free medium was added for 24 hours. Ten-fold concentrated WISP3 and control conditioned media were added in the presence and absence of IGF-I stimulation as described above. MTT reagents were added 24 hours later according to the manufacturer's protocol (Sigma), and the plate was read at a wavelength of 595 nm. The experiment was performed in triplicate.

Human Breast Tissues and Immunohistochemistry

WISP3 protein expression was studied by immunohistochemistry in normal human breast tissues obtained from 10 reduction mammoplasty procedures. Immunohistochemical analysis was performed by using a polyclonal anti-WISP3 antibody at 1:500 dilution with overnight incubation and microwave antigen retrieval [20]. The detection reaction followed the Dako Envision⁺ System Peroxidase kit protocol (Dako, Carpinteria, CA). Diaminobenzidine was used as chromogen and hematoxylin was used as counterstain. Positive and negative controls were tumor xenografts derived from cell lines shown to express high levels of WISP3 (SUM149 cell line stably transfected with WISP3) and from a cell line that does not express WISP3 (SUM149 wild type), respectively.

Results

WISP3 Protein Is Secreted by Human Breast Epithelial Cells

WISP3 protein contains a multimodular structure with a secretory signal peptide at the N-terminus. To investigate whether WISP3 is secreted by breast epithelial cells, SUM149 IBC cells previously characterized with a loss in WISP3 expression were stably transfected to express full-length WISP3. Conditioned media from SUM149/WISP3-overexpressing clones were collected and

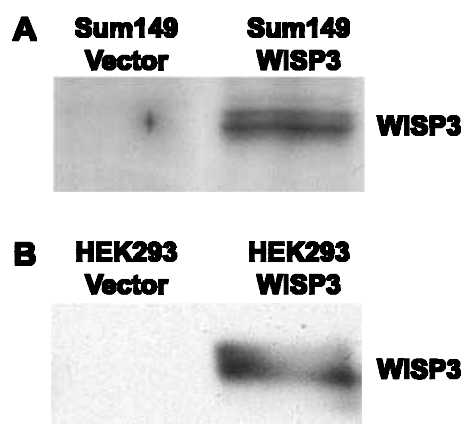


Figure 1. WISP3 protein is secreted and detected in the conditioned media. (A) Western immunoblot using anti-WISP3 polyclonal antibody detects WISP3 protein in the conditioned media of SUM149 cells transfected with WISP3 full-length cDNA. WISP3 protein is not detected in the conditioned media of SUM149 cells transfected with the empty vector. (B) Western immunoblot of the conditioned media of HEK-293 cells transfected with WISP3, detected using an anti-HIS antibody. WISP3 is not detected in the conditioned media of the control cells.

detected for WISP3 by Western blot analysis using a polyclonal anti-WISP3 antibody. WISP3 protein was detected in the media of SUM149-expressing WISP3 (SUM149/WISP3), and not in the media of empty vector-transfected SUM149 cells (SUM149/Flag) (Figure 1A). In order to explore these results from a different perspec-

tive, we performed transient transfections of WISP3 in SUM149 cells using a HIS⁻ tagged full-length WISP3 expression vector. In this case, WISP3 protein was detected in the conditioned media using both anti-WISP3 antibody and anti-HIS antibody (data not shown). To specifically address whether WISP3 would be detected in the conditioned media of a nonmammary cell, we repeated these experiments with the HEK293 cell line, derived from human embryonic kidney epithelial cells. WISP3 was detected in the conditioned media of these cells and not in the conditioned media of the empty vector controls (Figure 1B).

In situ expression of WISP3 protein was determined by immunohistochemical analysis of normal breast tissues derived from reduction mammoplasty procedures. In all 10 tissues examined, WISP3 protein was expressed at low levels in the cytoplasm of normal epithelial cells from ducts and acini and, interestingly, was present in the luminal secretions of ducts and lobules (Figure 2A). Xenografts derived from wild-type SUM149 cells (WISP3⁻) and from SUM149/WISP3⁺ cells were used as negative and positive controls, respectively (Figure 2, B and C).

WISP3 Containing Conditioned Media Reduces IGF-I-Induced IGF-IR Activation and Signaling Pathways

The effect of WISP3 on the activation of the IGF-I signaling pathway was studied in SUM149 cells derived from a primary IBC [5,6,19,21]. The activation of the IGF signaling

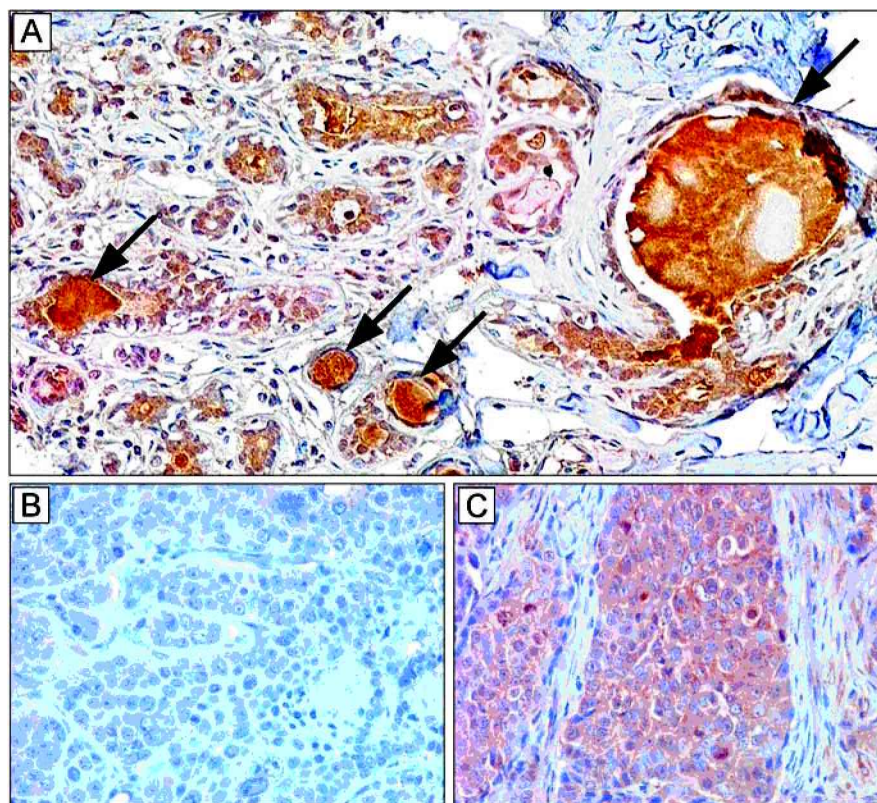


Figure 2. *In situ* expression of WISP3 protein in normal breast tissues. (A) Immunohistochemical analysis of normal breast tissues using a polyclonal anti-WISP3 antibody shows that WISP3 protein is expressed at low levels in the cytoplasm of normal epithelial cells and in the luminal secretions of ducts and acini (arrows) ($\times 200$). (B and C) Xenografts derived from wild-type SUM149 and SUM149/WISP3 cells were used as negative and positive controls, respectively ($\times 400$).

cascade plays a central role in breast cancer development and progression. To investigate whether the presence of WISP3 in the conditioned media has an effect on IGF-IR signaling pathways in IBC cells, phosphorylation of IGF-IR, IRS1, and ERK-1/2 was determined in wild-type SUM149 cells in the presence or absence of WISP3 in the conditioned media. Experiments were carried out under baseline conditions without addition of IGF-I and after stimulation with IGF-I. In the presence of WISP3 in the conditioned media, SUM149 cells exhibited decreased IGF-IR phosphorylation (Figure 3). The effect of WISP3 in the phosphorylation of the IGF-IR was evident in the presence of IGF-I stimulation because WISP3 was able to ameliorate the effect of IGF-I stimulation on the activation of the IGF-IR (Figure 3). Similarly, WISP3 conditioned media decreased the IGF-I-induced IRS1 and ERK-1/2 phosphorylation (Figures 4 and 5).

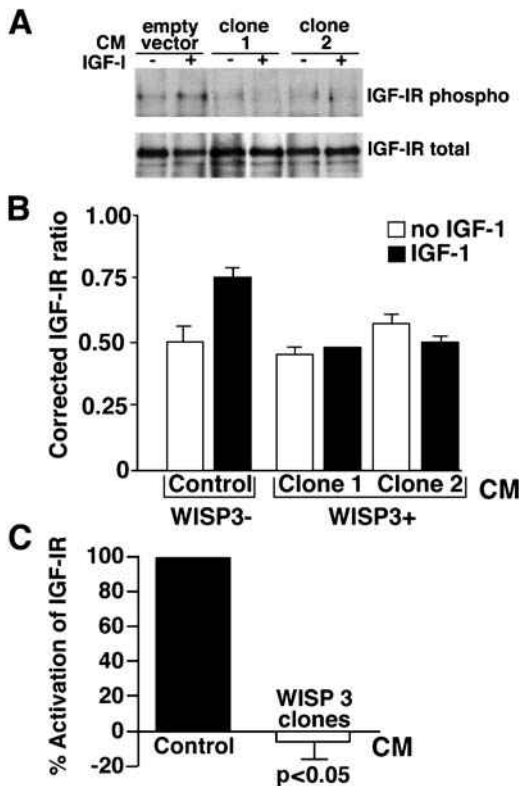


Figure 3. WISP3 decreases IGF-I-induced phosphorylation of the IGF-IR. (A) Western blot analysis of SUM149 cell lines bathed in WISP3⁺ and control (WISP3⁻) conditioned media. The experiment was carried out under baseline conditions (without IGF-I) and after stimulation with 20 ng/ml IGF-I. The IGF-IR was precipitated from 500 μg of protein lysate with an anti-IGF-IR mAb and subsequently detected by immunoblot with an anti-IGF-IR β subunit polyclonal Ab. Tyrosine phosphorylation of immunoprecipitated IGF-IR was assessed with an anti-phosphotyrosine mAb PY20. (B) Relative protein levels of IGF-IR phosphorylation normalized for total IGF-IR. Blots were scanned and the pixel intensity measured using Scn Image program. Results are expressed as mean ± SEM of three independent experiments. (C) Quantitation of the differences in the percent activation of the IGF-IR. The difference in normalized IGF-IR phosphorylation under baseline conditions and after IGF-I stimulation was calculated for each cell line. Results were corrected using the difference in IGF-IR phosphorylation in the absence of IGF-I stimulation as reference. WISP3 was able to decrease the IGF-I-induced activation of the IGF-IR (t test, P < .05).

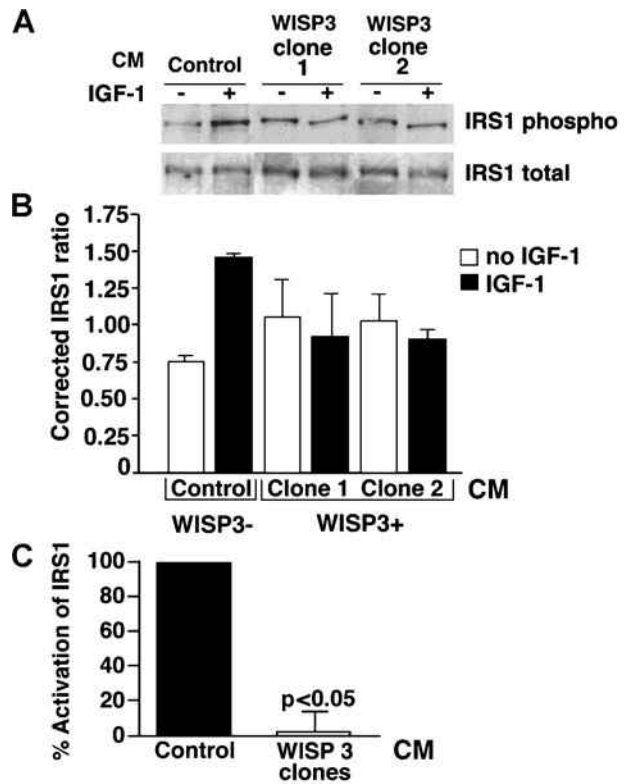


Figure 4. WISP3 decreases IGF-I-induced phosphorylation of IRS1. (A) Western blot analysis of SUM149 cell lines bathed in WISP3⁺ and control WISP3⁻ conditioned media. The experiment was carried out under baseline conditions (without IGF-I) and after stimulation with IGF-I. The expression of phosphorylated IRS1 was detected by Western blot using a polyclonal antibody against phosphorylated IRS1. The Western blot was stripped and probed with an antibody against total IRS1. (B) Relative protein levels of IRS1 phosphorylation normalized for total IRS1. Blots were scanned and the pixel intensity measured. Results are expressed as mean ± SEM of three independent experiments. (C) The differences in the percent activation of IRS-1 were quantitated. The difference in the corrected IRS1 phosphorylation under baseline conditions and after IGF-I stimulation was calculated for each cell line and results were normalized using the difference in IRS1 phosphorylation in the absence of IGF-I stimulation as reference. WISP3-rich conditioned media was able to decrease the phosphorylation of IRS-1 triggered by IGF-I (t test, P < .05).

WISP3 Containing Conditioned Media Reduces the Growth of IBC Cell Lines

After establishing that the presence of WISP3 in the conditioned media was able to modulate IGF-I signaling pathways, its effect on cellular proliferation was determined in the presence and absence of IGF-I stimulation. SUM149 cells bathed in the WISP3 conditioned media had significantly lower growth rates than the control SUM149 cells bathed in control (WISP3-deficient) conditioned media, both in the presence and absence of IGF-I stimulation (t test, P < .05; Figure 6).

Discussion

We have previously demonstrated that WISP3 is lost in 80% of IBC tumors and that it has tumor-suppressor functions in IBC [5,6]. Studies on the SUM149 IBC cell line showed that restoration of WISP3 expression has potent growth- and

angiogenesis-inhibitory functions *in vitro* and *in vivo* [6]. Restoration of WISP3 resulted in a significant decrease in anchorage-independent growth in soft agar and cellular proliferation, as well as a drastic decrease in the invasive capabilities of the SUM149 cells, which are highly invasive in their wild-type state. Furthermore, restoration of WISP3 expression in SUM149 cells resulted in a biologically relevant decrease in the level of angiogenic factors (VEGF, bFGF, and IL-6) in the conditioned media of the cells. *In vivo*, restoration of WISP3 expression in SUM149 cells caused a drastic decrease in tumor volume and rate of tumor growth when injected in nude mice [6]. Taken together, this body of work had strongly supported a tumor-suppressor role for WISP3 in mammary tumor progression. In the present study, we sought to discover the molecular mechanisms underlying the tumor-suppressor function of WISP3.

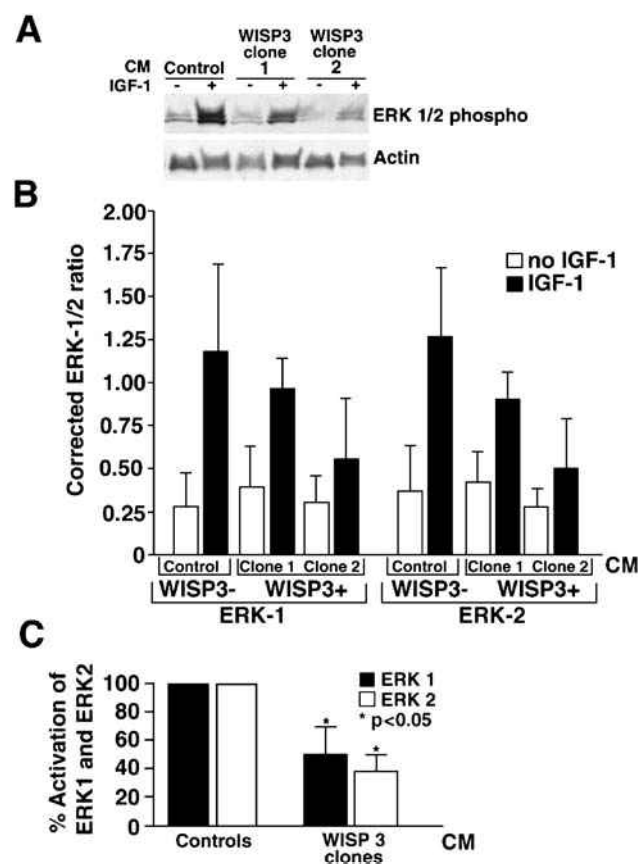


Figure 5. WISP3 decreases IGF-I–induced phosphorylation of ERK-1/2. (A) Western blot analysis of SUM149 cell lines bathed in WISP3⁺ and control (WISP3⁻) conditioned media, under baseline conditions (without IGF-I) and after stimulation with IGF-I. The expression of ERK-1/2 was detected by Western blot using a polyclonal antibody against phosphorylated ERK-1/2. The blot was stripped and probed with an antibody against β -actin. (B) Relative protein levels of ERK-1/2 phosphorylation normalized using actin. Blots were scanned and the pixel intensity measured. Results are expressed as mean \pm SEM of three independent experiments. (C) Quantitation of the differences in the percent activation of ERK-1/2. The difference in the corrected ERK-1/2 phosphorylation under baseline conditions and after IGF-I stimulation was calculated for each cell line. Results were normalized using the difference in ERK-1/2 phosphorylation in the absence of IGF-I stimulation as reference. WISP3-rich conditioned media ameliorated the phosphorylation of ERK 1 and ERK 2 induced by IGF-I stimulation (*t* test, *P* < .05).

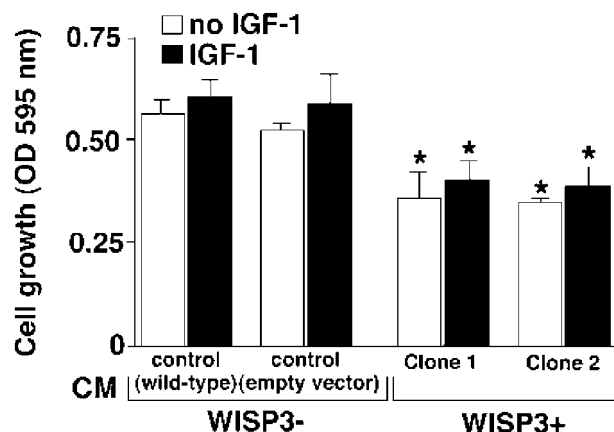


Figure 6. WISP3 decreases the growth of IBC cells. The growth of SUM149 cells was measured in the absence (WISP3⁻) and presence of WISP3 (WISP3⁺) in the conditioned media under baseline conditions (no IGF-I) and after IGF-I stimulation by an MTT assay. SUM149 cells were grown in 96-well plates at a density of 5×10^4 cells/ml. Serum-starved cells were incubated for 24 hours in the WISP3 and control conditioned media, with or without IGF-I stimulation. Results are expressed as mean \pm SEM of three independent experiments. WISP3⁺ conditioned media decreases significantly the growth of SUM149 cells (*t* test, *P* < .05 for both clones).

WISP3 belongs to the CCN family of proteins, which are highly conserved, putatively secreted proteins with important roles in development during chondrogenesis and skeletogenesis [7]. The CCN proteins have been recently also implicated in carcinogenesis [7,22–26]. It is not well understood, however, how the functions of the CCN proteins in development relate to their role in cancer. Moreover, their expression during tumorigenesis cannot be generalized across different tissue types. This may be due to tissue-specific functions of the CCN proteins, perhaps mediated by their multimodular structure and the presence of different affinities for binding partners and ligands in different tissues [7]. The presence of different receptors and differential processing of the CCN proteins (e.g., cleavage by proteases) may account also for their diverse functions in different tissues. In this paper, we focused on determining whether WISP3 is secreted into the conditioned media and its relationship to IGF signaling pathways.

Analysis of the protein sequence of WISP3 revealed that it contains a signal peptide at the N-terminal region that may participate in the secretion of the protein into the extracellular media [7–9]. Indeed, by Western blot, using two different specific antibodies, we were able to detect WISP3 protein in the conditioned media of SUM149 and HEK293 cells transfected with WISP3. Furthermore, consistent with these results, by immunohistochemical analysis, WISP3 protein was detected in the secretions accumulated in the lumens of ducts and lobules in normal breast tissues. The fact that WISP3 is secreted and present in the conditioned media (thereby alluding to its stability in solution) led us to the hypothesis that it may directly or indirectly regulate IGF signaling.

Although the signaling pathways that are required for the effects of IGF-I in breast cancer have not been completely elucidated, the contribution of IGF-I–induced IGF-IR

activation appears to be critical in hormone-dependent and -independent breast cancer [27–30]. IGF-I is locally released by breast cancer cells and stromal fibroblasts, and it is involved in autocrine and paracrine stimulation of the mammary epithelium [31]. In breast cancer cells, when IGF-I binds IGF-IR, signaling occurs mainly through activation of IRS-1 and RAS-dependent phosphorylation of MAP kinase with subsequent activation of nuclear transcription factors [32,33]. IGF-I signaling promotes cell growth, survival, and motility of breast cancer cells, as well as resistance to therapeutic interventions [10–12,14–18]. We hypothesized that expression of WISP3 could result in a series of molecular events that leads to the modulation of IGF-IR activation and downstream signaling. Contributing to this hypothesis is the fact that we have shown that WISP3 is secreted into the media where it has the opportunity to directly or indirectly modulate the strength of IGF signaling. Indeed, in the presence of IGF-I, WISP3 containing conditioned media decreased IGF-IR phosphorylation and the phosphorylation of two main downstream IGF-IR signaling molecules, IRS1 and ERK-1/2. This inhibition was not evident under baseline conditions, without stimulation with IGF-I. Our experiments thus show that even relatively small concentrations of WISP3 secreted by WISP3-transfected cells are able to modulate, directly or indirectly, IGF-I signaling in the setting of IGF-I stimulation.

A major growth-regulatory IGF-IR downstream pathway that regulates breast cancer growth and survival converges on ERK-1/2 cascade [34]. We observed a decrease in ERK-1/2 phosphorylation by addition of WISP3 containing conditioned media in the presence of IGF-I stimulation. ERK-1/2 influence chromatin remodeling and activation of gene expression, leading to enhanced cellular proliferation and decreased apoptosis [35–37]. Specifically, ERK-1/2 have been shown to activate the transcription of key genes involved in cell cycle progression including cyclin D1 and cyclin E. We have shown previously that restoration of WISP3 expression in the highly malignant SUM149 IBC cell line markedly decreased the levels of cyclin E and PCNA, a reliable marker of cellular proliferation [6].

The mechanism whereby WISP3 may modulate IGF-IR activation in the presence of IGF-I remains to be elucidated. WISP3 contains a highly conserved motif (GCGCCXXC) characteristic of IGF-BPs, which may provide the proper protein folding to interact with IGF-like ligands, thereby enabling interference with IGF signaling. Although initial studies reported that two other CCN proteins, CTGF (CTGF) and Nov, specifically bind to IGF-I [38,39], these results have not been subsequently built on and they remain to be duplicated by other investigators. Whether WISP3 physically binds to IGF-I warrants further investigation, in light of our data.

Another mechanism that may explain the modulation of IGF-IR phosphorylation by WISP3-containing conditioned media is the formation of a WISP3/IGF-I complex that may bind to the IGF-IR and occupy IGF binding sites, but the complex may be either inhibitory or may be only a weak agonist of the receptor. In another system [40], this hypoth-

esis is supported by recent data showing that IGF-I can still freely bind to the receptor even when complexed to a truncated N-terminal fragment of IGF-binding protein 5 (mini-IGFBP5); interestingly, the N-terminal portion of IGFBP5 has high homology to the N-terminal portion of WISP3. Mini-IGFBP5 binding to IGF-I resulted in incomplete inhibition of receptor binding [40]. In a similar manner, a WISP3/IGF-I complex might still bind to the IGF-IR but exert only a weak agonist effect, effectively resulting in physiologic antagonism of IGF-I action under conditions of high IGF-I stimulation. WISP3-rich conditioned media was able to significantly decrease the proliferation rate of IBC cells. The fact that this effect was seen both in the presence and absence of IGF-I stimulation suggests that, in addition to interfering with IGF-I signaling pathways, WISP3 may have IGF-independent functions in IBC. In sum, we show that WISP3 is a secreted protein that modulates IGF-I signaling pathways, leading to a decrease in the growth of IBC cells.

Acknowledgements

We thank Robin Kunkel and Elizabeth Horn for artwork; S. Ethier for the SUM149 and HME cell lines; Wendy Kutz and Matthew Warman from Case Western Reserve University for providing anti-WISP3 antibody; and Michelle LeBlanc and the Immunohistochemistry Core of the University of Michigan Cancer Center for tissue processing and immunohistochemistry.

References

- [1] Lee BJ (1924). Inflammatory carcinoma of the breast: a report of twenty-eight cases from the breast clinic of Memorial Hospital. *Surg Gynecol Obstet* **39**, 580–595.
- [2] Jaiyesimi IA, Buzdar AU, and Hortobagyi G (1992). Inflammatory breast cancer: a review. *J Clin Oncol* **10**, 1014–1024.
- [3] Merajver SD, Weber BL, Cody R, Zhang D, Strawderman M, Calzone KA, LeClaire V, Levin A, Irani J, Helvie M, August D, Wicha M, Lichter A, and Pierce LJ (1997). Breast conservation and prolonged chemotherapy for locally advanced breast cancer: the University of Michigan experience. *J Clin Oncol* **15**, 2873–2881.
- [4] Swain SM, Sorace RA, Bagley CS, Danforth Jr, DN, Bader J, Wesley MN, Steinberg SM, and Lippman ME (1987). Neoadjuvant chemotherapy in the combined modality approach of locally advanced nonmetastatic breast cancer. *Cancer Res* **47**, 3889–3894.
- [5] van Golen KL, Davies S, Wu ZF, Wang Y, Bucana CD, Root H, Chandrasekharappa S, Strawderman M, Ethier SP, and Merajver SD (1999). A novel putative low-affinity insulin-like growth factor-binding protein, LIBC (lost in inflammatory breast cancer), and RhoC GTPase correlate with the inflammatory breast cancer phenotype. *Clin Cancer Res* **5**, 2511–2519.
- [6] Kleer CG, Zhang Y, Pan Q, van Golen KL, Wu ZF, Livant D, and Merajver SD (2002). WISP3 is a novel tumor suppressor gene of inflammatory breast cancer. *Oncogene* **21**, 3172–3180.
- [7] Perbal B (2001). NOV (nephroblastoma overexpressed) and the CCN family of genes: structural and functional issues. *Mol Pathol* **54**, 57–79.
- [8] Pennica D, Swanson TA, Welsh JW, Roy MA, Lawrence DA, Lee J, Brush J, Taneyhill LA, Deuel B, Lew M, Watanabe C, Cohen RL, Melhem MF, Finley GG, Quirke P, Goddard AD, Hillan KJ, Gurney AL, Botstein D, and Levine AJ (1998). WISP genes are members of the connective tissue growth factor family that are up-regulated in wnt-1-transformed cells and aberrantly expressed in human colon tumors. *Proc Natl Acad Sci USA* **95**, 14717–14722.
- [9] Hurvitz JR, Suwairi WM, Van Hul W, El-Shanti H, Superti-Furga A, Roudier J, Holderbaum D, Pauli RM, Herd JK, Van Hul EV, Rezai-Delui

- H, Legius E, Le Merrer M, Al-Alami J, Bahabri SA, and Warman ML (1999). Mutations in the *CCN* gene family member *WISP3* cause progressive pseudorheumatoid dysplasia. *Nat Genet* **23**, 94–98.
- [10] Bartucci M, Morelli C, Mauro L, Ando S, and Surmacz E (2001). Differential insulin-like growth factor I receptor signaling and function in estrogen receptor (ER)-positive MCF-7 and ER-negative MDA-MB-231 breast cancer cells. *Cancer Res* **61**, 6747–6754.
- [11] Furstemberger G, and Senn HJ (2002). Insulin-like growth factors and cancer. *Lancet Oncol* **3**, 298–302.
- [12] Kleinberg DL, Feldman M, and Ruan W (2000). IGF-I: an essential factor in terminal end bud formation and ductal morphogenesis. *J Mammary Gland Biol Neoplasia* **5**, 7–17.
- [13] Surmacz E (2000). Function of the IGF-I receptor in breast cancer. *J Mammary Gland Biol Neoplasia* **5**, 95–105.
- [14] Byrne C, Colditz GA, Willett WC, Speizer FE, Pollak M, and Hankinson SE (2000). Plasma insulin-like growth factor (IGF) I, IGF-binding protein 3, and mammographic density. *Cancer Res* **60**, 3744–3748.
- [15] Turner BC, Haffty BG, Narayanan L, Yuan J, Havre PA, Gumbs AA, Kaplan L, Burgaud JL, Carter D, Baserga R, and Glazer PM (1997). Insulin-like growth factor-I receptor overexpression mediates cellular radioresistance and local breast cancer recurrence after lumpectomy and radiation. *Cancer Res* **57**, 3079–3083.
- [16] Resnik JL, Reichart DB, Huey K, Webster NJ, and Seely BL (1998). Elevated insulin-like growth factor I receptor autophosphorylation and kinase activity in human breast cancer. *Cancer Res* **58**, 1159–1164.
- [17] Rocha RL, Hilsenbeck SG, Jackson JG, VanDenBerg CL, Weng C, Lee AV, and Yee D (1997). Insulin-like growth factor binding protein-3 and insulin receptor substrate-1 in breast cancer: correlation with clinical parameters and disease-free survival. *Clin Cancer Res* **3**, 103–109.
- [18] Lee AV, Jackson JG, Gooch JL, Hilsenbeck SG, Coronado-Heinsohn E, Osborne CK, and Yee D (1999). Enhancement of insulin-like growth factor signaling in human breast cancer: estrogen regulation of insulin receptor substrate-1 expression *in vitro* and *in vivo*. *Mol Endocrinol* **13**, 787–796.
- [19] Ethier SP, Mahacek ML, Gullick WJ, Frank TS, and Weber BL (1993). Differential isolation of normal luminal mammary epithelial cells and breast cancer cells from primary and metastatic sites using selective media. *Cancer Res* **53**, 627–635.
- [20] Shi SR, Key ME, and Kalra KL (1991). Antigen retrieval in formalin-fixed, paraffin-embedded tissues: an enhancement method for immunohistochemical staining based on microwave oven heating of tissue sections. *J Histochem Cytochem* **39**, 741–748.
- [21] van Golen KL, Wu ZF, Qiao XT, Bao LW, and Merajver SD (2000). RhoC GTPase, a novel transforming oncogene for human mammary epithelial cells that partially recapitulates the inflammatory breast cancer phenotype. *Cancer Res* **60**, 5832–5838.
- [22] Soon LL, Yie TA, Shvarts A, Levine AJ, Su F, and Tchou-Wong KM (2003). Overexpression of WISP-1 down-regulated motility and invasion of lung cancer cells through inhibition of Rac activation. *J Biol Chem* **278**, 11465–11470.
- [23] Vilmos P, Gaudenz K, Hegedus Z, and Marsh JL (2001). The Twisted gastrulation family of proteins, together with the IGFBP and CCN families, comprise the TIC superfamily of cysteine rich secreted factors. *Mol Pathol* **54**, 317–323.
- [24] Kireeva ML, Mo FE, Yang GP, and Lau LF (1996). Cyr61, a product of a growth factor-inducible immediate-early gene, promotes cell proliferation, migration, and adhesion. *Mol Cell Biol* **16**, 1326–1334.
- [25] Tong X, Xie D, O'Kelly J, Miller CW, Muller-Tidow C, and Koeffler HP (2001). Cyr61, a member of CCN family, is a tumor suppressor in non-small cell lung cancer. *J Biol Chem* **276**, 47709–47714.
- [26] Xie D, Nakachi K, Wang H, Elashoff R, and Koeffler HP (2001). Elevated levels of connective tissue growth factor, WISP-1, and CYR61 in primary breast cancers associated with more advanced features. *Cancer Res* **61**, 8917–8923.
- [27] Godden J, Leake R, and Kerr DJ (1992). The response of breast cancer cells to steroid and peptide growth factors. *Anticancer Res* **12**, 1683–1688.
- [28] Jackson JG, White MF, and Yee D (1998). Insulin receptor substrate-1 is the predominant signaling molecule activated by insulin-like growth factor-I, insulin, and interleukin-4 in estrogen receptor-positive human breast cancer cells. *J Biol Chem* **273**, 9994–10003.
- [29] Jackson JG, and Yee D (1999). IRS-1 expression and activation are not sufficient to activate downstream pathways and enable IGF-I growth response in estrogen receptor negative breast cancer cells. *Growth Horm IGF Res* **9**, 280–289.
- [30] Peyrat JP, Bonneterre J, Dusanter-Fourt I, Leroy-Martin B, Djiane J, and Demaille A (1989). Characterization of insulin-like growth factor 1 receptors (IGF1-R) in human breast cancer cell lines. *Bull Cancer* **76**, 311–319.
- [31] Satyamoorthy K, Li G, Vaidya B, Patel D, and Herlyn M (2001). Insulin-like growth factor-1 induces survival and growth of biologically early melanoma cells through both the mitogen-activated protein kinase and beta-catenin pathways. *Cancer Res* **61**, 7318–7324.
- [32] Resnicoff M, and Baserga R (1998). The role of the insulin-like growth factor I receptor in transformation and apoptosis. *Ann NY Acad Sci* **842**, 76–81.
- [33] Baserga R (1999). The IGF-I receptor in cancer research. *Exp Cell Res* **253**, 1–6.
- [34] Santen RJ, Song RX, McPherson R, Kumar R, Adam L, Jeng MH, and Yue W (2002). The role of mitogen-activated protein (MAP) kinase in breast cancer. *J Steroid Biochem Mol Biol* **80**, 239–256.
- [35] Murphy LO, Smith S, Chen RH, Fingar DC, and Blenis J (2002). Molecular interpretation of ERK signal duration by immediate early gene products. *Nat Cell Biol* **4**, 556–564.
- [36] Volmat V, Camps M, Arkinstall S, Pouyssegur J, and Lenormand P (2001). The nucleus, a site for signal termination by sequestration and inactivation of p42/p44 MAP kinases. *J Cell Sci* **114**, 3433–3443.
- [37] Volmat V, and Pouyssegur J (2001). Spatiotemporal regulation of the p42/p44 MAPK pathway. *Biol Cell* **93**, 71–79.
- [38] Kim HS, Nagalla SR, Oh Y, Wilson E, Roberts CT Jr, and Rosenfeld RG (1997). Identification of a family of low-affinity insulin-like growth factor binding proteins (IGFBPs): characterization of connective tissue growth factor as a member of the IGFBP superfamily. *Proc Natl Acad Sci USA* **94**, 12981–12986.
- [39] Burren CP, Wilson EM, Hwa V, Oh Y, and Rosenfeld RG (1999). Binding properties and distribution of insulin-like growth factor binding protein-related protein 3 (IGFBP-rP3/NovH), an additional member of the IGFBP superfamily. *J Clin Endocrinol Metab* **84**, 1096–1103.
- [40] Zeslawski W, Beisel HG, Kamionka M, Kalus W, Engh RA, Huber R, Lang K, and Holak TA (2001). The interaction of insulin-like growth factor-1 with the N-terminal domain of IGFBP-5. *EMBO J* **20**, 3638–3644.

WISP3 is a novel tumor suppressor gene of inflammatory breast cancer

Celina G Kleer^{*1}, Yanhong Zhang¹, Quintin Pan², Kenneth L van Golen², Zhi-Fen Wu², D Livant³ and Sofia D Merajver²

¹Department of Pathology, University of Michigan Comprehensive Cancer Center, Ann Arbor, Michigan, USA; ²Department of Internal Medicine, Division of Hematology and Oncology, University of Michigan Comprehensive Cancer Center, Ann Arbor, Michigan, USA; ³Department of Radiation Oncology, University of Michigan Comprehensive Cancer Center, Ann Arbor, Michigan, USA

Inflammatory breast cancer (IBC) is an aggressive form of breast cancer with a 5-year disease-free survival of less than 45%. Little is known about the genetic alterations that result in IBC. In our previous work, we found that WISP3 was specifically lost in human IBC tumors when compared to stage-matched, non-IBC tumors. We hypothesize that WISP3 has tumor suppressor function in the breast and that it may be a key genetic alteration that contributes to the unique IBC phenotype. The full-length WISP3 cDNA was sequenced and cloned into an expression vector. The resulting construct was introduced into the SUM149 cell line that was derived from a patient with IBC and lacks WISP3 expression. In soft agar, stable WISP3 transfectants formed significantly fewer colonies than the controls. Stable WISP3 transfectants lost their ability to invade and had reduced angiogenic potential. WISP3 transfection was effective in suppressing *in vivo* tumor growth in nude mice. Mice bearing WISP3 expressing tumors had a significantly longer survival than those with vector-control transfectant tumors. Our data demonstrate that WISP3 acts as a tumor suppressor gene in the breast. Loss of WISP3 expression contributes to the phenotype of IBC by regulating tumor cell growth, invasion and angiogenesis.

Oncogene (2002) 21, 3172–3180. DOI: 10.1038/sj/onc/1205462

Keywords: WISP3; breast cancer; tumor suppressor gene; angiogenesis

Introduction

Inflammatory breast cancer (IBC) is the most lethal form of locally advanced breast cancer and accounts for approximately 6% of new breast cancer cases annually in the United States (Jaiyesimi *et al.*, 1992; Lee, 1924). It is also a very distinct clinical and

pathological form of breast carcinoma. It is characterized clinically by erythema, skin nodules, dimpling of the skin (termed ‘peau d’orange’) and by a rapid onset of disease, typically progressing within 6 months (Jaiyesimi *et al.*, 1992; Lee, 1924; Merajver *et al.*, 1997; Swain *et al.*, 1987). Pathologically, carcinomatous tumor emboli spread through the dermal lymphatics which are responsible for the clinical signs and symptoms (Lee, 1924). IBC is generally not associated with precursor lesions (Jaiyesimi *et al.*, 1992; Lee, 1924). From the outset, IBC is highly invasive and it appears to be capable of metastases from its inception. It is estimated that nearly all women with IBC have nodal involvement at the time of diagnosis, and over one-third have distant metastases (Merajver *et al.*, 1997; Swain *et al.*, 1987). In spite of new advances in breast cancer therapy, the overall 5-year disease-free survival rate is less than 45% (Merajver *et al.*, 1997; Swain *et al.*, 1987).

The genetic alterations underlying the development and progression of IBC were unknown until recently. Our laboratory identified two genes that are consistently and concordantly altered in human IBC when compared to stage-matched, non-IBC tumors: loss of WISP3 and over-expression of RhoC-GTPase (van Golen *et al.*, 1999).

WISP3 has been identified as a member of the CCN family of proteins, which have important biological functions in normal physiology as well as in carcinogenesis (Perbal, 2001). There are only two publications in the literature on the biological effects of WISP3 and very little is known about the expression pattern and function of this novel gene (Hurvitz *et al.*, 1999; Pennica *et al.*, 1998). We hypothesize that WISP3 may function as a growth-suppressing factor in breast carcinogenesis and that it may be a key genetic alteration in IBC in particular. To test this hypothesis, we set out to determine whether restoring WISP3 expression in an IBC cell line, SUM149, could abrogate or modulate the highly malignant IBC phenotype. We observed that stably transfected SUM149/WISP3 cells exhibited a striking decrease in proliferation rate, anchorage independent growth, invasion, and tumor growth in nude mice compared to empty vector transfectants. This work suggests new insights into the role of WISP3 in carcinogenesis in general.

*Correspondence: CG Kleer, 2G332 University Hospital, Department of Pathology, University of Michigan Medical School, 1500 East Medical Center Drive, Ann Arbor, Michigan MI 48109-0054, USA; E-mail: kleer@umich.edu

Received 18 October 2001; revised 11 January 2002; accepted 4 March 2002

Results

Transfection with the SUM149 cell line with WISP3 cDNA

Figure 1 shows the Western blot analysis of WISP3 protein in whole cell lysates from four clones of SUM149/WISP3 stable transfectants, SUM149/Flag (transfection controls), SUM149 wild type, and HME cells (human mammary epithelial cells). We used a specific anti-WISP3 antibody (gift from Dr Mathew Warman).

Statistically significant differences were found when each SUM149/WISP3 clone was compared to the SUM149/Flag control ($P < 0.04$, t -test).

WISP3 induces a striking morphologic change in IBC cell line

After stable transfection with WISP3 cDNA, we observed marked morphologic differences between the SUM149/WISP3 clones and SUM149/Flag control (Figure 2a). Whereas the control SUM149/Flag cells had a characteristic tightly packed, cobblestone appearance, with a cuboidal shape and high nuclear to cytoplasmic ratio, the SUM149/WISP3 transfectants were heterogeneous in size and morphology. They became large, round, and flat with abundant granular and vacuolated cytoplasm and ill-defined cell borders. A detailed ultrastructural analysis by electron microscopy demonstrate that the WISP3 transfectants exhibited numerous cytoplasmic lysosomal bodies surrounded by a membrane, some containing electron-dense material and invaginated and convoluted nuclei (Figure 2b). These morphologic features have been described in cells undergoing senescence (Romanov *et al.*, 2001; Tsugu *et al.*, 2000).

WISP3 partially abrogates angiogenesis in IBC

As illustrated in Figure 3a, SUM149/WISP3 clones produce significantly decreased levels of FGF2 (bFGF)

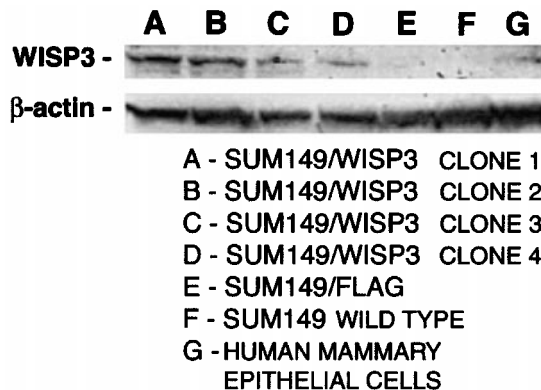


Figure 1 Western blot using a specific anti-WISP3 antibody demonstrates successful transfection and expression of WISP3 in SUM149 cells (lanes A–D). Lane E: transfection control (SUM149/Flag). Lane F: wild-type SUM149. Lane G: HME cells with normal expression of WISP3

and VEGF, key pro-angiogenic factors. The levels of IL-6, another pro-angiogenic cytokine were significantly decreased. To investigate whether the decreased production of angiogenic factors induced by restoration of WISP3 expression resulted in the inhibition of neovascularization, we carried out rat aortic ring assays. After 10 days of incubating a rat aortic ring with a $10\times$ concentration of the cell culture supernatant, fewer vessels were formed by SUM149/WISP3 cells when compared to the controls (Figure 3b). The SUM149/WISP3 transfectants formed a mean number of 26.33 new vessels (s.e.m. = 1.63), and the SUM149/Flag control cells formed a mean number of 69.33 new vessels (s.e.m. = 4.15) (t -test, $P = 0.0003$). These results show that expression of WISP3 depressed the strength of the tumor-induced signal for angiogenesis.

Expression of WISP3 reduces the proliferation rate, anchorage-independent growth, and the invasive ability of IBC cells

As anchorage independent growth is a hallmark of malignant transformation, we investigated whether expression of WISP3 in highly malignant SUM149 cell line abolished this feature. After 14 days of growth in soft agar four WISP3 expressing clones formed significantly fewer and smaller colonies than the control cells ($P < 0.05$), (Figure 4a,b). Figure 4c shows the results of the MTT assay and illustrates that the

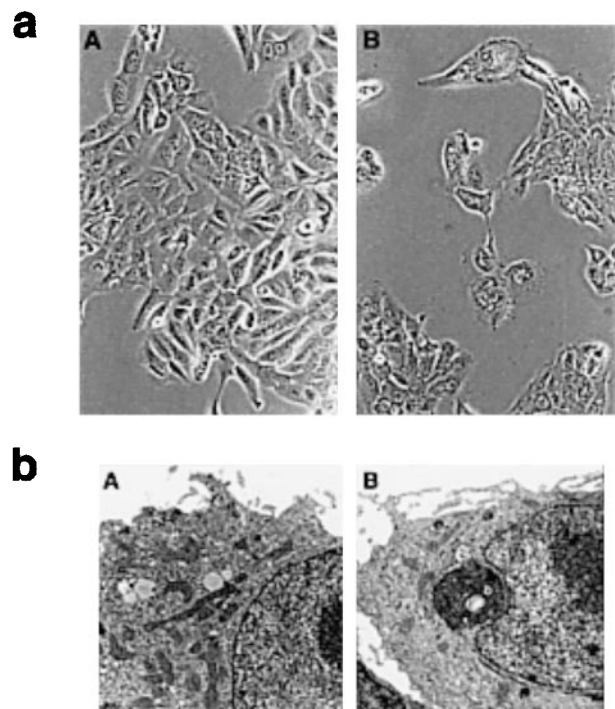


Figure 2 (a) Phase contrast microscopy showing the vacuolization and morphologic changes induced by restoring WISP3 expression in SUM149 cells. A: SUM149/Flag (controls). B: SUM149/WISP3 (X 200). (b) Electron microscopy. A: SUM149/Flag, and B: SUM149/WISP3 transfectant cell showing a prominent intracytoplasmic dense vacuole

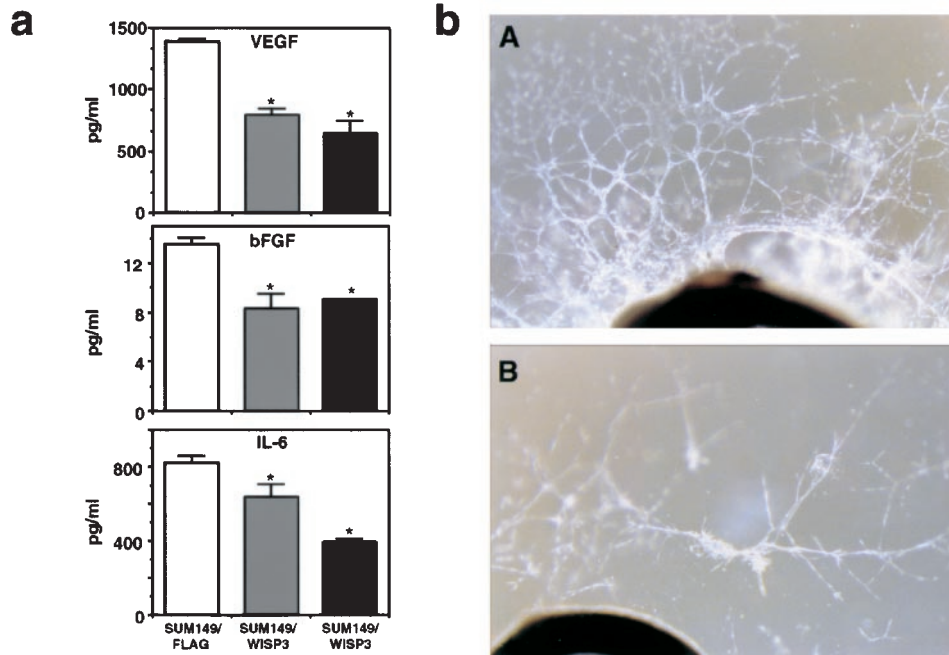


Figure 3 (a) Decrease in key angiogenic factors measured by ELISA, as a result of restoration of WISP3 expression in SUM149 cells. Results are expressed as mean \pm s.d. * $P < 0.05$. (b) Rat aortic ring assay showing marked decreased in new vessel formation from the pre-existing aortic ring bathed in conditioned media from SUM149/WISP3 (B), and SUM149/Flag controls (A). (100 \times)

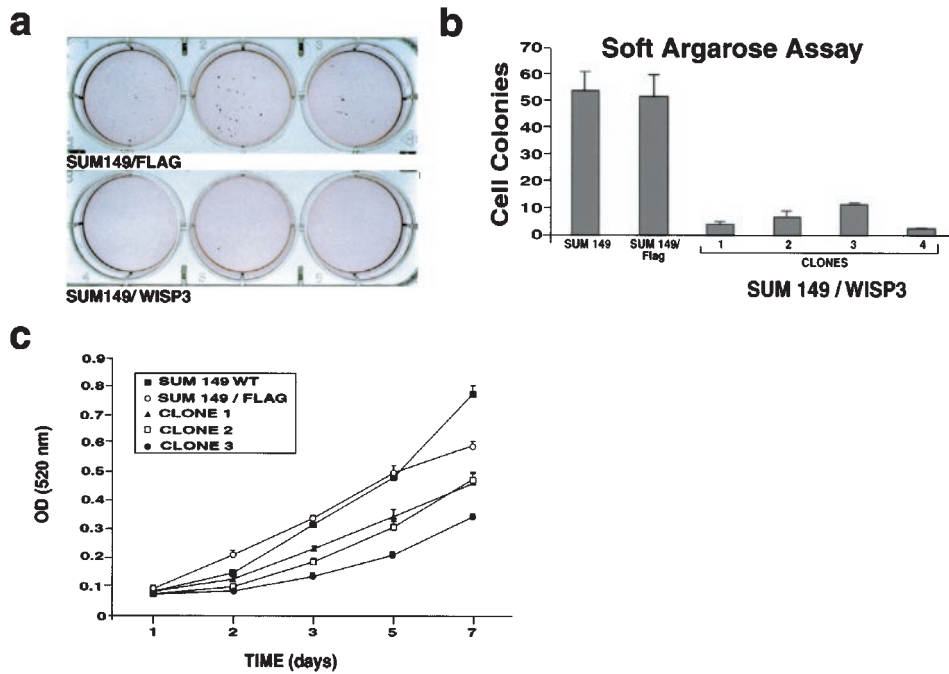


Figure 4 (a) and (b) Anchorage-independent growth in soft agar. Restoration of WISP3 in SUM149 cell line greatly decreased the number of the colonies formed. (c) Effect of stable WISP3 transfection on the proliferation of SUM149 cells studied with the MTT assay. Results are expressed as mean \pm s.d. of three independent experiments. Three thousand cells were assessed in each plate ($P < 0.05$)

proliferation rate of three different clones of SUM149 cells transfected with WISP3 decreased significantly when compared to controls ($P < 0.05$). The ability of the transfectants to invade and intravasate was studied

using the sea urchin extracellular membrane (SU-ECM) invasion assay. This assay provides a naturally serum-free, selectively permeable basement membrane that closely mimics the type of extracellular matrix that

cells encounter *in vivo*. Mean invasion percentages were calculated from three independent analyses of 50–100 random cells. We found that transfection with WISP3 cDNA completely abolished the ability of IBC cells to invade, compared to the control (the mean \pm s.d. for invasion of SUM149/flag cells was 14 ± 3 , when compared to 0 for both clones of SUM149/WISP3).

WISP3 expression inhibits cellular growth by inducing accumulation of p27^{kip1} and p21^{waf1} in cancer cells and induces apoptosis

Based on the morphologic changes induced by transfection with WISP3, we set out to investigate whether WISP3 caused alterations in the regulation of the cell cycle, that could in turn be contributing to the inhibition of cellular proliferation, anchorage-independent growth, and *in vivo* tumor growth. To elucidate the possible effect of WISP3 on the cell cycle regulators, the round and vacuolated cells (SUM149/WISP3) were assayed for the presence of several key cell cycle regulators by Western immunoblots. Interestingly, when compared to the control cells, the level of p27^{kip1} and p21^{waf1} were increased in the WISP3 transfectants when compared to SUM149/flag control cells ($P=0.0003$ and $P=0.003$ for p27^{kip1} expression for clones 1 and 2 respectively, and $P=0.001$ and $P=0.06$ for p21^{waf1} expression for clones 1 and 2 respectively, *t*-test, Figure 5). Concordantly, SUM149/WISP3 cells exhibited decreased levels of cyclin E and PCNA, a reliable marker for cellular proliferation, when compared to the SUM149/flag control cells ($P=0.02$ and $P=0.02$ for cyclin E expression for clones 1 and 2 respectively, and $P=0.0003$ and $P=0.003$ for PCNA expression for clones 1 and 2 respectively, *t*-test, Figure 5).

We noticed an increased percentage of apoptotic cells after stable transfection with WISP3 detected by the Annexin V assay by flow cytometry. SUM149/WISP3 transfectants had 30% apoptotic cells when compared to SUM149/Flag control cell line with only 13% apoptotic cells.

WISP3 inhibits in vivo tumor growth and improves survival of mice

Given that WISP3 affects cell cycle regulation, proliferation rates and anchorage independent growth, we investigated the effect of restoration of WISP3 expression on SUM149 xenograft tumor growth and survival of the host mice. Three groups of 10–11 mice were injected with two clones of SUM149/WISP3 stable transfectants and a control group (SUM149/Flag and SUM149 wild-type, five mice each). Mice with orthotopically implanted tumor cells were monitored weekly for tumor formation over an 8-week period. By the 8th and final week of the experiment, palpable tumors developed in 20 of the 21 mice that received injection of the SUM149/WISP3 clones and in nine out of 10 mice given injection of control clones (five injected with SUM149/Flag and five injected with

wild-type SUM149). The rate of tumor formation between WISP3 transfectants and controls differed (Table 1). Specifically, the clones transfected with WISP3 formed tumors at a slower rate than the controls (logistic regression analysis adjusted for longitudinal correlation, $P=0.05$). Moreover, when tumor volume was compared at each week (starting at week 2), it was significantly lower in the tumors formed by SUM149/WISP3 transfectants than in the tumors formed by the controls ($P=0.05$). When the slopes of the regression lines were compared, striking differences were found between the WISP3 transfectants and control cells ($P<0.001$, Figure 6a,b). At week 5, two tumors from each clone and from the control were excised. WISP3 mRNA expression was confirmed by quantitative RT-PCR. Levels of WISP3 expression were found to be similar to those of preinjection. Taken together, these results demonstrate that tumors formed by SUM149/WISP3 take longer to grow and are smaller than controls.

To address whether the tumors formed by the transfectants expressing WISP3 were pathologically different from the control, histopathologic study of the tumors was carried out. As shown in Figure 6c, SUM149/Flag tumors were highly anaplastic, had

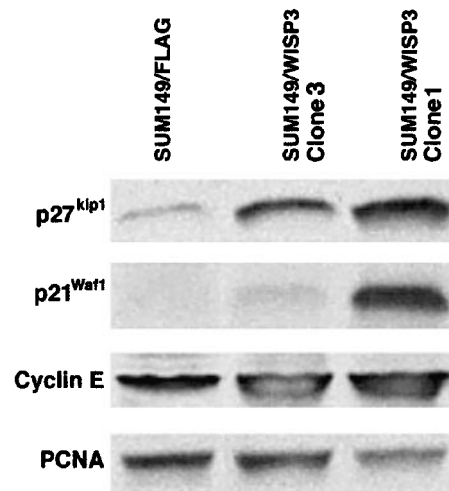


Figure 5 Western immunoblot of cell culture media of control (SUM149/FLAG), and two WISP3 expressing clones using antibodies for p27^{kip1}, p21^{waf1}/cip1, cyclin E, and PCNA

Table 1 Rate of tumor formation after orthotopic injection in the mammary fat pad of SUM149 wild-type, SUM149/Flag, and two stable clones of SUM149/WISP3 transfectants in female athymic nude mice. Tumors formed by the WISP transfectants took a longer time to develop than tumors formed by the control cells ($P=0.05$, logistic regression analysis)

	2 weeks n (%)	4 weeks n (%)	6 weeks n (%)	8 weeks n (%)
SUM149 wild-type	5/5 (100)	5/5 (100)	5/5 (100)	5/5 (100)
SUM149/Flag	4/5 (80)	4/5 (80)	4/5 (80)	4/5 (80)
SUM149/WISP3 Clone 1	9/11 (82)	10/11 (91)	10/11 (91)	10/11 (91)
SUM149/WISP3 Clone 3	3/10 (30)	5/10 (50)	9/10 (90)	10/10 (100)

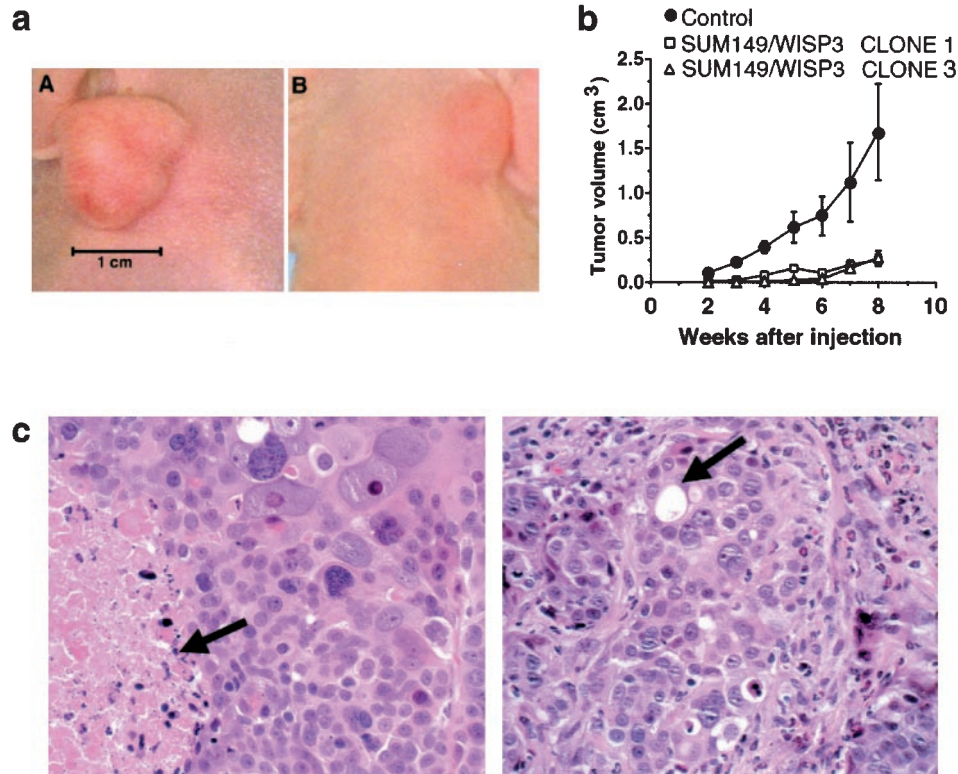


Figure 6 (a) SUM149 cells transfected with WISP3 (A) formed smaller tumors than SUM149/Flag controls. Pictures were taken 5 weeks after injection (B). (b) Effect on tumor volume of restoration of WISP3 in SUM149 cells. When the slopes of the curves were compared, a significant difference was found between the transfectants and controls ($P < 0.001$). Results are expressed as mean \pm s.e.m. Wild-type SUM149 were represented together with SUM149/FLAG because no statistically significant difference between the 2 groups was found. (c) Pathological features of the tumors. The tumors formed by SUM149/Flag controls are pleomorphic, with extensive necrosis (arrow) and mitoses. The tumors formed by the SUM149/WISP3 clones are better differentiated, the cells are smaller, there is less necrosis and mitoses. The arrow points to a glandular lumen. (Hematoxylin and eosin stain, light microscopy, $\times 400$)

strikingly atypical cells forming solid aggregates, with no glandular formation, a sign of poor differentiation, and extensive areas of necrosis. The cells exhibited high mitotic activity (mean 88 mitoses per 10 high power field ($400\times$)) and numerous abnormal mitoses. In contrast, the tumors derived from SUM149/WISP3 clones had less nuclear pleomorphism and slightly better differentiation evidenced by occasional gland formation. These tumors had less necrosis and the mitotic activity was greatly decreased (mean 11 mitoses per 10 high power fields).

Discussion

WISP3 is located in chromosome 6q21–22 and encodes for a 354 amino acid, 39292 Da protein with the modular architecture of the CCN family of proteins which includes connective tissue growth factor (CTGF), Cyr61, Nov, WISP1 and WISP2 (Babic *et al.*, 1998; Hashimoto *et al.*, 1998; Hurvitz *et al.*, 1999; Kireeva *et al.*, 1996; O'Brien and Lau, 1992; Pennica *et al.*, 1998; Perbal, 2001; Wong *et al.*, 1997; Xu *et al.*, 2000). The CCN proteins participate in fundamental biological processes such as cell proliferation, migra-

tion, wound healing, angiogenesis and tumorigenesis (Perbal, 2001). They have a range of biological properties that might be dependent upon the cellular context (Perbal, 2001).

In tumorigenesis, Cyr61 and WISP1 were reported to act as positive regulators of cell growth (Babic *et al.*, 1998; Hashimoto *et al.*, 1998; Kireeva *et al.*, 1996; O'Brien and Lau, 1992; Pennica *et al.*, 1998; Wong *et al.*, 1997; Xu *et al.*, 2000); Nov expression was found to correlate with the development of metastases in Ewing's sarcomas, prostate cancer, and renal cell carcinomas (Perbal, 2001), whereas it was found to act as a negative growth regulator of glioblastoma cell lines (Li *et al.*, 1996). Furthermore, in primary human colonic adenocarcinomas, the expression of WISP2 was significantly decreased compared to normal colon (Pennica *et al.*, 1998), and it was not detected in the epithelial tumor cells of mammary carcinoma obtained from Wnt-1 transgenic mice (Pennica *et al.*, 1998). Similarly, in our study we could not detect WISP3 mRNA expression in 80% of the IBC human tissues studied (van Golen *et al.*, 1999). The expression of ELM1/WISP1, which had been reported to suppress the metastatic potential of murine melanoma cells (Hashimoto *et al.*, 1998), was significantly increased in

most human colonic carcinomas (Pennica *et al.*, 1998; Xu *et al.*, 2000). These data provide compelling evidence that the CCN proteins may have opposing functions in carcinogenesis in different cell types and tissues.

There are only two previous publications in the literature on the biologic properties of WISP3 (Hurvitz *et al.*, 1999; Pennica *et al.*, 1998). In one of these studies, the WISP3 gene was significantly over-expressed in human colon carcinoma (Pennica *et al.*, 1998) whereas Hurvitz *et al.* (1999) found loss of function mutations in the WISP3 gene to be associated with progressive pseudorheumatoid dysplasia in humans (Hurvitz *et al.*, 1999). Patients with progressive pseudorheumatoid dysplasia due to WISP3 loss-of-function mutations have not been reported to have higher rates of cancer; however this has not been systematically sought in this cohort (Hurvitz *et al.*, 1999). Our data provide evidence that WISP3 has tumor suppressor function in the mammary gland.

Using a modified version of the differential display technique and *in situ* hybridization of human breast cancer tissues, we found that WISP3 is lost in 80% of IBC and in 21% of stage matched, non IBC tumors ($P=0.0013$, Fisher's exact test) (van Golen *et al.*, 1999). WISP3 loss was found in concert with RhoC-GTPase over-expression in 90% of archival IBC patient samples, but not in stage-matched non-IBC tumors (van Golen *et al.*, 1999). Our laboratory demonstrated that RhoC-GTPase over-expression produces a motile and invasive phenotype in human mammary epithelial cells, primarily through formation of actin stress fibers and focal adhesion points (van Golen *et al.*, 2000b). We hypothesized that loss of expression of WISP3 contributes to the development of the IBC phenotype by altering angiogenesis and tumor growth, therefore complementing the role of RhoC-GTPase over-expression.

One of the features that define the IBC phenotype as unique is its rapid progression, with fast growth and invasion, making it the most lethal form of locally advanced breast cancer (Jaiyesimi *et al.*, 1992; Lee, 1924; Merajver *et al.*, 1997; Swain *et al.*, 1987). IBC is characterized by a rapid onset of disease, typically arising within 6 months, and by the time of diagnosis, the majority of patients have locoregional and distant metastatic disease (Jaiyesimi *et al.*, 1992; Lee, 1924; Merajver *et al.*, 1997; Swain *et al.*, 1987). Transfection of the IBC cell line SUM149 with WISP3 cDNA inhibited some of these key phenotypic characteristics.

The proliferation rate of highly aggressive SUM149 cell line was decreased, and growth under anchorage independent conditions was greatly reduced in the stable WISP3 transfectants. In comparison with the control cells, the WISP3 transfectants produced 6–16-fold less colonies than the control cells. Similarly, the effect of transfection with WISP3 in cancer cell invasion was striking. Using the sea urchin invasion assay, a system that closely resembles the extracellular matrix that cells encounter *in vivo*, the WISP3

transfectants did not invade, when compared to controls. Furthermore, transfection with WISP3 cDNA greatly reduced tumor growth *in vivo*. Interestingly, transfection with WISP3 also resulted in a decrease in the rate of tumor uptake.

Another feature that makes IBC unique is its high angiogenic and angioinvasive potential. We proved that WISP3 suppressed pathologic neovascularization by reducing the levels of key pro-angiogenic factors, FGF2, VEGF, and IL-6.

Although the mechanism of action of the CCN proteins in general and of WISP3 in particular has not been elucidated, there are several candidates. The first of these could be by regulating nuclear cycling and/or apoptotic functions (Lopez-Bermejo *et al.*, 2000; Sprenger *et al.*, 1999). We observed a marked morphologic change in the SUM149 cell line after transfection with WISP3 cDNA. Histopathologic study of the tumors developed in nude mice revealed that those derived from the WISP3 transfectants had a significant reduction in the mitotic activity, as well as better differentiation and less cellular and nuclear pleomorphism. To better understand these morphologic changes, we studied the levels of key cell cycle regulators and apoptosis. The levels of the cell cycle inhibitors p27^{kip1} and p21^{waf1} were markedly increased by WISP3 expression, and cyclin E was concordantly decreased. Consistent with these cell-cycle specific gene expression changes, the percentage of apoptotic cells was also increased in the WISP3 transfectants. These data suggest that in the mammary gland, WISP3 expression may inhibit cancer cell growth through modulation of the cell-cycle regulation and apoptosis.

A second possible mode of tumor suppression activity for WISP3 is by regulating angiogenesis (Babic *et al.*, 1998; Perbal, 2001). As the tumor grows, it requires and promotes an increase in neovascularization. This activation of the angiogenic switch involves the up-regulation of angiogenic inducers and/or down-regulation of angiogenic inhibitors. Our results show that WISP3 expression induces a reduction in the level of key pro-angiogenic factors which results in a decrease in functional neovascularization.

A third mechanism of WISP3 tumor suppression could be by binding IGF-like ligands. WISP3 has the modular architecture of the CCN proteins and consists of four domains: an IGF-binding protein domain, a Von Willebrand factor domain, a thrombospondin 1 domain, and a C terminal domain (Babic *et al.*, 1998; Hashimoto *et al.*, 1998; Hurvitz *et al.*, 1999; Pennica *et al.*, 1998; Perbal, 2001). The N-terminal domain includes the first 12 cysteine residues and contains the highly conserved IGF binding consensus sequence (GCGCCXXC) which provides the proper folding of the protein to bind IGF (Byun *et al.*, 2001; Kim *et al.*, 1997; Oh *et al.*, 1996). Although this sequence is believed to be required for IGF-binding, the actual binding site may be slightly downstream of it (Imai *et al.*, 2000; Kalus *et al.*, 1998). The thrombospondin type 1 domain (TSP1) is presumably involved in inhibition

of angiogenesis (Perbal, 2001). The carboxy-terminal domain (CT) is present in most CCN proteins described to date and forms a cysteine knot. The protein is folded into two highly twisted antiparallel pairs of beta-strands and contains three disulfide bonds that may participate in dimerization and receptor binding. The CT domain does not appear to be as critical in IGF binding as the N-terminal region that contains the IGF-binding protein motif (Imai *et al.*, 2000; Kalus *et al.*, 1998). Although WISP3 may function in tumorigenesis through modulation of IGF binding, this is less likely since IGF-binding activity could not be demonstrated for other members of the CCN family (Perbal, 2001). We are currently investigating this possibility in mammary tissue.

In summary, we have proven that restoring expression of WISP3 into an aggressive IBC cell line, SUM149, inhibited cellular proliferation, drastically decreased angiogenesis, inhibited invasion, and decreased anchorage-independent growth, all hallmarks of malignant transformation. Restoration of WISP3 expression resulted in a morphologic alteration and induced tumor cell apoptosis with concordant molecular changes in cell cycle specific gene, p27^{kip1} and p21^{waf1}. Finally, when SUM149 cells transfected with WISP3 were injected into female athymic nude mice, the rate of tumor formation and the tumor volume were markedly decreased when compared to controls. These studies demonstrate for the first time that WISP3 has strong tumor suppressor function in the mammary gland. Given the seemingly specific role that WISP3 plays in the development of IBC, our work may lead to the development of novel therapies that replace or mimic WISP3 function to treat this particularly challenging form of breast cancer.

Materials and methods

Cell culture

The derivation of SUM149 cell line has been described previously by Ethier *et al.* (1993). This cell line was developed from a human primary inflammatory breast cancer and has lost WISP3 expression (Figure 1, lane F). Cells were cultured in Ham's F-12 medium supplemented with 5% FBS, hydrocortisone (1 μ g/ml), insulin (5 μ g/ml), fungizone (2.5 μ g/ml), Gentamycin (5 μ g/ml) and each of Penicillin/streptomycin (100 μ g/ml) at 37°C under 10% CO₂.

Construction of expression vector and stable transfection

Total RNAs were isolated from human mammary epithelial cells (HME) using a Trizol kit (Life Technologies, Inc., Gaithersburg, MD, USA). First-strand cDNA synthesis was performed using 1 μ g of total RNA with AMV reverse transcriptase (Promega, Madison, WI, USA) and oligo (dT) as a primer. Two μ l of the reaction mixture were used for PCR amplification. Human WISP3 cDNA was amplified by PCR using the following forward and reverse primers: 5'-ATGCAGGGGCTCCTCTTCTGC-3' and 5'-ACTTTTCCC-CATTTGCTTG-3', under the following conditions: denaturing for 1 min at 94°C, annealing for 1 min at 58°C, and

elongation for 2 min at 72°C for 35 cycles. The PCR product was cloned into pGEM-T Easy vector (Promega, Madison, WI, USA). The 1.1 kb full-length cDNA encoding WISP3 was excised by *EcoRI* and subcloned into the *EcoRI* site of pFLAG-CV4 vector (Sigma, Saint Louis, MO, USA). The insert was confirmed by DNA sequencing. The plasmids were purified. Subsequently, the SUM149 cells were transfected with pFLAG-WISP3 and pFlag control vector by FuGene TM 6 transfection reagent (Roch-Boehringer Mannheim, Mannheim, Germany), and selected in the medium containing 150 μ g/ml G418. The cells surviving during selection were expanded and maintained in the selected medium.

Western immunoblots

Western immunoblots were performed using the following primary antibodies: WISP3 polyclonal antibody (gift from Dr Matthew Warman), p27^{kip1}, p21^{waf1}, PCNA (Zymed, San Francisco, CA, USA) cyclin E (SC-247, Santa Cruz, CA, USA), cyclin D1 (SC-246, Santa Cruz, CA, USA), and actin (Sigma Chemical Co.). Cells were lysed in RIPA buffer (1 \times PBS, 1% Nonidet P-40, 0.5% sodium deoxycholate, 0.1% SDS, 0.1 mg/ml PMSF, 1 mM sodium orthovanadate, and 0.3 mg/ml aprotinin; Sigma Chemical Co.). Whole cell lysates (50 μ g) were boiled in Laemmli buffer for 5 min, separated by 10% SDS-PAGE and transferred to PVDF membrane. Non-specific binding was blocked by incubation with 1.5% BSA in Tris-buffered saline with 0.5% Tween-20 (Sigma Chemical Co.). Antibody-antigen complexes were detected with an enhanced chemiluminescence kit (ECL, Amersham, Arlington Height, IL, USA) following the manufacturer's instructions.

Anchorage-independent growth

Cells from four SUM149/WISP3 stable clones and controls were seeded at a density of 1×10^3 per 35-mm plated in 0.3% agar and Ham's F-12 supplemented with 10% FBS, and plated on a base of 0.6% agar, Ham's F-12 and 10% FBS. Each assay was performed in triplicate. Plates were maintained at 37°C under 10% CO₂ for 3 weeks. Colonies greater than or equal to 100 μ m in diameter were counted.

Annexin V-FITC binding assay

This assay was performed using the Apo Alert Annexin V kit (Clontech, CA, USA). Three clones of stably transfected SUM149/WISP3 and SUM149/Flag control cells (1×10^6) were trypsinized, washed and incubated in binding buffer (1 \times) containing 1 μ g/ml of Annexin V-FITC conjugate (Clontech, CA, USA) for 10 min in the dark. Cells were next stained with propidium iodide (20 μ g/ml) and analysed by flow cytometry (Martin *et al.*, 1995).

Monolayer growth rate

Monolayer culture growth rate was determined by qualitative measurement of the conversion of MTT (3-(4,5-Dimethylthiazol-2-yl)-2,5-diphenyltetrazolium bromide, Sigma Chemical Co.) to a water insoluble formazan by viable cells. Three thousand cells in 200 μ l of culture medium were plated in 96-well plates and grown under normal conditions. Cultures were assayed at 0, 1, 3, 4 and 5 days by the addition of MTT and incubation for 1 h at 37°C. The MTT containing medium was aspirated and 100 μ l DMSO (Sigma Chemical Co.) was added to lyse the cells and solubilize the formazan. Absorbance values of the lysates were determined on a Dynatech MR 5000 microplate reader at 540 nm.

Invasion and intravasation

To study invasion, the sea urchin extracellular membrane (SU-ECM) invasion assay was used (Livant *et al.*, 1995). Cells were layered onto sea urchin embryo extracellular basement membrane and allowed to invade for 4 h. The cells on the SU-ECM were fixed using paraformaldehyde and visualized under a microscope. Mean invasion percentages were calculated from two independent analyses of 50–100 randomly chosen cells in contact with the surfaces of the basement membranes.

Angiogenesis and angiogenic factor analysis

To study whether WISP3 modulated the angiogenic activity of IBC, the levels of key pro-angiogenic factors known to be secreted by IBC (VEGF, FGF2, IL-6, and IL-8) were measured in the cell supernatants by ELISA (van Golen *et al.*, 2000a). A functional analysis of angiogenesis of the conditioned media was performed. We used the rat aortic assay in which we assessed the amount of new blood vessel growth elicited by the conditioned medium of the WISP3 transfected cells (Nissanov *et al.*, 1995). Approximately 1-mm thick rings were cut from the aorta of a freshly sacrificed rat and embedded into Matrigel in the center of a 35-mm dish. Vessel outgrowth from the aorta into the Matrigel was visually quantified by counting the branching points in six randomly chosen fields for the SUM149/WISP3 and control SUM149/flag cells under a light microscope and compared at 7 and 10 days after planting. Statistical analysis was performed using the *t*-test.

In vivo tumor formation

Groups of 5–11, 10-week old, nude, athymic female mice were orthotopically injected into the mammary fat pad with

2×10^6 cells. Each group was injected with either a control (SUM149/Flag, or wild-type SUM149) clone, or one of two WISP3-expressing clones. The clones were selected according to their anchorage-independent growth characteristics. Mice were then monitored weekly for tumor formation for 8 weeks and for signs of wasting and cachexia as surrogates of survival for 18 weeks. If tumors were present, tumor volume was calculated using the formula $(l \times w^2)/2$ (where l = length and w = width of tumor). Rates of tumor formation were analysed by the Kruskal-Wallis method; and tumor volumes were assessed between the groups by the Mann-Whitney *U*-test. After the mice developed signs and symptoms of cachexia, they were sacrificed and their tumors were removed. A portion of each tumor (1/3) was digested with 0.1% collagenase (Type I) and 50 μ g/ml DNase (Worthington Biochemical Corp. Freehold, NJ, USA), and RNA was collected for RT-PCR analysis. The remainder of the tumor tissues were used for histopathological study. After removal of the tumors, part of the tissues were fixed in 10% buffered formalin and processed for histopathological evaluation by paraffin-embedding and hematoxylin and eosin staining. Histological features studied included degree of anaplasia, mitotic activity, presence and amount of necrosis, and degree of differentiation (e.g. glandular formation).

Acknowledgments

We thank Wendy Kutz and Matthew Warman from Case Western Reserve University for providing anti-WISP3 polyclonal antibody. We thank Satoru Hayasaka for statistical support, and Elizabeth Horn and Robin Kunkel for artwork. Work supported in part by DOD grant DAMD17-00-1-0636 (CG Kleer), and NIH grants RO1CA77612 (SD Merajver), P30CA46592, M01-RR00042 and DAMD17-00-0345 (SD Merajver).

References

- Babic AM, Kireeva ML, Kolesnikova TV and Lau LF. (1998). *Proc. Natl. Acad. Sci. USA*, **95**, 6355–6360.
- Byun D, Mohan S, Baylink DJ and Qin X. (2001). *J. Endocrinol.*, **169**, 135–143.
- Ethier SP, Mahacek ML, Gullick WJ, Frank TS and Weber BL. (1993). *Cancer Res.*, **53**, 627–635.
- Hashimoto Y, Shindo-Okada N, Tani M, Nagamachi Y, Takeuchi K, Shiroishi T, Toma H and Yokota J. (1998). *J. Exp. Med.*, **187**, 289–296.
- Hurvitz JR, Suwairi WM, Van Hul W, El-Shanti H, Superti-Furga A, Roudier J, Holderbaum D, Pauli RM, Herd JK, Van Hul EV, Rezai-Delui H, Legius E, Le Merrer M, Al-Alami J, Bahabri SA and Warman ML. (1999). *Nat. Genet.*, **23**, 94–98.
- Imai Y, Morales A, Andag U, Clarke JB, Busby Jr WH and Clemmons DR. (2000). *J. Biol. Chem.*, **275**, 18188–18194.
- Jaiyesimi IA, Buzdar AU and Hortobagyi G. (1992). *J. Clin. Oncol.*, **10**, 1014–1024.
- Kalus W, Zweckstetter M, Renner C, Sanchez Y, Georgescu J, Grol M, Demuth D, Schumacher R, Dony C, Lang K and Holak TA. (1998). *EMBO J.*, **17**, 6558–6572.
- Kim HS, Nagalla SR, Oh Y, Wilson E, Roberts Jr CT and Rosenfeld RG. (1997). *Proc. Natl. Acad. Sci. USA*, **94**, 12981–2986.
- Kireeva ML, Mo FE, Yang GP and Lau LF. (1996). *Mol. Cell Biol.*, **16**, 1326–1334.
- Lee BJA and ND. (1924). *Surg. Gynecol. Obstet.*, **39**, 580–595.
- Li W, Martinierie C and Zumkeller W. (1996). *Mol. Pathol.*, **49**, 91–97.
- Livant DL, Linn S, Markwart and Shuster J. (1995). *Cancer Res.*, **55**, 5085–5093.
- Lopez-Bermejo A, Buckway CK, Devi GR, Hwa V, Plymate SR, Oh Y and Rosenfeld RG. (2000). *Endocrinology*, **141**, 4072–4080.
- Martin SJ, Reutelingersperger CP, McGahon AJ, Rader JA, van Schie RC, LaFace DM and Green DR. (1995). *J. Exp. Med.*, **182**, 1545–1556.
- Merajver SD, Weber BL, Cody R, Zhang D, Strawderman M, Calzone KA, LeClaire V, Levin A, Irani J, Halvie M, August D, Wicha M, Lichter A and Pierce LJ. (1997). *J. Clin. Oncol.*, **15**, 2873–2881.
- Nissanov J, Tuman RW, Gruver LM and Fortunato JM. (1995). *Lab. Invest.*, **73**, 734–739.
- O'Brien TP and Lau LF. (1992). *Cell Growth Differ.*, **3**, 645–654.
- Oh Y, Nagalla SR, Yamanaka Y, Kim HS, Wilson E and Rosenfeld RG. (1996). *J. Biol. Chem.*, **271**, 30322–30325.
- Pennica D, Swanson TA, Welsh JW, Roy MA, Lawrence DA, Lee J, Brush J, Taneyhill LA, Deuel B, Lew M, Watanabe C, Cohen RL, Melhem MF, Finley GG, Quirke P, Goddard AD, Hillan KJ, Gurney AL, Botstein D and Levine AJ. (1998). *Proc. Natl. Acad. Sci. USA*, **95**, 14717–14722.
- Perbal B. (2001). *Mol. Pathol.*, **54**, 57–79.

- Romanov SR, Kozakiewicz BK, Holst CR, Stampfer MR, Haupt LM and Tlsty TD. (2001). *Nature*, **409**, 633–637.
- Sprenger CC, Damon SE, Hwa V, Rosenfeld RG and Plymate SR. (1999). *Cancer Res.*, **59**, 2370–2375.
- Swain SM, Sorace RA, Bagley CS, Danforth Jr DN, Bader J, Wesley MN, Steinberg SM and Lippman ME. (1987). *Cancer Res.*, **47**, 3889–3894.
- Tsugu A, Sakai K, Dirks PB, Jung S, Weksberg R, Fei YL, Mondal S, Ivanchuk S, Ackerley C, Hamel PA and Rutka JT. (2000). *Am. J. Pathol.*, **157**, 919–932.
- van Golen KL, Davies S, Wu ZF, Wang Y, Bucana CD, Root H, Chandrasekharappa S, Strawderman M, Ethier SP and Merajver SD. (1999). *Clin. Cancer Res.*, **5**, 2511–2519.
- van Golen KL, Wu ZF, Qiao XT, Bao L and Merajver SD. (2000a). *Neoplasia*, **2**, 418–425.
- van Golen KL, Wu ZF, Qiao XT, Bao LW and Merajver SD. (2000b). *Cancer Res.*, **60**, 5832–5838.
- Wong M, Kireeva ML, Kolesnikova TV and Lau LF. (1997). *Dev. Biol.*, **192**, 492–508.
- Xu L, Corcoran RB, Welsh JW, Pennica D and Levine AJ. (2000). *Genes Dev.*, **14**, 585–595.

Research article

WISP3 and RhoC guanosine triphosphatase cooperate in the development of inflammatory breast cancer

Celina G Kleer^{1,3}, Yanhong Zhang^{1,3}, Quintin Pan^{2,3}, Gary Gallagher^{1,3}, Mei Wu^{1,2}, Zhi-Fen Wu^{2,3} and Sofia D Merajver^{2,3}

¹Department of Pathology, University of Michigan, Ann Arbor, MI, USA

²Department of Internal Medicine, University of Michigan, Ann Arbor, MI, USA

³Comprehensive Cancer Center, University of Michigan, Ann Arbor, MI, USA

Correspondence: Sofia D Merajver (e-mail: smerajve@umich.edu)

Received: 17 Jun 2003 Revisions requested: 28 Aug 2003 Revisions received: 4 Dec 2003 Accepted: 5 Dec 2003 Published: 19 Dec 2003

Breast Cancer Res 2004, **6**:R110-R115 (DOI 10.1186/bcr755)

© 2004 Kleer et al., licensee BioMed Central Ltd (Print ISSN 1465-5411; Online ISSN 1465-542X). This is an Open Access article: verbatim copying and redistribution of this article are permitted in all media for any purpose, provided this notice is preserved along with the article's original URL.

Abstract

Background: Inflammatory breast cancer (IBC) is the most lethal form of locally advanced breast cancer. We found concordant and consistent alterations of two genes in 90% of IBC tumors when compared with stage-matched non-IBC tumors: overexpression of RhoC guanosine triphosphatase and loss of WNT-1 induced secreted protein 3 (WISP3). Further work revealed that RhoC is a transforming oncogene for human mammary epithelial (HME) cells. Despite the aggressiveness of the RhoC-driven phenotype, it does not quantitatively reach that of the true IBC tumors. We have demonstrated that WISP3 has tumor growth and angiogenesis inhibitory functions in IBC. We proposed that RhoC and WISP3 cooperate in the development of IBC.

Methods: Using an antisense approach, we blocked WISP3 expression in HME cells. Cellular proliferation and growth were determined using the 3-[4,5-dimethylthiazol-2-yl]-2,5-diphenyl-

tetrazolium bromide (MTT) assay and anchorage-independent growth in a soft agar assay. Vascular endothelial growth factor (VEGF) was measured in conditioned medium by enzyme-linked immunosorbent assay.

Results: Antisense inhibition of WISP3 in HME cells increased RhoC mRNA levels and resulted in an increase in cellular proliferation, anchorage-independent growth and VEGF levels in the conditioned medium. Conversely, restoration of WISP3 expression in the highly malignant IBC cell line SUM149 was able to decrease the expression of RhoC protein.

Conclusion: WISP3 modulates RhoC expression in HME cells and in the IBC cell line SUM149. This provides further evidence that these two genes act in concert to give rise to the highly aggressive IBC phenotype. We propose a model of this interaction as a starting point for further investigations.

Keywords: CCN proteins, motility, oncogene, tumor suppressor gene, vascular endothelial growth factor, WNT-pathway

Introduction

Inflammatory breast cancer (IBC) is the most lethal form of locally advanced breast cancer and accounts for approximately 6% of new breast cancer cases annually in the United States [1,2]. IBC has distinct clinical and pathological features. Patients present with erythema, skin nodules, dimpling of the skin (termed 'peau d'orange'), all features that develop rapidly, typically progressing within 6 months [1-4]. One salient feature of IBC that is observed in tissue

sections is that cancer cells form emboli that spread through the dermal lymphatics. The dermatotropism of IBC is believed to be responsible for the clinical signs and symptoms and probably enables effective dissemination to distant sites [2]. These observations lead us to conclude that IBC is highly invasive and that it is capable of metastases from its inception. Indeed, at the time of diagnosis, most patients have locoregional and/or distant metastatic disease [3,4]. In spite of new advances in breast cancer

FBS = fetal bovine serum; GTPase = guanosine triphosphatase; HME = human mammary epithelial; IBC = inflammatory breast cancer; MTT = 3-[4,5-dimethylthiazol-2-yl]-2,5-diphenyltetrazolium bromide; PCR = polymerase chain reaction; RT-PCR = reverse transcriptase PCR; VEGF = vascular endothelial growth factor; WISP3 = WNT-1 induced secreted protein 3.

therapy including multimodality approaches, the 5-year disease-free survival rate is less than 45% [3,4].

Until recently, no biological markers defined the IBC phenotype. We proposed that a limited number of genetic alterations, occurring in rapid succession or concordantly, are responsible for the rapidly progressive and distinct clinical and pathological features of IBC. Using a modified version of the differential display technique and *in situ* hybridization of human tumors, we identified two genes that are consistently and concordantly altered in human IBC when compared with stage-matched non-IBC tumors: loss of WISP3 and overexpression of RhoC guanosine triphosphatase (GTPase) [5].

WNT-1 induced secreted protein 3 (WISP3) is a member of the CCN family of proteins, which have important biological functions in normal physiology as well as in carcinogenesis [6–8]. We found that WISP3 has growth and angiogenesis inhibitory functions in IBC *in vitro* and *in vivo* [9]. RhoC GTPase is a member of the Ras superfamily of small GTPases. Activation of Rho proteins leads to assembly of the actin–myosin contractile filaments into focal adhesion complexes that bring about cell polarity and facilitate motility [10–12]. Our laboratory has characterized RhoC as a transforming oncogene for human mammary epithelial (HME) cells; its overexpression results in a highly motile and invasive phenotype that recapitulates the IBC phenotype. Predicated on the high rate of concordance of RhoC and WISP3 changes in IBC, we propose that these two genes cooperate to determine this highly metastatic, unique breast cancer phenotype.

Materials and methods

Cell culture

The derivation of the SUM149 cell line has been described previously by Ethier et al [13]. This cell line was developed from a human primary IBC and has lost WISP3 expression [9]. HME cells were immortalized with human papilloma virus E6/E7 and were characterized as being keratin 19 positive, ensuring that they are from the same differentiation lineage as the SUM149 IBC tumor cell line [14,15]. MCF10A cells are spontaneously immortalized human mammary epithelial cells. Cells were cultured in Ham's F-12 medium supplemented with 5% fetal bovine serum (FBS), hydrocortisone (1 µg/ml), insulin (5 µg/ml), fungizone (2.5 µg/ml), gentamycin (5 µg/ml), penicillin (100 U/ml) and streptomycin (10 µg/ml) at 37°C under 10% CO₂.

Construction of expression vectors and stable transfections

Total RNAs were isolated from HME cells with a Trizol kit (Life Technologies, Inc, Gaithersburg, MD). First-strand cDNA synthesis was performed by using 1 µg of total RNA with AMV reverse transcriptase (Promega, Madison,

WI) and oligo(dT) as a primer. A 2 µl portion of the reaction mixture was used for amplification by polymerase chain reaction (PCR). Human WISP3 cDNA was amplified by PCR with the forward and reverse primers 5'-ACGAATTCAATGAACAAGCGGCG-3' and 3'-GCGAATTCTTTACAGAATCTTG-5', respectively, under the following conditions: denaturing for 1 min at 94°C, annealing for 1 min at 58°C, and elongation for 1 min at 72°C, for 35 cycles. PCR products were cloned into pGEM-T Easy vector (Promega). The 1.1 kb full-length cDNA encoding WISP3 was excised by *EcoRI* and subcloned into the *EcoRI* site of pFlag-CMV4 vector (Sigma, St Louis, MO). The insert was confirmed by DNA sequencing. The plasmids were purified. Subsequently, the SUM149 cells were transfected with pFlag-WISP3 sense (SUM149/WISP3), and HME cells were transfected with pFlag-WISP3 anti-sense (HME/AS WISP3). MCF10A cells were stably transfected with full-length RhoC cDNA (MCF10A/RhoC). pFlag control vectors were used as controls (FuGene TM 6 transfection reagent; Roch–Boehringer-Mannheim, Germany). Transfectants were selected in the medium containing 150 µg/ml G418. The cells surviving during selection were expanded and maintained in the selected medium.

Reverse transcriptase PCR (RT-PCR) analysis

Total RNA (1 µg) from HME/AS WISP3 clones and empty vector controls were reverse-transcribed with Superscript reverse transcriptase (Invitrogen) using oligo(dT) and random hexanucleotide primer for first-strand cDNA synthesis. PCRs were performed directly on 1 µl of first-strand cDNA using 500 nmol of each of the following gene-specific primers: WISP3, 5'-ATGCAGGGGCTCCTCTTCTGC-3' (forward primer) and 5'-ACTTTTCCCCATTGCTTG-3' (reverse primer); RhoC, 5'-ATGGCTGCAATCCGAAAAG-3' (forward primer) and 5'-GATCTCAGAGAATGGGACAGC-3' (reverse primer); GAPDH, 5'-CGGAGTCAACGGATTG-GTCGTAT-3' (forward primer) and 5'-AGCCTTCTCCATG-GTGGTGAAGAC-3' (reverse primer). The 100 µl reaction volume consisted of 50 mM KCl, 10 mM Tris-HCl pH 8.3, 1.5 mM MgCl₂, and deoxynucleotide triphosphates (each at 200 µM). PCR was performed for initial denaturation at 94°C for 5 min, followed by 35 cycles of denaturation (94°C, 1 min), annealing (55°C, 1 min), and extension (72°C, 1 min) with 5 units of *Taq* polymerase (Invitrogen). This was followed by a final extension step at 72°C for 10 min. The products were analyzed on 1% agarose gels stained with ethidium bromide and detected with ultraviolet illumination.

Western immunoblots

Western immunoblots were performed with polyclonal anti-RhoC and anti-WISP3 antibodies. Cultured cells were washed in ice-cold phosphate-buffered saline, lysed in lysis buffer (10% glycerol, 50 mM Tris-HCl pH 7.4, 100 mM NaCl, 1% Nonidet P40, 2 mM MgCl₂, 1 µg/ml leupeptin, 1 µg/ml aprotinin, 1 mM phenylmethylsulphonyl

fluoride) on ice for 5 min, and then centrifuged for 5 min at 4°C. Cleared lysates (each containing 50 µg of protein) were subjected to SDS–polyacrylamide-gel electrophoresis and transferred to poly(vinylidene difluoride) membrane. Western blots were performed as described previously, with anti-RhoC rabbit polyclonal antibody and anti-β-actin goat antibody (Sigma) at dilutions of 1 : 1500 and 1 : 2000, respectively [16].

Anchorage-independent growth

For studies of anchorage-independent growth we performed soft agar assays on stable clones of HME/AS WISP3, HME/Flag, and SUM149 cells. Each well of a six-well plate was first layered with 0.6% agar diluted with 10% FBS-supplemented Ham's F-12 medium complete with growth factors. The cell layer was then prepared by diluting agarose to concentrations of 0.3% and 0.6% with 10³ cells in 2.5% FBS-supplemented Ham's F-12/1.5 ml/well. Plates were maintained at 37°C under 10% CO₂ for 3 weeks. Colonies 100 µm or more in diameter were counted under the microscope with a grid.

Monolayer growth rate

Monolayer culture growth rate was determined by qualitative measurement of the conversion of 3-(4,5-dimethylthiazol-2-yl)-2,5-diphenyltetrazolium bromide (MTT; Sigma) to a water-insoluble formazan by viable cells. In all, 3000 cells obtained for HME/AS WISP3 clones, HME/Flag, and HME wild-type cells, suspended in 200 µl of culture medium, were plated in 96-well plates and grown under normal conditions. Cultures were assayed at 0, 2, 4, 6, and 8 days by the addition of MTT and incubation for 1 hour at 37°C. The MTT-containing medium was aspirated and 100 µl of dimethyl sulphoxide (Sigma) was added to lyse the cells and solubilize the formazan. Optical densities of the lysates were determined on a Dynatech MR 5000 microplate reader at 595 nm.

Analysis of vascular endothelial growth factor

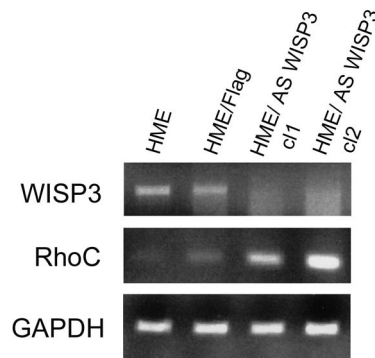
Conditioned medium was generated by incubating HME/AS WISP3 cells, HME/Flag cells, and SUM149 cells in serum-free medium. After 3 days the medium was collected, cleared of cell debris by centrifugation, concentrated approximately 10-fold through a Centriplus YM-10 column (Millipore, Bedford, MA). The levels of vascular endothelial growth factor (VEGF), which is a factor known to be secreted by IBC, were measured in the cell culture supernatants by enzyme-linked immunosorbent assay, as described previously [9,17].

Results

Inhibition of WISP3 increases RhoC mRNA levels in immortalized HME cells and induces proliferation, anchorage-independent growth, and VEGF production

To study the effects of inhibition of WISP3 expression on the phenotype of HME cells, we established clones of

Figure 1



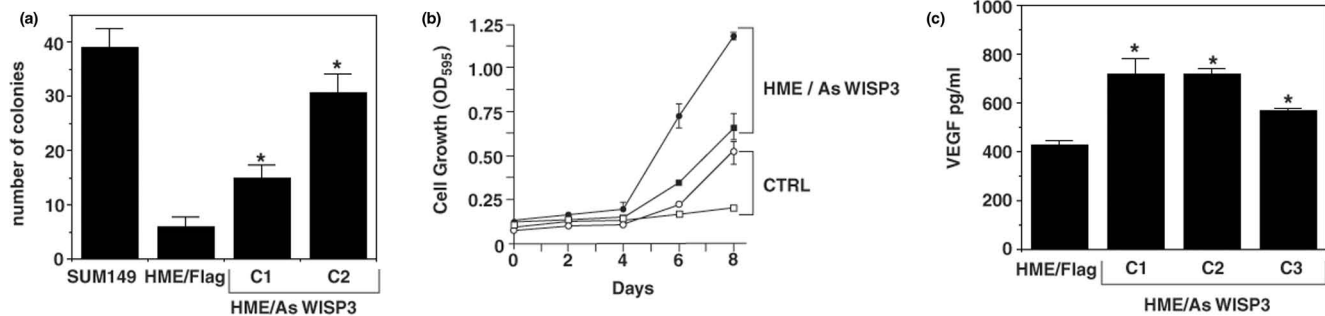
Inhibition of WISP3 in human mammary epithelial (HME) cells results in an increase in RhoC transcript levels. Reverse transcriptase polymerase chain reaction was conducted on vector and HME cells that have inhibition of WISP3 expression using full-length WISP3 antisense mRNA. HME/AS WISP3 cells showed increased levels of RhoC transcript in comparison with controls.

HME cells stably transfected with antisense WISP3 constructs (HME/AS WISP3). Effective inhibition of WISP3 expression was confirmed by RT–PCR (Fig. 1). Inhibition of WISP3 expression in HME cells resulted in increased expression of RhoC transcript in comparison with HME cells transfected with the control empty vector (Fig. 1). After 14 days of growth in soft agar, inhibition of WISP3 expression in HME cells resulted in a significant increase in the number of colonies formed in comparison with the empty vector control (*t*-test, $P < 0.05$ for both clones; Fig. 2a). Inhibition of WISP3 expression resulted in an increase in cellular proliferation (*t*-test, $P < 0.05$; Fig. 2b).

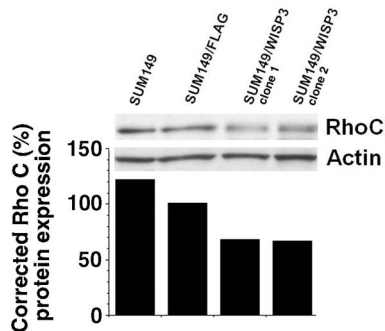
Previously, we had shown that restoration of WISP3 expression in an IBC cell line decreases the production of VEGF, a major pro-angiogenic factor secreted by IBC [9]. To determine the effect of WISP3 inhibition on the secretion of VEGF, we measured the concentration of VEGF in the conditioned medium of the stably transfected HME/AS WISP3 cells. Figure 2c shows that inhibition of WISP3 expression resulted in increased levels of VEGF in the conditioned medium (*t*-test, $P < 0.05$ for all clones).

Restoration of WISP3 expression in SUM149 cells decreases RhoC expression

Because decreased expression of WISP3 in HME cells induced a significant increase in RhoC expression and some features of RhoC induced functional changes including anchorage-independent growth and production of VEGF, we sought to determine whether restoration of WISP3 expression in the SUM149 IBC cell line, which has lost WISP3 expression in the wild type, has an effect in RhoC expression. To test this, we stably transfected WISP3 in SUM149 cells and measured RhoC expression

Figure 2

Inhibition of WISP3 induces anchorage-independent growth, proliferation and secretion of vascular endothelial growth factor (VEGF) in human mammary epithelial (HME) cells. **(a)** Inhibition of WISP3 expression in HME cells. HME cells greatly increased the number of colonies formed in soft agar in comparison with empty vector control (HME/Flag; *t*-test, $P < 0.05$ for both clones). **(b)** Effect of inhibition of WISP3 expression on the proliferation of HME cells was studied with the 3-(4,5-dimethylthiazol-2-yl)-2,5-diphenyltetrazolium bromide (MTT) assay. The stable HME/AS WISP3 cells have a significant increase in the proliferation rate in comparison with the empty vector control. Results are expressed as means \pm SEM of three independent experiments. In all, 3000 cells were assessed in each plate (*t*-test, $P < 0.05$). **(c)** Increase in VEGF measured by enzyme-linked immunosorbent assay, as a result of inhibition of WISP3 expression in HME cells. Results are expressed as means \pm SEM; *t*-test, $P < 0.05$ for all clones.

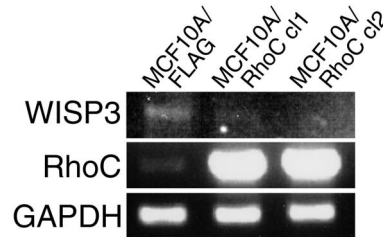
Figure 3

Restoration of WISP3 expression in SUM149 inflammatory breast cancer cells decreases RhoC protein expression. Western immunoblot of cell culture of SUM 149 cells, empty vector control (SUM149/Flag), and two WISP3-expressing clones with antibodies against RhoC and actin. Gels were scanned and pixel intensity values were obtained. Values for RhoC were corrected for loading by dividing the RhoC pixel intensity by the actin pixel intensity.

by Western blotting. Restoration of WISP3 expression in SUM149 cells resulted in a decrease in RhoC protein expression in comparison with the empty vector control (Fig. 3). To investigate whether the relationship between WISP3 and RhoC expression is reciprocal, we developed MCF10A cells stably transfected with RhoC. These cells showed a 2.5-fold decrease in WISP3 mRNA expression (Fig. 4).

Discussion

Our previous work showed that the overexpression of RhoC GTPase and the loss of WISP3 expression are alterations that occur concordantly, more often in IBC than

Figure 4

RhoC overexpression in MCF10A cells results in a decrease in WISP3 mRNA level. Reverse transcriptase polymerase chain reaction was conducted on vector and MCF10A cells stably overexpressing RhoC. RhoC-overexpressing cells had decreased levels of WISP3 mRNA.

in slow-growing locally advanced breast cancers. WISP3 loss was found in concert with RhoC GTPase overexpression in 90% of archival patient samples of IBC, but rarely in stage-matched non-IBC tumors. Our laboratory further demonstrated that RhoC GTPase is a transforming oncogene for HME cells and that WISP3 has tumor inhibitory functions in IBC. However, neither alteration occurring in isolation seems to be sufficient to develop the full-blown, highly malignant IBC phenotype. Here we postulate that dysregulation of WISP3 might upregulate RhoC GTPase and thus enhance the aggressiveness of the phenotype that results when these two alterations are present.

We have shown that overexpression of RhoC GTPase in immortalized HME cells produced a striking tumorigenic effect that, for the most part, recapitulates the phenotype of the SUM149 IBC cell line. HME cells stably transfected with RhoC exhibited greatly increased growth under anchorage-independent conditions [15]. HME cells over-

expressing RhoC produced up to 100-fold more colonies than the controls, about 60% of the level of colony formation of the SUM149 IBC cell line. RhoC overexpression induced motility and invasion in HME cells, and markedly induced the production of angiogenic mediators including VEGF [17]. The HME/RhoC transfectants formed tumors when injected into the mammary fat pad of athymic nude mice [15].

Importantly, restoration of WISP3 in SUM149 cells ameliorated these features of the malignant phenotype. The SUM149/WISP3⁺ cells exhibited decreased growth *in vitro* and *in vivo* in comparison with SUM149 cells transfected with the empty vector. The invasiveness of SUM149 cells was greatly decreased by restoring WISP3 expression. We also found that WISP3 markedly decreased the concentration of angiogenic mediators in the conditioned medium, especially VEGF, basic fibroblast growth factor, and interleukin-6 [9]. Given the high specificity of WISP3 and RhoC alterations in IBC and their interrelated functions in tumorigenesis, we propose that they cooperate in the development of IBC.

Using an antisense approach, inhibition of WISP3 expression in HME cells resulted in a threefold increase of RhoC GTPase transcript levels. The HME/AS WISP3 cells also exhibited increased cellular proliferation and anchorage-independent growth in soft agar. The HME/AS WISP3 cells produced significantly more colonies in soft agar in comparison with the control cells, an average of 58% of the level of colonies formed by the SUM149 IBC cells. HME/AS WISP3 cells also exhibited decreased production of VEGF in the conditioned medium.

The relationship between RhoC and WISP3 expression seems to be reciprocal. Restoration of WISP3 expression in SUM149 cells, which have lost WISP3 in the wild-type state, induced a 1.5-fold decrease in RhoC GTPase expression. These results are intriguing because changes in expression in Rho proteins by subtle factors such as 1.5–1.8 can be sufficient to modulate cellular behavior. Overexpression of RhoC in spontaneously immortalized HME cells, MCF10A, resulted in a 2.5-fold decrease in WISP3 mRNA expression.

In summary, overexpression of RhoC GTPase and loss of WISP3 are key genetic alterations in the development of IBC, and they have complementary functions. RhoC GTPase has a primary role in motility, invasion, and angiogenesis [15,17]. WISP3 has a pivotal role in tumor growth, invasion, and angiogenesis [9]. Here we have further strengthened the evidence that these genes cooperate in the development of IBC, because WISP3 expression modulates the expression of RhoC GTPase and its functions.

Conclusion

IBC is the most lethal form of locally advanced breast cancer, with a 5-year disease-free survival of less than 45%. Our work focused on determining the genetic alterations that result in this aggressive breast cancer phenotype. Previously, we have found that RhoC and WISP3 are consistently and concordantly altered in IBC tissues. RhoC functions as an oncogene, and WISP3 as a tumor suppressor gene. Here we provide evidence supporting the hypothesis that these two genes act in concert to give rise to the highly aggressive IBC phenotype. We propose a model of this interaction as a starting point for further investigations.

Competing interests

None declared.

Acknowledgements

This work was supported in part by DOD grants DAMD17-02-1-0490 and DAMD17-02-1-0491 (CGK), DOD grants DAMD17-00-1-0345 and DAMD17-02-1-0492 (SDM), and NIH grants K08CA090876-01A2 (CGK), RO1CA77612 (SDM), P30CA46592 and M01-RR00042. We thank S Ethier for supplying the SUM149 and HME cell lines and R Kunkel for art work.

References

- Jaiyesimi IA, Buzdar AU, Hortobagyi G: **Inflammatory breast cancer: a review.** *J Clin Oncol* 1992, **10**:1014-1024.
- Lee BJ, Tannenbaum ND: **Inflammatory carcinoma of the breast: a report of twenty-eight cases from the breast clinic of Memorial Hospital.** *Surg Gynecol Obstet* 1924, **39**:580-595.
- Merajver SD, Weber BL, Cody R, Zhang D, Strawderman M, Calzone KA, LeClaire V, Levin A, Irani J, Halvie M, August D, Wicha M, Lichter A, Pierce LJ: **Breast conservation and prolonged chemotherapy for locally advanced breast cancer: the University of Michigan experience.** *J Clin Oncol* 1997, **15**: 2873-2881.
- Swain SM, Sorace RA, Bagley CS, Danforth DN Jr, Bader J, Wesley MN, Steinberg SM, Lippman ME: **Neoadjuvant chemotherapy in the combined modality approach of locally advanced nonmetastatic breast cancer.** *Cancer Res* 1987, **47**: 3889-3894.
- van Golen KL, Davies S, Wu ZF, Wang Y, Bucana CD, Root H, Chandrasekharappa S, Strawderman M, Ethier SP, Merajver SD: **A novel putative low-affinity insulin-like growth factor-binding protein, LIBC (lost in inflammatory breast cancer), and RhoC GTPase correlate with the inflammatory breast cancer phenotype.** *Clin Cancer Res* 1999, **5**:2511-2519.
- Perbal B: **NOV (nephroblastoma overexpressed) and the CCN family of genes: structural and functional issues.** *Mol Pathol* 2001, **54**:57-79.
- Pennica D, Swanson TA, Welsh JW, Roy MA, Lawrence DA, Lee J, Brush J, Taneyhill LA, Deuel B, Lew M, Watanabe C, Cohen RL, Melhem MF, Finley GG, Quirke P, Goddard AD, Hillan KJ, Gurney AL, Botstein D, Levine AJ: **WISP genes are members of the connective tissue growth factor family that are up-regulated in wnt-1-transformed cells and aberrantly expressed in human colon tumors.** *Proc Natl Acad Sci USA* 1998, **95**:14717-14722.
- Hurvitz JR, Suwairi WM, Van Hul W, El-Shanti H, Superti-Furga A, Roudier J, Holderbaum D, Pauli RM, Herd JK, Van Hul EV, Rezai-Delui H, Legius E, Le Merrer M, Al-Alami J, Bahabri SA, Warman ML: **Mutations in the CCN gene family member WISP3 cause progressive pseudorheumatoid dysplasia.** *Nat Genet* 1999, **23**:94-98.
- Kleer CG, Zhang Y, Pan Q, van Golen KL, Wu ZF, Livant D, Merajver SD: **WISP3 is a novel tumor suppressor gene of inflammatory breast cancer.** *Oncogene* 2002, **21**:3172-3180.
- Kimura K, Ito M, Amano M, Chihara K, Fukata Y, Nakafuku M, Yamamori B, Feng J, Nakano T, Okawa K, Iwamatsu A, Kaibuchi

- K: Regulation of myosin phosphatase by Rho and Rho-associated kinase (Rho-kinase).** *Science* 1996, **273**:245-248.
11. Leung T, Chen XQ, Manser E, Lim L: **The p160 RhoA-binding kinase ROK alpha is a member of a kinase family and is involved in the reorganization of the cytoskeleton.** *Mol Cell Biol* 1996, **16**:5313-5327.
 12. Nobes CD, Hall A: **Rho, rac, and cdc42 GTPases regulate the assembly of multimolecular focal complexes associated with actin stress fibers, lamellipodia, and filopodia.** *Cell* 1995, **81**: 53-62.
 13. Ethier SP, Mahacek ML, Gullick WJ, Frank TS, Weber BL: **Differential isolation of normal luminal mammary epithelial cells and breast cancer cells from primary and metastatic sites using selective media.** *Cancer Res* 1993, **53**:627-635.
 14. Band V, Zajchowski D, Kulesa V, Sager R: **Human papilloma virus DNAs immortalize normal human mammary epithelial cells and reduce their growth factor requirements.** *Proc Natl Acad Sci USA* 1990, **87**:463-467.
 15. van Golen KL, Wu ZF, Qiao XT, Bao LW, Merajver SD: **RhoC GTPase, a novel transforming oncogene for human mammary epithelial cells that partially recapitulates the inflammatory breast cancer phenotype.** *Cancer Res* 2000, **60**:5832-5838.
 16. Kleer CG, van Golen KL, Zhang Y, Wu ZF, Rubin MA, Merajver SD: **Characterization of RhoC expression in benign and malignant breast disease : a potential new marker for small breast carcinomas with metastatic ability.** *Am J Pathol* 2002, **160**:579-584.
 17. van Golen KL, Wu ZF, Qiao XT, Bao L, Merajver SD: **RhoC GTPase overexpression modulates induction of angiogenic factors in breast cells.** *Neoplasia* 2000, **2**:418-425.

Correspondence

Sofia D Merajver, 7217 CCGC, 1500 East Medical Center Drive, Ann Arbor, MI 48109-0948, USA. Tel: +1 734 936 6884; fax: +1 734 936 7376; e-mail: smerajve@umich.edu

The Polycomb Group Protein EZH2 Impairs DNA Repair in Breast Epithelial Cells¹

Michael Zeidler*, Sooryanarayana Varambally*[†], Qi Cao*, Arul M. Chinnaiyan*^{†,‡}, David O. Ferguson*, Sofia D. Merajver*[§] and Celina G. Kleer*[†]

*Department of Pathology, University of Michigan, Arbor, MI, USA; [†]Comprehensive Cancer and Geriatrics Center, University of Michigan, Arbor, MI, USA; [‡]Department of Urology, University of Michigan, Arbor, MI, USA; [§]Department of Internal Medicine, University of Michigan, Arbor, MI, USA

Abstract

The Polycomb group protein EZH2 is a transcriptional repressor involved in controlling cellular memory and has been linked to aggressive and metastatic breast cancer. Here we report that EZH2 decreased the expression of five RAD51 paralog proteins involved in homologous recombination (HR) repair of DNA double-strand breaks (RAD51B/RAD51L1, RAD51C/RAD51L2, RAD51D/RAD51L3, XRCC2, and XRCC3), but did not affect the levels of *DMC1*, a gene that only functions in meiosis. EZH2 overexpression impaired the formation of RAD51 repair foci at sites of DNA breaks. Overexpression of EZH2 resulted in decreased cell survival and clonogenic capacity following DNA damage induced independently by etoposide and ionizing radiation. We suggest that EZH2 may contribute to breast tumorigenesis by specific downregulation of RAD51-like proteins and by impairment of HR repair. We provide mechanistic insights into the function of EZH2 in mammalian cells and uncover a link between EZH2, a regulator of homeotic gene expression, and HR DNA repair. Our study paves the way for exploring the blockade of EZH2 overexpression as a novel approach for the prevention and treatment of breast cancer.

Neoplasia (2005) 7, 1011–1019

Keywords: EZH2, breast cancer, homologous recombination, RAD51 paralogs, DNA repair.

Introduction

Breast cancer is the most common malignancy and second leading cause of cancer-related deaths in women in the Western world [1]. Despite advances in early detection and treatment, once distant metastases develop, the disease is (at present) incurable. There is a need to better understand the molecular events that lead to breast cancer development and progression to improve the design of clinical tests and novel targeted treatments.

Perturbations of the transcriptional memory of a cell may lead to developmental defects and cancer [2,3]. Two groups of proteins have long been found to be involved in the maintenance of heritable transcription patterns: the

Polycomb group proteins (PcG) and their counterpart, the Trithorax group proteins (TrxG) [3]. Both maintain spatial patterns of homeotic box gene expression, which occur early during embryonic development of *Drosophila*. TrxG act as activators and maintain the “on stage” of gene expression, whereas PcG act as repressors and maintain the “off stage” of gene expression. At least two PcG complexes with distinct functions and target genes have been found: Polycomb Repression Complex (PRC)-2, which consists of EZH2/embryonic ectoderm development (EED) [4] and Su(z)12 [5], among other proteins, and PRC-1 [6], which consists of Ring1, Mel18, Mph1, Bmi1, and Mpc2, among other proteins. In human malignancies, PcG and TrxG have been found to be dysregulated first in neoplasms of hematopoietic origin, but also in solid tumors, including breast and prostate carcinomas [7–16].

EZH2 is the human homologue of the PcG Enhancer of Zeste and is involved in gene silencing [3]. EZH2 contains a SET domain, a highly conserved domain found in many chromatin-associated histone methyltransferases. EZH2 and its binding partners EED and Suz(12) interact directly with type 1 histone deacetylases (HDACs), and this has been suggested to be part of the silencing mechanism [17–19]. Furthermore, recent studies have demonstrated that PRC-2 complexes methylate H3-K9 and K27 *in vitro*, with a strong preference for K27 [20–25]. Methylation of both H3-K9 and H3-K27 is thought to be involved in targeting PRC-1 to specific genetic loci [23,26]. At present, the mechanism of function of EZH2 in the development of malignant tumors is unknown.

The mammalian genome is at constant risk of mutation as a result of damage to DNA. This can occur due to extrinsic or intrinsic insults. Hampered DNA double-strand break (DSB) repair may lead to structural chromosomal abnormalities and

Abbreviations: HR, homologous recombination; DSB, double-strand break; PcG, Polycomb group proteins

Address all correspondence to: Celina G. Kleer, MD, Department of Pathology, University of Michigan Medical School, 3510C MSRB1, 1150 West Medical Center Drive, Ann Arbor, MI 48109-0605. E-mail: kleer@umich.edu

¹This work was supported, in part, by National Institutes of Health grants R01CA107469 (C.G.K.), CA090876-K08 (C.G.K.), and R01CA77612 (A.M.C.); Army grants DAMD17-02-1-0490 and DAMD17-02-1-491 (C.G.K.); the Burroughs Wellcome Research Fund (S.D.M.); and the Breast Cancer Research Foundation (S.D.M.).

Received 18 July 2005; Revised 26 August 2005; Accepted 29 August 2005.

Copyright © 2005 Neoplasia Press, Inc. All rights reserved 1522-8002/05/\$25.00
DOI 10.1593/neo.05472

aneuploidy, which may result in cell death or neoplastic transformation [27–30]. The two main mechanisms used to repair DSB are homologous recombination (HR), which promotes accurate repair of DSB by copying intact information from an undamaged homologous DNA template, and nonhomologous end joining (NHEJ), which is a homology-independent mechanism that rejoins broken ends, regardless of sequence [31].

In vertebrates, HR requires the recombinase RAD51 and its five paralogs RAD51B/RAD51L1, RAD51C/RAD51L2, RAD51D/RAD51L3, XRCC2, and XRCC3 [32]. The sixth paralog, *DMC1*, is thought to be only active in meiotic cells [32,33]. The RAD51 paralogs share up to 20% amino acid identity with the human RAD51 protein and with each other. Null mutations of any of the paralogs prevent RAD51 from assembling at damaged sites, resulting in decreased RAD51 repair foci formation, hampered HR, and increased sensitivity to DNA cross-linking drugs [34–40]. Although the functions and mechanisms of the regulation of the RAD51 paralogs are still elusive, an emerging body of data indicates that the RAD51 paralogs are important in maintaining chromosomal integrity and function in the early and later stages of HR [32,41].

We have previously reported that overexpression of the PcG EZH2 plays an important role in breast cancer by promoting the growth and invasion of breast epithelial cells [14]. Moreover, EZH2 is a promising novel biomarker of aggressive breast cancer, being elevated in invasive and metastatic tumors, when compared to normal breast tissues. Indeed, EZH2 is an independent predictor of breast cancer recurrence and death [14]. In breast tissues, EZH2 protein expression increases steadily from normal epithelium to epithelial hyperplasia, ductal carcinoma *in situ*, invasive carcinoma, and distant metastasis, supporting the finding that EZH2 plays a central role in neoplastic transformation [14]. In this study, we show that EZH2 overexpression downregulates all five RAD51 paralogs, which are necessary for HR in breast epithelial cells. This downregulation is associated with an impaired survival capacity of breast epithelial cells amidst the DNA-damaging effects of etoposide and ionizing radiation. Taken together, these data uncover a link between regulators of homeotic gene expression and the DNA repair pathway, and they propose a novel mechanism for EZH2 function in breast tumorigenesis.

Experimental Design

Cell Lines

Spontaneously immortalized human mammary epithelial MCF10A cells (ATCC, Manassas, VA) were grown in DMEM/F-12 (Cellgro) supplemented with nonessential amino acids, penicillin/streptomycin, L-glutamine, Fungizone, 5% horse serum, 20 ng/ml embryonic growth factor, 100 ng/ml cholera toxin, 10 μ g/ml insulin, and 500 ng/ml hydrocortisone. Cells were kept at 37°C and 10% CO₂. For detaching, cells were treated with 0.25% trypsin for 5 minutes. MCF7 breast cancer cells (ATCC) were grown in a DMEM/F12 mixture supplemented with 5% FBS. SUM102 human breast cancer cells

were grown in F12 supplemented with 5% FBS, 10 μ g/ml insulin, and 500 ng/ml hydrocortisone.

Adenoviral Constructs

Adenoviral constructs were generated by *in vitro* recombination. Full-length EZH2 (av-EZH2) was inserted into an adenoviral shuttle [pACCMVpLpA(–) loxP-SSP] provided by the University of Michigan (Ann Arbor, MI) vector core. The virus was complemented in a 293 helper cell line, propagated in 911 cells, and purified on a CsCl gradient. The virus was stored in 10 mM Tris–HCl (pH 7.4), 137 mM NaCl, 5 mM KCl, and 1 mM MgCl₂ in 10% (vol/vol) glycerol. As control, adenovirus containing no transgene was used. As an additional control, the full-length luciferase gene, an unrelated gene, was inserted in an adenovirus (av-luciferase).

Quantitative Reverse Transcriptase Analysis

RNA was harvested from MCF10A cells infected with vector or av-EZH2 constructs using TRIZOL (Invitrogen, Carlsbad, CA), according to the manufacturer's instructions. One microgram of RNA was reverse-transcribed using Superscript II (Invitrogen) following the manufacturer's instructions and reconstituted in 20 μ l of RNase-free water. One microliter of cDNA product was used for quantitative real-time PCR analysis. Reaction mixes were made by combining 12.5 μ l of 2 \times SYBR green RT-PCR master mix, 0.5 μ l of RNase inhibitor (Promega, Madison, WI), primer, template, and H₂O to a final volume of 25 μ l into Smart Cycler Tubes (Cepheid, Sunnyvale, CA). Primers were used at a final concentration of 0.25 μ M:

RAD51L1: 5'-TTT CCC CAC TGG AGC TTA TG-3', 5'-CTT CGT CCA AAG CAG AAA GG-3'
 RAD51L2: 5'-GCA TAC CCA GGG CTT CAT AAT C-3', 5'-TTT CGG TGT TCC TCT CCC TTG TGT TTT TCT-3'
 RAD51L3: 5'-CAG TGG TGG ACC TGG TTT CT-3', 5'-CTG GGC CTC CTA CAA TTT CA-3'
 XRCC2: 5'-TTC CAT AGG GCT GAG TCT GG-3', 5'-CCG GAG CAT ATC AAA GTG GT-3'
 XRCC3: 5'-AAG AAG GTC CCC GTA CTG CT-3', 5'-AAA CAC GTT CGT CCC AGA AC-3'
 DMC1: 5'-AAT GGC ACT TTT TCG AGT GG-3', 5'-CAG GCA TCT CAG GAC TGT CA-3'
 β -Actin: 5'-CTG GAC TTC GAG CAA GAG-3', 5'-AAG GAA GGC TGG AAG AGT-3'.

Primers were selected using LocusLink software and spanned an intron–exon junction to prevent amplification of genomic DNA. To confirm the absence of nonspecific amplification, a no-template control was included. Forty cycles were programmed as follows: 15 seconds of denaturation at 94°C, followed by 1 minute of extension at 60°C. Results were quantified against a β -actin standard set in relation to the vector control using Excel.

Western Immunoblot

MCF10A, MCF7, and SUM102 cells were infected with vector or av-EZH2. After 2 days, cells were lysed in 10% glycerol, 150 mM KCl, 10 mM MgCl₂, 25 mM HEPES, 2 mM

DTT, and one Complete Mini protease inhibitor tablet (Roche, Nutley, NJ) and sonicated 4 × 30 seconds at medium speed. Samples were separated on a precast gel (10% Tris–glycine; Cambrex, Rockville, MD) and transferred to nitrocellulose membrane using a Transblot Semidry Transfer Cell (Bio-Rad, Hercules, CA). Membranes were blocked in 5% (wt/vol) milk at room temperature for 1 hour. After three washes in Tris-buffered saline–Tween (TBS-T), primary antibodies against RAD51L2 (Abcam, Cambridge, MA), RAD51L3 (Novus Biologicals, Littleton, CO), RAD51L3, XRCC2, and XRCC3 (Abcam), at a dilution of 1/1000, were added in PBS-T [PBS containing 0.1% (vol/vol) Triton X-100] containing 3% BSA. The membranes were incubated overnight at 4°C, washed three times for 15 minutes in TBS-T, and incubated with anti-mouse horseradish peroxidase (Amersham, Buckinghamshire, UK) at a dilution of 1/2500. After incubation for 1 hour and three more washes, immunoreactive proteins were visualized using ECL reagents (Amersham), following the manufacturer's instructions.

Immunofluorescence

MCF10A cells were plated onto chamber slides and infected with av-EZH2 or av-vector. On the next day, the cells were treated with 0.3 mM etoposide for 24 hours. Following incubation, the cells were washed three times with PBS and fixed in 3% (wt/vol) paraformaldehyde in PBS-T and 0.15% (wt/vol) BSA for 20 minutes. Prior to incubation with antibodies against RAD51 (Santa Cruz Biotechnology, Santa Cruz, CA) or Myc (Cell Signaling, Beverly, MA) at a dilution of 1/1000 for 16 hours, the slides were rinsed twice in PBS-T. After incubation, the slides were washed 4 × 15 minutes in PBS-T. The slides were incubated for 4 hours with Alexa Fluor 488 or Texas Red antibody (Molecular Probes, Carlsbad, CA) at a dilution of 1/500, washed 4 × 15 minutes in PBS-T, and mounted with ProLong antifade reagent with DAPI (Molecular Probes). Images were obtained with an Olympus F500 inverted confocal microscope using ×10, ×40, and ×60 oil immersion objectives. The frequencies of cells containing RAD51 foci were determined by counting at least 250 nuclei in each slide in three independent experiments. Following strict published criteria, only nuclei containing ≥10 RAD51 foci were classified as RAD51-positive [42].

Survival Assays

For colony outgrowth assays, 500 MCF10A, 500 MCF7, and 500 SUM102 cells were plated onto a Petri dish 4 hours before infection. Cells were infected with vector or av-EZH2 constructs. An av-luciferase was used as additional control. One day after infection, the culture medium was changed and cells were continuously treated with increasing concentrations of etoposide (0.1, 0.3, and 0.5 mM). After 7 to 9 days, when colonies had been observed, the cells were washed twice in PBS, and colonies were fixed and stained using methylene blue (Merck, Whitehouse Station, NJ), following the manufacturers' instructions. Colonies with more than 50 cells were counted as positive.

For clonogenic survival assays, 500 MCF10A, 500 MCF7, and 500 SUM102 cells were plated 4 hours before infection.

Cells were infected with av-vector, av-EZH2, or av-luciferase constructs. One day after infection, the culture medium was changed and cells were treated for 24 hours with increasing concentrations of etoposide (0.1, 0.3, and 0.5 mM). After 7 to 9 days, colonies were already visible. Cells were washed twice with PBS, fixed, and stained using methylene blue (Merck), following the manufacturer's instructions. Colonies exceeding 50 cells were counted.

For ionizing radiation experiments, 4000 MCF10A, 4000 MCF7, and 4000 SUM102 cells were plated and infected with av-vector, av-EZH2, or av-luciferase. Two days after infection, the cells were irradiated with doses of 0, 300, 600, 900, and 1200 rad using a ¹³⁷Cs Mark I irradiator. Seven days post-infection, the colonies were stained with crystal violet and counted as described in the above paragraph. For all assays, transient gene expression of EZH2 in MCF10A, MCF7, and SUM102 cells was validated by Western blot analysis.

Metaphase Analysis

MCF10A cells were grown to 20% confluency and infected with av-EZH2 or vector control. Two days postinfection, 0.004 μg/ml KaryoMax Colcemid (Gibco, Carlsbad, CA) was added. Sixteen hours later, the cells were trypsinized and washed in PBS. After centrifugation, the cells were resuspended in 250 μl of PBS. Eight milliliters of 0.06 M KCl was carefully added while gently shaking the cells at 37°C in a water bath. Cells were incubated at 37°C for 30 minutes and then fixed with 2 ml of methanol:glacial acetic acid (3:1). After 5 minutes of centrifugation at 1000 rpm, the cells were resuspended in 8 ml of fixative, centrifuged again, and finally resuspended in 1 ml of fixative.

Cells were dropped from a pipette onto a wet frosted slide (Fisher, Pittsburgh, PA) from a height of about 50 cm. The slides were dried for 15 minutes at 37°C. ProLong Gold (Molecular Probes) antifade reagent with DAPI was used to fix the cover slip. Slides were dried overnight and then analyzed using Spectral Imaging SkyView software (Applied Spectral Imaging, Vista, CA). The number of chromosomes in 75 to 100 cells in metaphase was counted independently by three investigators (M.Z., D.O.F., and C.G.K.). Experiments were performed in triplicate.

Results

EZH2-Overexpressing Mammary Epithelial Cells Exhibit Lower Transcription of RAD51L1, RAD51L2, RAD51L3, XRCC2, and XRCC3, But Not of DMC1

In our previous studies, we demonstrated that EZH2 promoted growth and invasion in human mammary epithelial cells, which resulted in an aggressive and metastatic breast cancer phenotype [14]. Patients with tumors with high EZH2 expression had a worse disease-free and overall survival than those with low levels of EZH2 [14]. EZH2 has been reported to function as a transcriptional repressor in mammalian cells [14,19,43]. Preliminary data from our laboratory of a cDNA microarray comparing EZH2-overexpressing breast epithelial cells to vector controls prompted us to

investigate the possible influence of EZH2 on the expression of the RAD51 paralogs (data not shown). Notably, quantitative real-time PCR on av-EZH2- and av-vector-infected human mammary epithelial cells revealed that EZH2 overexpression led to a drastic decrease in the transcripts of the five RAD51 paralogs. As shown in Figure 1A, *RAD51L1*, *RAD51L2*, *RAD51L3*, *XRCC2*, and *XRCC3* transcripts are significantly decreased in EZH2-overexpressing MCF10A cells. These five RAD51 paralogs have crucial nonredundant roles in the HR DNA repair pathway. *DMC1*, a RAD51 paralog that is active only in meiosis, was not affected (Figure 1A). Immunoblot analyses of MCF10A, MCF7, and SUM102 cells showed that EZH2 overexpression was associated with decreased protein levels of RAD51L1, RAD51L2, RAD51L3, XRCC2, and XRCC3 (Figure 1B).

Attenuated RAD51 Repair Foci Formation in EZH2-Overexpressing Breast Epithelial Cells

RAD51L1, RAD51L2, RAD51L3, XRCC2, and XRCC3 are required for the formation of DNA damage-induced RAD51

repair foci. This is a crucial event in HR repair as studies have demonstrated that RAD51 foci formation is significantly attenuated in mutant cells defective in any of the RAD51 paralogs [34–37,40,41,44,45]. EZH2 overexpression in MCF10A cells resulted in a marked decrease in RAD51 foci formation after induction of DSB by etoposide (Figure 2). To investigate the effect of EZH2 overexpression on the repair foci formation ability of breast cells, we determined the number of cells with ≥ 10 RAD51 foci in EZH2-overexpressing and control cells at 0, 6, 12, and 24 hours following a 24-hour treatment with etoposide. Figure 2B shows that, immediately after removal of etoposide, EZH2-overexpressing cells displayed only about 50% of repair foci compared to the controls. These cells could not compensate for the hampered foci formation by sustaining a low level of repair over a longer period of time. Thus, 6 hours after etoposide withdrawal, the number of cells with RAD51 foci was significantly decreased in all cells, but the number of foci in EZH2-overexpressing cells was still significantly lower than that in the respective controls. After 12 hours, EZH2-overexpressing cells and controls had about the same number of cells with RAD51 repair foci. Twenty-four hours after etoposide withdrawal, RAD51 foci formation ceased almost completely in EZH2-overexpressing cells and controls. These data suggest that HR repair in EZH2-overexpressing cells is less effective than that in the controls.

EZH2-Overexpressing Cells Have Reduced Survival to Etoposide- and Radiation-Induced DNA Damage and Increased Number of Chromosomes

The above experiments demonstrated that EZH2 overexpression results in a marked downregulation of the RAD51 paralogs involved in HR and an attenuated formation of RAD51 foci after induced DSB. We next investigated the effects of EZH2 overexpression on cell survival after induction of DSB in the spontaneously immortalized human mammary epithelial cell line MCF10A and two breast cancer cell lines MCF7 and SUM102. In addition, to control for possible effects of protein overexpression, we infected these cells with *av-luciferase*, a gene unrelated to EZH2 that is not involved in HR repair. To induce DSB, we chose to independently use etoposide and ionizing radiation—both previously shown to cause DNA DSBs that are repaired by the HR pathway [42]. As presented in Figure 3, EZH2 overexpression significantly decreased the survival, clonogenic capacity, and colony-forming ability of the three breast cell lines after exposure to ionizing radiation and etoposide. Overall, our experiments suggest that overexpression of EZH2 hampers HR repair of DSB, at least in part, by downregulation of the five RAD51 paralogs RAD51L1, RAD51L2, RAD51L3, XRCC2, and XRCC3.

Knockout of the RAD51 paralogs has been shown to cause multiple forms of genetic instability, including chromosome aberrations, centrosome fragmentation, and missegregation of chromosomes [32,34–37,40,41,44,45]. In particular, a defect in chromosomal segregation leading to aneuploidy appears to be specific for HR repair defects, as it has not been found for cells deficient in alternative repair pathways (for

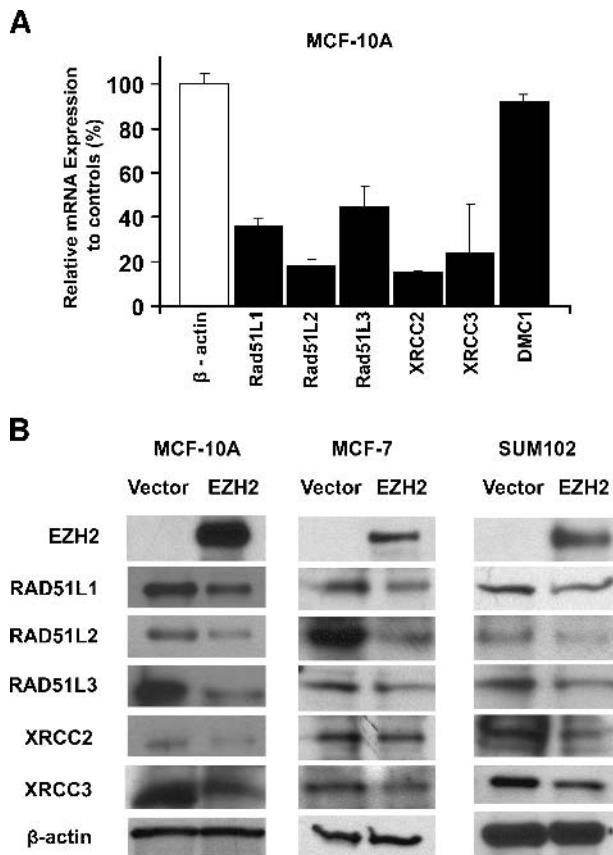


Figure 1. *RAD51L1*, *RAD51L2*, *RAD51L3*, *XRCC2*, and *XRCC3* transcripts and proteins are downregulated in EZH2-overexpressing mammary epithelial cells. (A) Quantitative real-time PCR. The graph shows transcription of the RAD51 paralogs in EZH2-overexpressing cells relative to control cells. Standard deviations from at least three independent experiments are depicted. The transcription of the five RAD51 paralogs involved in HR is significantly downregulated. Only DMC1, which is active in meiotic cells, stays unmodified. (B) Western immunoblots for EZH2 and the five RAD51 paralogs in EZH2-overexpressing MCF10A, MCF7, SUM102 cells and in vector-infected controls. A representative β -actin is shown for MCF10A cells. β -Actin is shown for MCF7 and SUM102 cells.

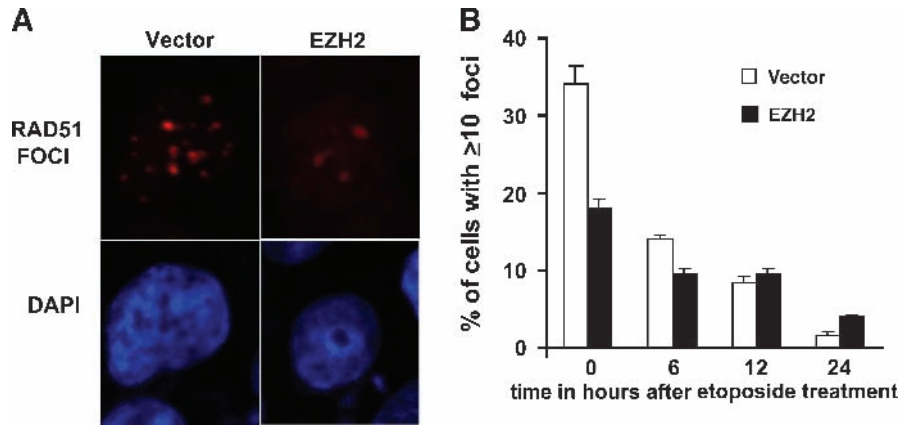


Figure 2. EZH2 overexpression reduces RAD51 foci formation. (A) Visualization of RAD51 foci in MCF10A cells infected with vector control or av-EZH2 after etoposide-induced DSBs. Shown are two representative cells. Lower panel: respective DAPI stain. (B) Mean percentage of vector control or av-EZH2 cells containing ≥ 10 RAD51 foci (columns) after a 24-hour etoposide treatment. Standard deviations (error bars) from three independent experiments for each time point are depicted.

instance, simple end joining of DNA breaks) [32,46,47]. Cytogenetic analysis of EZH2-overexpressing MCF10A cells and vector controls showed that EZH2 overexpression led to a shift in the number of chromosomes. Table 1 shows that, although the control cells show the characteristic chromosomal changes of immortal but untransformed MCF10A cells, EZH2-overexpressing cells have an increased number of chromosomes, with over 65% of cells having 49 to 54 chromosomes (*t*-test, $P < .0001$). Adenovirus infection did not affect the number and integrity of the chromosomes, as adenovirus-infected and uninfected MCF10A cells had the same low-level (baseline) aneuploidy characteristic of MCF10A cells [48–53].

Discussion

In this study, we provide evidence for a hitherto unknown mechanism of action for EZH2 in the development of breast cancer. We report that EZH2 overexpression results in specific downregulation of five RAD51 paralogs RAD51L1, RAD51L2, RAD51L3, XRCC2, and XRCC3, which are crucial for the normal function of the HR pathway of DNA DSB repair in mammalian cells [36,37,40]. Coupled with this effect on gene expression, EZH2 overexpression attenuates RAD51 foci formation at sites of DNA damage, impairing the ability of human breast epithelial cells to repair DNA by HR. Our results show that EZH2 overexpression leads to a lower survival after DNA-damaging insults. We suggest that suppression of the RAD51 paralogs by EZH2 is a likely mechanism of EZH2-driven malignant transformation of breast epithelial cells.

EZH2 is a member of the PcG of early-onset gene repressors involved in maintaining heritable gene expression profiles, thus regulating cell type identity [22–25]. There is compelling evidence that EZH2 overexpression leads to cancer. EZH2 is involved in the pathogenesis of myeloid leukemia, Hodgkin's disease, B-cell lymphoma, and multiple myeloma [9,10,12]. Our group and other investigators have reported that EZH2 promotes the development and progression of breast cancer, prostate cancer, and other solid tumors [11,13–15]. By performing an *in silico* analysis of published

cDNA datasets using ONCOMINE [54], we found that, in addition to breast cancer, *EZH2* mRNA is overexpressed in lung, liver, prostate, bladder, and adrenal carcinomas when compared to their normal epithelial counterparts (data not shown). These data suggest that misexpression of EZH2 may be a fundamental event in the transition from normal state to cancer in several organs. At present, the mechanism of action of EZH2 in cancer is unknown.

There are several lines of evidence supporting a role for the RAD51 gene family in cancer development, especially in light of the functional links between RAD51 and the *BRCA* genes [32]. In breast cancer, it has been shown that *BRCA2* mutation carriers are at greater risk for breast cancer when they also carry the RAD51 variant G135CD [55–57]. XRCC2 codon 188 variant may carry an increased risk for breast cancer [58]. The variant Glu233Gly of RAD51L3 may increase the risk of breast cancer in families without *BRCA* gene mutations [59]. The emerging association between the RAD51 gene family and cancer is not surprising given the critical role of RAD51 and its paralogs in HR repair, which is essential for the maintenance of genomic stability and tumor avoidance. Cell lines deficient in XRCC2 and XRCC3 have a high frequency of chromosomal instability, with especially high frequencies of chromosome exchange and aneuploidy [32,46,47,60]. XRCC2- and XRCC3-deficient hamster cells have been shown to have increased missegregation of chromosomes resulting in aneuploidy, likely due to a centrosome defect [46,47]. It has been suggested that loss of RAD51 paralog genes leads, in particular, to a chromosomal segregation defect that results in aneuploidy [32,46,47]. Studies have shown that aneuploidy causes imbalances in groups of proteins involved in chromosome segregation, synthesis, and repair, possibly leading to malignant transformation of the cell [27–30].

In the present study, we found that EZH2 overexpression in human mammary epithelial cells resulted in a drastic downregulation of the transcripts of the five RAD51 paralogs involved in HR repair (*RAD51L1*, *RAD51L2*, *RAD51L3*, *XRCC2*, and *XRCC3*). Notably, the expression of the sixth paralog, *DMC1*, and of RAD51 (data not shown) was not

affected by EZH2. In light of these data, it is likely that EZH2 may play a role in the transcriptional regulation of the RAD51 paralogs and thus modulate the function of HR DNA repair. In *Drosophila*, PcG exert their function through a DNA motif called Polycomb response element (PRE) [61,62]. Although a mammalian PRE has not been found yet, a recent study found that the EZH2 complex is able to associate with the

hDAB2IP promoter in prostate cells and is able to recruit HDAC1 to the promoter region [19]. Whether the EZH2 complex also associates with the promoters of the RAD51 paralogs is intriguing and warrants investigation.

Consistent with the observed decrease in RAD51L1, RAD51L2, RAD51L3, XRCC2, and XRCC3, EZH2-over-expressing mammary epithelial cells had an attenuated

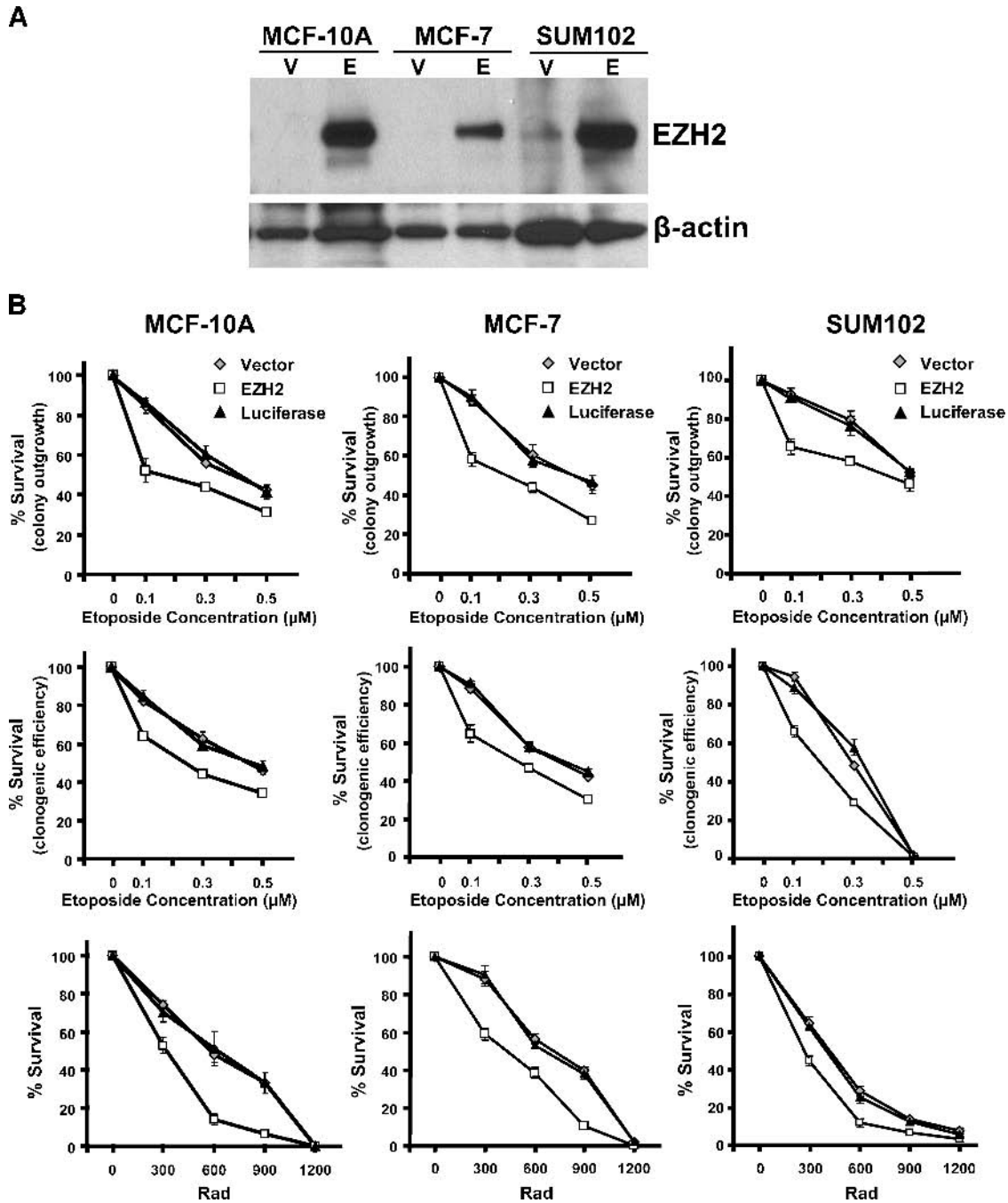


Figure 3. EZH2 overexpression decreases cell survival following etoposide treatment and ionizing radiation. MCF10A, MCF7, and SUM102 cells were infected with av-EZH2 and the control vector. (A) Western blot analysis for EZH2 and β -actin. (B) Three independent toxicity assays for MCF10A, MCF7, and SUM102 cells. The legend for all experiments is shown in the upper right corner. The upper panel shows a colony outgrowth of cells infected with av-EZH2, a luciferase control, or a vector control. Cells were treated continuously with etoposide. Colony-forming ability was measured after 7 to 9 days by counting colonies with more than 50 cells. The means (symbols) and standard deviations (bars) from three different experiments are shown. The middle panel shows clonogenic efficiency after 24 hours of treatment with etoposide. The means (symbols) and standard deviations (bars) from four different experiments are shown. The lower panel shows the surviving cells after different doses of ionizing irradiation. Colonies were counted after 9 days, as described above.

Table 1. Effect of EZH2 Overexpression on the Chromosome Number of MCF10A Cells.

	% of Metaphases According to the Number of Chromosomes			P value
	46–48	49–50	51–54	
MCF10A/vector	87.1	6.5	6.4	< .05
MCF10A/EZH2	31.4	28.6	40	

formation of RAD51 repair foci after treatment with etoposide. EZH2 overexpression resulted in a marked decrease in the number of cells with repair foci when compared to controls. The attenuated RAD51 foci formation most likely led to unrepaired chromosomal breaks. Although most cells would succumb to the damage, a subset of cells may survive and acquire additional genetic alterations, which may lead to neoplastic transformation.

We next tested the hypothesis that attenuated DNA repair foci formation may lead to defective HR. Indeed, EZH2-overexpressing cells exhibited decreased survival ability following etoposide and ionizing radiation, both of which cause DNA DSBs that necessitate HR repair [42,63–67]. EZH2 overexpression not only affected HR repair in the spontaneously immortalized human mammary epithelial cell line MCF10A, but had a similar effect on two breast cancer cell lines MCF7 and SUM102. Furthermore, EZH2-overexpressing MCF10A cells exhibited an increase in the number of chromosomes when compared to controls. These results are not surprising given the important role of HR not only in DNA repair, but also in the resolution of crossover during cell divisions [32]. Taken together, our data suggest that EZH2 overexpression occurs early in neoplastic transformation and may be important for the development of prevention strategies for breast cancer based on blockade of EZH2. Our data open the way to future investigations on the detection of EZH2 overexpression in histologically normal breast epithelial cells as a harbinger of carcinoma. This could result in the development of a new clinically applicable tissue-based test to determine the individual risk of breast cancer before histologic atypia is evident.

Our data are in agreement with previous studies demonstrating that aneuploidy is particularly seen in association with defects in HR, but not in association with defects in other DNA repair mechanisms such as NHEJ repair [32,46,47]. These data suggest further investigations to elucidate whether EZH2 overexpression induces random or specific chromosomal alterations. Our data strengthen the emerging link between decreased expression of the RAD51 paralogs, aneuploidization, and cancer development.

In summary, we have identified and delineated a new functional role for EZH2 in the HR mechanism of DNA repair, which may cause aneuploidy in breast epithelial cells. We provide a mechanistic basis for our initial observations implicating EZH2 in promoting breast cancer development and also uncover a role for EZH2 in the regulation of a central pathway in DNA repair and in maintaining the stability of the genome.

Acknowledgements

We thank Diane Roulston (University of Michigan Medical School) for critical reading of the manuscript and suggestions, Lei Ding for assistance with ONCOMINE, as well as other members of the Kleer laboratory for their constructive suggestions throughout the execution of this project, and Karilynn Schneider and Robin Kunkel for artwork.

References

- [1] Jemal A, Murray T, Samuels A, Ghafoor A, Ward E, and Thun MJ (2003). Cancer statistics, 2003. *CA Cancer J Clin* **53**, 5–26.
- [2] Jacobs JJ and van Lohuizen M (1999). Cellular memory of transcriptional states by Polycomb-group proteins. *Semin Cell Dev Biol* **10**, 227–235.
- [3] Laible G, Wolf A, Dorn R, Reuter G, Nislow C, Lebersorger A, Popkin D, Pillus L, and Jenuwein T (1997). Mammalian homologues of the Polycomb-group gene Enhancer of zeste mediate gene silencing in *Drosophila* heterochromatin and at *S. cerevisiae* telomeres. *EMBO J* **16**, 3219–3232.
- [4] Sewalt RG, van der Vlag J, Gunster MJ, Hamer KM, den Blaauwen JL, Satijn DP, Hendrix T, van Driel R, and Otte AP (1998). Characterization of interactions between the mammalian polycomb-group proteins Enx1/EZH2 and EED suggests the existence of different mammalian polycomb-group protein complexes. *Mol Cell Biol* **18**, 3586–3595.
- [5] Birve A, Sengupta AK, Beuchle D, Larsson J, Kennison JA, Rasmuson-Lestander A, and Muller J (2001). Su(z)12, a novel *Drosophila* Polycomb group gene that is conserved in vertebrates and plants. *Development* **128**, 3371–3379.
- [6] Shao Z, Raible F, Mollaaghababa R, Guyon JR, Wu CT, Bender W, and Kingston RE (1999). Stabilization of chromatin structure by PRC1, a Polycomb complex. *Cell* **98**, 37–46.
- [7] Haupt Y, Alexander WS, Barri G, Klincken SP, and Adams JM (1991). Novel zinc finger gene implicated as myc collaborator by retrovirally accelerated lymphomagenesis in E mu-myc transgenic mice. *Cell* **65**, 753–763.
- [8] Haupt Y, Barri G, and Adams JM (1992). Nucleotide sequence of *bup*, an upstream gene in the *bmi-1* proviral insertion locus. *Mol Biol Rep* **17**, 17–20.
- [9] Raaphorst FM, van Kemenade FJ, Blokzijl T, Fieret E, Hamer KM, Satijn DP, Otte AP, and Meijer CJ (2000). Coexpression of *BMI-1* and *EZH2* polycomb group genes in Reed-Sternberg cells of Hodgkin's disease. *Am J Pathol* **157**, 709–715.
- [10] Visser HP, Gunster MJ, Kluin-Nelemans HC, Manders EM, Raaphorst FM, Meijer CJ, Willemze R, and Otte AP (2001). The Polycomb group protein EZH2 is upregulated in proliferating, cultured human mantle cell lymphoma. *Br J Haematol* **112**, 950–958.
- [11] Bracken AP, Pasini D, Capra M, Prosperini E, Colli E, and Helin K (2003). EZH2 is downstream of the pRB–E2F pathway, essential for proliferation and amplified in cancer. *EMBO J* **22**, 5323–5335.
- [12] Croonquist PA and Van Ness B (2005). The polycomb group protein enhancer of zeste homolog 2 (*EZH2*) is an oncogene that influences myeloma cell growth and the mutant ras phenotype. *Oncogene* **24**, 6269–6280.
- [13] Varambally S, Dhanasekaran SM, Zhou M, Barrette TR, Kumar-Sinha C, Sanda MG, Ghosh D, Pienta KJ, Sewalt RG, Otte AP, et al. (2002). The polycomb group protein EZH2 is involved in progression of prostate cancer. *Nature* **419**, 624–629.
- [14] Kleer CG, Cao Q, Varambally S, Shen R, Ota I, Tomlins SA, Ghosh D, Sewalt RG, Otte AP, Hayes DF, et al. (2003). EZH2 is a marker of aggressive breast cancer and promotes neoplastic transformation of breast epithelial cells. *Proc Natl Acad Sci USA* **100**, 11606–11611.
- [15] Raaphorst FM, Meijer CJ, Fieret E, Blokzijl T, Mommers E, Buerger H, Packeisen J, Sewalt RA, Otte AP, and van Diest PJ (2003). Poorly differentiated breast carcinoma is associated with increased expression of the human polycomb group *EZH2* gene. *Neoplasia* **5**, 481–488.
- [16] Haupt Y, Bath ML, Harris AW, and Adams JM (1993). *bmi-1* transgene induces lymphomas and collaborates with myc in tumorigenesis. *Oncogene* **8**, 3161–3164.
- [17] Cao R and Zhang Y (2004). SUZ12 is required for both the histone methyltransferase activity and the silencing function of the EED–EZH2 complex. *Mol Cell* **15**, 57–67.
- [18] Pasini D, Bracken AP, Jensen MR, Denchi EL, and Helin K (2004). Suz12 is essential for mouse development and for EZH2 histone methyltransferase activity. *EMBO J* **23**, 4061–4071.

- [19] Chen H, Tu SW, and Hsieh JT (2005). Down-regulation of human *DAB2IP* gene expression mediated by polycomb Ezh2 complex and histone deacetylase in prostate cancer. *J Biol Chem* **280**, 22437–22444.
- [20] Sewalt RG, Lachner M, Vargas M, Hamer KM, den Blaauwen JL, Hendrix T, Melcher M, Schweizer D, Jenuwein T, and Otte AP (2002). Selective interactions between vertebrate polycomb homologs and the SUV39H1 histone lysine methyltransferase suggest that histone H3-K9 methylation contributes to chromosomal targeting of Polycomb group proteins. *Mol Cell Biol* **22**, 5539–5553.
- [21] Kuzmichev A, Jenuwein T, Tempst P, and Reinberg D (2004). Different EZH2-containing complexes target methylation of histone H1 or nucleosomal histone H3. *Mol Cell* **14**, 183–193.
- [22] Kuzmichev A, Nishioka K, Erdjument-Bromage H, Tempst P, and Reinberg D (2002). Histone methyltransferase activity associated with a human multiprotein complex containing the Enhancer of Zeste protein. *Genes Dev* **16**, 2893–2905.
- [23] Cao R, Wang L, Wang H, Xia L, Erdjument-Bromage H, Tempst P, Jones RS, and Zhang Y (2002). Role of histone H3 lysine 27 methylation in Polycomb-group silencing. *Science* **298**, 1039–1043.
- [24] Czermin B, Melfi R, McCabe D, Seitz V, Imhof A, and Pirrotta V (2002). *Drosophila* enhancer of Zeste/ESC complexes have a histone H3 methyltransferase activity that marks chromosomal Polycomb sites. *Cell* **111**, 185–196.
- [25] Muller J, Hart CM, Francis NJ, Vargas ML, Sengupta A, Wild B, Miller EL, O'Connor MB, Kingston RE, and Simon JA (2002). Histone methyltransferase activity of a *Drosophila* Polycomb group repressor complex. *Cell* **111**, 197–208.
- [26] Plath K, Fang J, Mlynczyk-Evans SK, Cao R, Worringer KA, Wang H, de la Cruz CC, Otte AP, Panning B, and Zhang Y (2003). Role of histone H3 lysine 27 methylation in X inactivation. *Science* **300**, 131–135.
- [27] Hede K (2005). Which came first? Studies clarify role of aneuploidy in cancer. *J Natl Cancer Inst* **97**, 87–89.
- [28] Wang RH, Yu H, and Deng CX (2004). A requirement for breast-cancer-associated gene 1 (*BRCA1*) in the spindle checkpoint. *Proc Natl Acad Sci USA* **101**, 17108–17113.
- [29] Daniels MJ, Wang Y, Lee M, and Venkitaraman AR (2004). Abnormal cytokinesis in cells deficient in the breast cancer susceptibility protein *BRCA2*. *Science* **306**, 876–879.
- [30] Duesberg P, Fabarius A, and Hehlmann R (2004). Aneuploidy, the primary cause of the multilateral genomic instability of neoplastic and preneoplastic cells. *IUBMB Life* **56**, 65–81.
- [31] Mills KD, Ferguson DO, and Alt FW (2003). The role of DNA breaks in genomic instability and tumorigenesis. *Immunol Rev* **194**, 77–95.
- [32] Thacker J (2005). The *RAD51* gene family, genetic instability and cancer. *Cancer Lett* **219**, 125–135.
- [33] Bugreev DV, Golub EI, Stasiak AZ, Stasiak A, and Mazin AV (2005). Activation of human meiosis-specific recombinase *DMC1* by Ca^{2+} . *J Biol Chem* **280**, 26886–26895.
- [34] Tebbs RS, Zhao Y, Tucker JD, Scheerer JB, Siciliano MJ, Hwang M, Liu N, Legerski RJ, and Thompson LH (1995). Correction of chromosomal instability and sensitivity to diverse mutagens by a cloned cDNA of the *XRCC3* DNA repair gene. *Proc Natl Acad Sci USA* **92**, 6354–6358.
- [35] Liu N, Lamerdin JE, Tebbs RS, Schild D, Tucker JD, Shen MR, Brookman KW, Siciliano MJ, Walter CA, Fan W, et al. (1998). *XRCC2* and *XRCC3*, new human Rad51-family members, promote chromosome stability and protect against DNA cross-links and other damages. *Mol Cell* **1**, 783–793.
- [36] Takata M, Sasaki MS, Tachiiri S, Fukushima T, Sonoda E, Schild D, Thompson LH, and Takeda S (2001). Chromosome instability and defective recombinational repair in knockout mutants of the five Rad51 paralogs. *Mol Cell Biol* **21**, 2858–2866.
- [37] Godthelp BC, Wiegant WW, van Duijn-Goedhart A, Scharer OD, van Buul PP, Kanaar R, and Zdzienicka MZ (2002). Mammalian Rad51C contributes to DNA cross-link resistance, sister chromatid cohesion and genomic stability. *Nucleic Acids Res* **30**, 2172–2182.
- [38] Fuller LF and Painter RB (1988). A Chinese hamster ovary cell line hypersensitive to ionizing radiation and deficient in repair replication. *Mutat Res* **193**, 109–121.
- [39] Caldecott K and Jeggo P (1991). Cross-sensitivity of gamma-ray-sensitive hamster mutants to cross-linking agents. *Mutat Res* **255**, 111–121.
- [40] Bishop DK, Ear U, Bhattacharya A, Calderone C, Beckett M, Weichselbaum RR, and Shinohara A (1998). *Xrcc3* is required for assembly of Rad51 complexes *in vivo*. *J Biol Chem* **273**, 21482–21488.
- [41] Yokoyama H, Sarai N, Kagawa W, Enomoto R, Shibata T, Kurumizaka H, and Yokoyama S (2004). Preferential binding to branched DNA strands and strand-annealing activity of the human Rad51B, Rad51C, Rad51D and *Xrcc2* protein complex. *Nucleic Acids Res* **32**, 2556–2565.
- [42] Lundin C, Schultz N, Arnaudeau C, Mohindra A, Hansen LT, and Helleday T (2003). *RAD51* is involved in repair of DNA damage associated with DNA replication in mammalian cells. *J Mol Biol* **328**, 521–535.
- [43] Varambally S, Dhanasekaran SM, Zhou M, Barrette TR, Kumar-Sinha C, Sanda MG, Ghosh D, Pienta KJ, Sewalt RG, Otte AP, et al. (2002). The polycomb group protein EZH2 is involved in progression of prostate cancer. *Nature* **419**, 624–629.
- [44] Johnson RD, Liu N, and Jasin M (1999). Mammalian *XRCC2* promotes the repair of DNA double-strand breaks by homologous recombination. *Nature* **401**, 397–399.
- [45] Pierce AJ, Johnson RD, Thompson LH, and Jasin M (1999). *XRCC3* promotes homology-directed repair of DNA damage in mammalian cells. *Genes Dev* **13**, 2633–2638.
- [46] Griffin CS, Simpson PJ, Wilson CR, and Thacker J (2000). Mammalian recombination-repair genes *XRCC2* and *XRCC3* promote correct chromosome segregation. *Nat Cell Biol* **2**, 757–761.
- [47] Hut HM, Lemstra W, Blaauw EH, Van Cappellen GW, Kampinga HH, and Sibon OC (2003). Centrosomes split in the presence of impaired DNA integrity during mitosis. *Mol Biol Cell* **14**, 1993–2004.
- [48] Yoon DS, Wersto RP, Zhou W, Chrest FJ, Garrett ES, Kwon TK, and Gabrielson E (2002). Variable levels of chromosomal instability and mitotic spindle checkpoint defects in breast cancer. *Am J Pathol* **161**, 391–397.
- [49] Santner SJ, Dawson PJ, Tait L, Soule HD, Eliason J, Mohamed AN, Wolman SR, Heppner GH, and Miller FR (2001). Malignant MCF10CA1 cell lines derived from premalignant human breast epithelial MCF10AT cells. *Breast Cancer Res Treat* **65**, 101–110.
- [50] Wolman SR, Mohamed AN, Heppner GH, and Soule HD (1994). Chromosomal markers of immortalization in human breast epithelium. *Genes Chromosomes Cancer* **10**, 59–65.
- [51] Miller FR, Soule HD, Tait L, Pauley RJ, Wolman SR, Dawson PJ, and Heppner GH (1993). Xenograft model of progressive human proliferative breast disease. *J Natl Cancer Inst* **85**, 1725–1732.
- [52] Pauley RJ, Soule HD, Tait L, Miller FR, Wolman SR, Dawson PJ, and Heppner GH (1993). The MCF10 family of spontaneously immortalized human breast epithelial cell lines: models of neoplastic progression. *Eur J Cancer Prev* **2** (Suppl 3), 67–76.
- [53] Soule HD, Maloney TM, Wolman SR, Peterson WD Jr, Brenz R, McGrath CM, Russo J, Pauley RJ, Jones RF, and Brooks SC (1990). Isolation and characterization of a spontaneously immortalized human breast epithelial cell line, MCF-10. *Cancer Res* **50**, 6075–6086.
- [54] Rhodes DR, Yu J, Shanker K, Deshpande N, Varambally R, Ghosh D, Barrette A, Pandey A, and Chinnaiyan AM (2004). ONCOMINE: a cancer microarray database and integrated data-mining platform. *Neoplasia* **6**, 1–6.
- [55] Levy-Lahad E, Lahad A, Eisenberg S, Dagan E, Paperna T, Kasinetz L, Catane R, Kaufman B, Beller U, Renbaum P, et al. (2001). A single nucleotide polymorphism in the *RAD51* gene modifies cancer risk in *BRCA2* but not *BRCA1* carriers. *Proc Natl Acad Sci USA* **98**, 3232–3236.
- [56] Wang WW, Spurdle AB, Kolachana P, Bove B, Modan B, Ebbers SM, Suthers G, Tucker MA, Kaufman DJ, Doody MM, et al. (2001). A single nucleotide polymorphism in the 5' untranslated region of *RAD51* and risk of cancer among *BRCA1/2* mutation carriers. *Cancer Epidemiol Biomark Prev* **10**, 955–960.
- [57] Kadouri L, Kote-Jarai Z, Hubert A, Durocher F, Abeliovich D, Glaser B, Hamburger T, Eeles RA, and Peretz T (2004). A single-nucleotide polymorphism in the *RAD51* gene modifies breast cancer risk in *BRCA2* carriers, but not in *BRCA1* carriers or noncarriers. *Br J Cancer* **90**, 2002–2005.
- [58] Rafii S, O'Regan P, Xinarianos G, Azmy I, Stephenson T, Reed M, Meuth M, Thacker J, and Cox A (2002). A potential role for the *XRCC2* R188H polymorphic site in DNA-damage repair and breast cancer. *Hum Mol Genet* **11**, 1433–1438.
- [59] Rodriguez-Lopez R, Osorio A, Ribas G, Pollan M, Sanchez-Pulido L, de la Hoya M, Ruibal A, Zamora P, Arias JI, Salazar R, et al. (2004). The variant E233G of the *RAD51D* gene could be a low-penetrance allele in high-risk breast cancer families without *BRCA1/2* mutations. *Int J Cancer* **110**, 845–849.
- [60] Deans B, Griffin CS, O'Regan P, Jasin M, and Thacker J (2003). Homologous recombination deficiency leads to profound genetic instability in cells derived from *Xrcc2*-knockout mice. *Cancer Res* **63**, 8181–8187.

- [61] Sengupta AK, Kuhrs A, and Muller J (2004). General transcriptional silencing by a Polycomb response element in *Drosophila*. *Development* **131**, 1959–1965.
- [62] Bloyer S, Cavalli G, Brock HW, and Dura JM (2003). Identification and characterization of polyhomeotic PREs and TREs. *Dev Biol* **261**, 426–442.
- [63] Vispe S, Cazaux C, Lesca C, and Defais M (1998). Overexpression of Rad51 protein stimulates homologous recombination and increases resistance of mammalian cells to ionizing radiation. *Nucleic Acids Res* **26**, 2859–2864.
- [64] Yanez RJ and Porter AC (1999). Gene targeting is enhanced in human cells overexpressing hRAD51. *Gene Ther* **6**, 1282–1290.
- [65] Erixon K and Cedervall B (1995). Linear induction of DNA double-strand breakage with X-ray dose, as determined from DNA fragment size distribution. *Radiat Res* **142**, 153–162.
- [66] Hand R (1978). Eucaryotic DNA: organization of the genome for replication. *Cell* **15**, 317–325.
- [67] Jeggo PA, Caldecott K, Pidsley S, and Banks GR (1989). Sensitivity of Chinese hamster ovary mutants defective in DNA double strand break repair to topoisomerase II inhibitors. *Cancer Res* **49**, 7057–7063.

Report

RhoC-GTPase is a novel tissue biomarker associated with biologically aggressive carcinomas of the breast

Celina G. Kleer^{1,5}, Kent A. Griffith^{2,5}, Michael S. Sabel^{3,5}, Gary Gallagher¹, Kenneth L. van Golen^{4,5}, Zhi-Fen Wu^{4,5}, and Sofia D. Merajver^{4,5}

¹Department of Pathology and Internal Medicine; ²Department of Biostatistics and Internal Medicine; ³Department of Surgery and Internal Medicine; ⁴Division of Hematology/Oncology; ⁵Comprehensive Cancer Center, University of Michigan, Ann Arbor, MI, USA

Key words: RhoC, breast cancer, biomarkers, tissue microarrays, inflammatory breast cancer, pathology

Summary

Background. There is a need for reliable predictors of breast cancer aggressiveness that will further refine the staging classification and help guide the implementation of novel therapies. We have identified RhoC as being nearly always overexpressed in the most aggressive form of breast cancer, inflammatory breast cancer (IBC); in subsequent work we identified RhoC to be a promising marker of aggressive behavior in breast cancers less than 1 cm in diameter. We hypothesized that RhoC expression would identify aggressive, non-IBC tumors breast cancer patients at any stage with worse outcomes defined as recurrence and/or metastasis.

Methods. We constructed four high-density tissue microarrays (TMAs) using 801 tissue cores from 280 patients. These tissues represent a wide range of normal breast and breast disease, including intraductal hyperplasia, ductal carcinoma *in situ* (DCIS), invasive carcinomas, and distant metastases. The TMAs were immunostained using a polyclonal anti-RhoC antibody developed in our laboratory. Cytoplasmic RhoC expression was scored as negative, weak, moderate, or strong by a previously validated scoring schema.

Results. RhoC expression increases with breast cancer progression. All samples of normal breast epithelium had negative to weak staining, whereas staining intensity increased in hyperplasia, DCIS, invasive carcinoma, and metastases (Kruskal–Wallis $p < 0.001$). In patients with invasive carcinoma, high RhoC expression was associated with features of aggressive behavior including high histologic grade, positive lymph nodes, and negative hormonal receptor status. High RhoC expression was a predictor of overall survival in patients with breast cancer (log rank test, $p = 0.002$) and was associated with 100% increase in the risk of death as compared to patients with low RhoC expression. Importantly, high RhoC was an independent predictor of poor response to doxorubicin-based chemotherapy with a hazard ratio of 3.1 and a 95% CI of 1.2–7.7 ($p = 0.02$).

Conclusion. RhoC expression increases with breast cancer progression and RhoC protein level in tumor tissue is strongly associated with biologically aggressive invasive carcinomas of the breast. RhoC expression, if validated, may identify patients who are less likely benefit from doxorubicin therapy and suggests RhoC overexpression as a new target for intervention.

Introduction

Breast cancer remains the second most common cause of cancer related deaths for women in the United States [1]. With the most advanced current treatment options, it is a fact that once patients develop distant metastases, they succumb to the disease [2]. The most important prognostic indicators in breast cancer that are in current use in the clinic are components of the staging system, such as primary tumor size and the presence of lymph node metastases [3]. Although these parameters are the most powerful prognostic factors available, they are not as precise as desired in predicting which tumors will recur locally and/or metastasize distally [4]. There are small invasive carcinomas that follow an aggressive clinical

course and large tumors that do not recur or metastasize. Approximately one-third of women with node-negative breast cancer experience recurrences, whereas approximately one-third of patients with positive lymph nodes are free of disease 10 years after the primary tumor diagnosis. In addition to size and lymph nodes, other morphologic features, such as histological grade, vascular invasion, and molecular markers have been investigated for their potential to predict outcome, but in general, they have had limited value so far [4–6]. These data highlight the need for more sensitive and specific markers of aggressive behavior.

Through a modified version of the differential display technique and *in situ* hybridization of breast tissues, we previously identified RhoC, a gene involved in cell

polarity and motility, as being overexpressed in the most lethal form of locally advanced breast cancers, inflammatory breast cancer (IBC) [7]. We demonstrated that RhoC functions as a transforming oncogene for human mammary epithelial cells giving rise to a highly motile and invasive phenotype [8,9]. Invasive breast carcinomas that developed metastases exhibited higher levels of RhoC protein than invasive carcinomas that did not metastasize [10]. This body of work led us to hypothesize that RhoC overexpression may occur early in breast cancer progression and that it may identify a group of invasive, non-IBC tumors with a highly aggressive phenotype.

Methods

Selection of patients and tissue microarray development

Breast tissues were obtained from the Surgical Pathology files at the University of Michigan with Institutional Review Board approval. A total of 280 cases ($n = 801$ tissue microarray elements) were reviewed by the study pathologist (CGK) and arrayed in four high-density tissue microarrays (TMAs), as previously described [11,12]. At least three tissue cores (0.6 mm diameter) were sampled from each block to account for tumor heterogeneity. The TMAs contained the whole spectrum of breast pathology, with samples of normal breast ($n = 76$), intraductal hyperplasia ($n = 26$), ductal carcinoma *in situ* ($n = 22$), invasive carcinoma ($n = 639$), and breast cancer metastases ($n = 38$). The invasive carcinomas were obtained from 233 largely consecutive patients ($n = 639$ tissue microarray elements) with follow-up information at the University of Michigan between 1987 and 1991. Clinical and outcome information on the 233 patients was obtained by chart review performed by the surgeon on the study (MSS) with IRB approval. In our cohort of 233 breast cancer patients, 211 had follow-up information. The median duration of follow-up was 3.6 years (range 15 days–17 years). Clinical and pathological variables were determined following well-established criteria. The histologic grade was assessed according to the method described by Elston and Ellis [13]; angiolymphatic invasion was classified as either present or absent.

Immunohistochemical studies

Immunohistochemistry was performed on the TMAs by using a standard biotin–avidin complex technique and a polyclonal antibody against RhoC that was previously validated by immunoblot and immunohistochemistry [10]. RhoC expression was evaluated at least three times for every tissue microarray element and at least nine times for each tumor, using an internet based tool (TMA Profiler, University of Michigan, Ann Arbor, MI) [11,14]. Using this method, the pathologist is blinded to tumor stage and clinical information. The median value of all measurements from a single individual was used for

subsequent analyses. As observed previously [10], RhoC protein was strongly expressed in the cytoplasm of myoepithelial cells and vascular smooth muscle cells, which served as consistent internal positive controls. Cytoplasmic RhoC expression was scored from 1 to 4 by comparison to the positive internal controls [10,11,15]. Strong, diffuse staining was considered score = 4, whereas moderate and low diffuse staining was scored as 3 and 2, respectively. Negative staining was scored as 1. Based on our previous work dealing with the biological characterization of RhoC as an oncogene, we defined high RhoC expression when there was strong staining (score = 4) and low RhoC expression, when staining was negative, weak, or moderate (scores = 1–3).

Statistical analysis

The association between RhoC protein expression and the pathologic diagnoses of the tissue microarray element was assessed using the general estimating equation. The ordinal expression categories for RhoC were modeled using the multinomial distribution with the cumulative logit link. Tissue microarray elements were clustered by patient. The model calculates the odds of a higher expression score versus a lower score, with the odds ratio and 95% confidence intervals reported.

The median RhoC expression score by patient was calculated for the subset of invasive carcinoma microarray elements. In instances where the calculated median was the midpoint between expression categories, the median was rounded to the higher category. Possible associations between the median RhoC expression score and clinical and pathologic features of the patient were assessed using the cumulative-logit multinomial model. Also called the proportional-odds model, the model calculates the odds of a higher expression score compared to a lower score across the ordinal categories of expression. The appropriateness of the proportional-odds assumption across categories was tested using the χ^2 score test. The odds ratio and 95% confidence intervals are reported.

Overall survival time, time to breast cancer specific mortality, and time to treatment failure were calculated from the date of surgery until the subjects' date of death, date of death due to breast cancer, or the date of diagnosed treatment failure, respectively. Patients experiencing competing events were censored at the date of the competing event. For example, for calculations of breast cancer specific mortality, patients dying from other causes were censored on that date. Treatment failures included the diagnosis of local recurrence and the development of regional and distant metastases. Patients not experiencing any failure events were censored on their last date of follow-up or date of death. The analyzable sample included those patients with primary invasive tumor specimens arrayed for whom clinical follow-up data were available ($N = 211$).

Univariate associations between time-to-event endpoints and the clinical and pathologic characteristics,

which included median RhoC expression, were assessed using the log-rank test statistic. The probability of events was estimated using the product-limit method of Kaplan and Meier. Multivariate associations were modeled using Cox proportional hazards regression. Clinical and pathologic characteristics with univariate log-rank test statistics with *p*-values less than 10% were included in multivariate models. The most parsimonious multivariate models were constructed using backward, stepwise elimination, with a *p*-value less than or equal to 5% necessary for a covariate to be retained. Hazard ratios and 95% confidence intervals are reported.

Results

RhoC protein expression is elevated in breast cancer

On the basis of our previous work characterizing RhoC as an oncogene in IBC and its protein expression in breast tissues, we sought to determine whether RhoC is upregulated as breast cancer develops. To this end, we

evaluated the expression of RhoC protein in a wide range of breast tissues (280 cases, *n* = 801 tissue microarray elements) by immunohistochemistry, to characterize its expression *in situ*. RhoC expression was observed mainly in the cytoplasm (Figure 1(a)), consistent with our previous observations [10]. Invasive breast carcinomas that expressed high levels of RhoC and those that expressed low levels of RhoC were readily apparent. RhoC protein levels were elevated in invasive carcinoma when compared to normal, intraductal hyperplasia, and DCIS (Table 1 and Figure 1). The odds of a higher RhoC expression levels were 2 times, 8 times, 12 times, and 8 times higher than normal epithelium, for intraductal hyperplasia, DCIS, invasive carcinoma, and metastatic deposits, respectively (Table 2).

Elevated RhoC expression is associated with aggressive breast cancer and poor prognosis

By using our breast cancer tissue microarray data, we evaluated the clinical pathological associations of RhoC

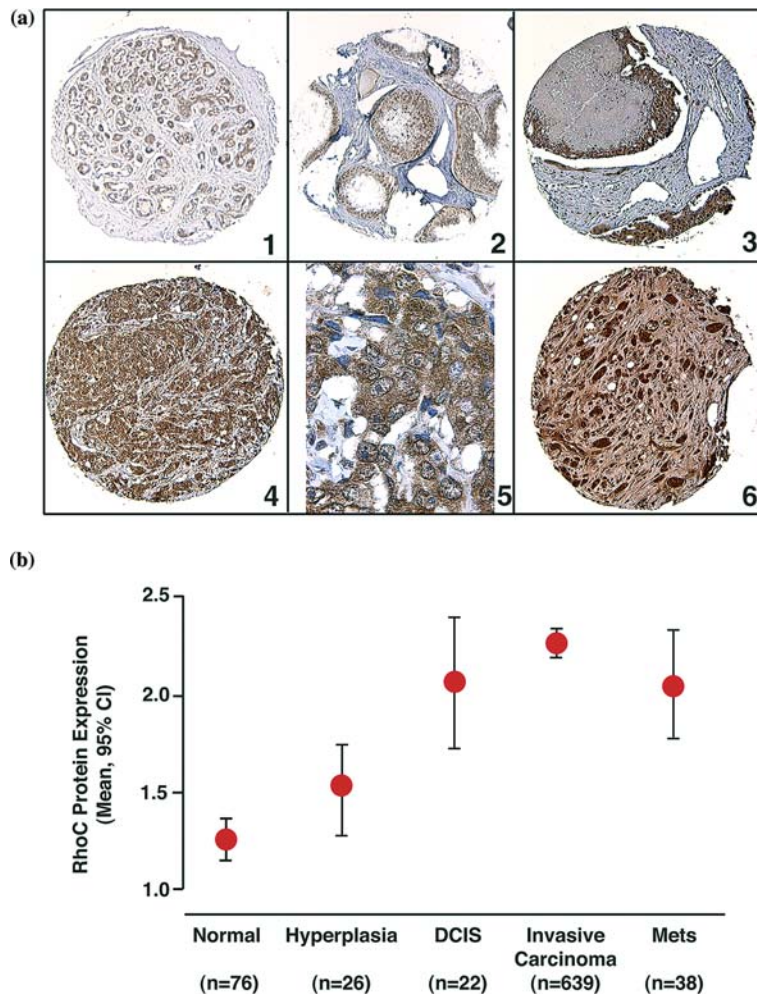


Figure 1. RhoC protein expression increases with breast cancer progression. (a) Tissue microarray samples of a normal breast lobule (1) and intraductal hyperplasia (2) with negative and weak RhoC expression. Ductal carcinoma *in situ* with comedo-necrosis (3) and invasive ductal carcinoma (4) with moderate and high RhoC expression, respectively. High power magnification of an invasive ductal carcinoma showing cytoplasmic accumulation of RhoC protein (5) Metastatic breast carcinoma in bone (6) with high expression of RhoC. (b) Mean RhoC expression increases with the severity of the diagnosis. Original magnification 40× and 100×.

Table 1. Frequency of RhoC protein expression in breast tissue samples as determined by immunohistochemistry

Breast tissue	Cores	Staining intensity, <i>n</i> (%)				Mean intensity
		1	2	3	4	
Normal epithelium	76	58 (76)	16 (21)	2 (3)	0	1.26
Intraductal hyperplasia	26	14 (54)	11 (42)	1 (4)	0	1.50
Ductal carcinoma <i>in situ</i>	22	6 (27)	9 (41)	7 (32)	0	2.05
Invasive carcinoma	639	140 (22)	249 (39)	203 (32)	47 (7)	2.25
Metastasis	38	12 (32)	13 (34)	13 (34)	0	2.03
Total	801					2.11

Table 2. Odds of higher RhoC expression according to the tissue diagnosis

Diagnosis	Odds ratio	95% CI	<i>p</i> -Value
Normal epithelium	1.00		
Intraductal hyperplasia	2.46	1.01–6.00	0.0487
Ductal carcinoma <i>in situ</i>	8.41	3.35–21.14	<0.0001
Invasive carcinoma	12.16	7.00–21.14	<0.0001
Metastasis	8.03	3.64–17.70	<0.0001

protein levels in breast cancer. In our cohort of 233 breast cancer patients ($n = 801$ samples), 211 had follow-up information. The median age of the study population was 58 years (range 28–99 years). The clinical and pathological characteristics of the patients are summarized in Table 3. The breakdown of treatment modalities in this group of patients is summarized in Table 4. Ninety-three patients (44.1%) received chemotherapy following surgery. In 90 of 93 patients (97%) the treatment consisted of a doxorubicin and cyclophosphamide combination regimen, with the remaining three patients receiving taxol alone.

After a median follow-up of 3.6 years (range: 15 days–17 years), 42 of the 226 patients (18.6%) died of breast cancer. The 5- and 10-year disease specific survival rates for the entire cohort of patients were 60% and 38%, respectively.

High RhoC expression was present in a subset of invasive carcinomas (13 of 211, 6.2%). The association between RhoC protein levels and clinical characteristics is shown on Table 5. RhoC expression was strongly associated with the presence of positive axillary lymph nodes (Fisher's exact test, $p = 0.0026$), one of the strongest known predictors of survival. High RhoC expression was also associated with increasing histologic tumor grade (Fisher's exact test, $p = 0.016$), a measure of the degree of tumor differentiation and poor prognostic indicator. Grade II and III tumors were three and six times more likely to have a high RhoC expression when compared to grade I tumors, respectively. High RhoC expression was associated with negative estrogen receptor status (Fisher's exact test, $p = 0.033$) and negative progesterone receptor status (Fisher's exact test, $p = 0.004$). Notably, despite the small number of tumors, RhoC overexpression was strongly associated

with features of poor outcome in patients with breast cancer.

We next investigated the prognostic value of RhoC protein expression by interrogating the dataset about its prediction of aspects of the outcome in patients with newly diagnosed breast cancer. As expected, at the univariate level, the stage of disease, lymph node status, and histological tumor grade were associated with overall and disease-specific survival (Tables 6 and 7). Hormone receptor status was inversely associated with outcome. We found a strong and consistent association between RhoC protein levels and overall patient outcome. Higher RhoC protein levels were associated with all the important clinical outcomes that comprise 'poor prognosis': shorter disease-free interval after initial surgical treatment, lower overall survival, and a high probability of breast cancer-specific death (Figure 2). The 10-year overall survival for patients with tumors expressing high RhoC levels was 23% and by contrast to 53% for low levels of RhoC (log rank, $p = 0.002$, Figure 2b).

The best multivariable model predictive of overall survival included tumor stage, negative PR, the presence of vascular invasion, and treatment with radiotherapy, chemotherapy and tamoxifen (Table 8). High RhoC expression was a marginally significant independent predictor of outcome. Patients with high RhoC levels had a 100% higher risk of death when compared to patients with low RhoC expression (hazard ratio 2, 95% CI 1.0–4.1, $p = 0.067$).

RhoC is a promising predictive factor of response to doxorubicin-based chemotherapy

In our cohort of 211 breast cancer patients, 93 (44.1%) received adjuvant chemotherapy consisting in 90 of the 93 patients of a doxorubicin and cyclophosphamide combination regimen (Table 4). We sought to determine whether RhoC expression could predict survival in chemotherapy treated patients. Tumor stage, positive lymph node status, estrogen and progesterone receptor status, lymphovascular invasion, tamoxifen use, and median RhoC expression all had significant univariate associations with survival for chemotherapy treated patients. The multivariate model indicates that median RhoC expression was found to be independently

Table 3. Clinico-pathologic characteristics of the 211 patients with invasive carcinomas

Characteristics	N (%) [†]
Race	
White	172 (81.5)
Black	26 (12.3)
Other/Unknown	13 (6.2)
Menopause status	
Pre	43 (20.4)
Peri	19 (9.0)
Post	129 (61.1)
Unknown	20 (9.5)
Breast cancer type	
Ductal	149 (70.6)
Lobular	19 (9.0)
Ductal and Lobular	9 (4.3)
Other/Unknown	34 (16.1)
Tumor stage	
I	65 (30.8)
II	72 (34.1)
III	47 (22.3)
IV	5 (2.4)
Unknown	22 (10.4)
Tumor size (cm)	
≤ 2	109 (51.7)
> 2	85 (40.3)
Unknown	17 (8.0)
Tumor grade	
I	24 (11.4)
II	92 (43.6)
III	77 (36.5)
Unknown	18 (8.5)
Estrogen receptor	
Positive	137 (64.9)
Negative	68 (32.2)
Unknown	6 (2.8)
Progesterone receptor	
Positive	113 (53.6)
Negative	92 (43.6)
Unknown	6 (2.8)
Her2/Neu status	
Positive over expressed	36 (17.7)
Negative not over expressed	165 (77.6)
Unknown	10 (4.7)
Lymphovascular invasion	
Present	61 (28.9)
Absent	147 (69.7)
Unknown	3 (1.4)
Lymph nodes	
Negative	92 (43.6)
1–3 positive nodes	46 (21.8)
> 4 positive nodes	39 (18.5)
Unknown	34 (16.1)

Table 3. Continued

Characteristics	N (%) [†]
Median RhoC expression	
1	33 (15.6)
2	94 (44.6)
3	71 (33.7)
4	13 (6.2)

Table 4. Treatment characteristics of the patients with invasive carcinomas (N = 211)

Characteristics	N (%) [†]
Neoadjuvant chemotherapy	
Yes	17 (8.1)
No	192 (91.0)
Unknown	2 (0.9)
Surgery type	
Mastectomy	132 (62.6)
Lumpectomy	74 (35.1)
None/Unknown	5 (2.4)
Adjuvant chemotherapy	
Yes	93 (44.1)
No	108 (51.2)
Unknown	10 (4.7)
Adjuvant radiotherapy	
Yes	95 (45.0)
No	104 (49.3)
Unknown	12 (5.7)
Tamoxifen therapy	
Yes	96 (45.5)
No	99 (46.9)
Unknown	16 (7.6)

associated with overall survival following chemotherapy, with a hazard ratio of 3.1 and a 95% CI of 1.2–7.7 ($p = 0.0176$) (Table 9).

Discussion

In this study based on unselected patients with primary invasive carcinomas of the breast treated by standard of care at our institution between 1987 and 1991, we tested the hypothesis that RhoC protein levels are associated with highly aggressive breast cancer. Furthermore, we examined the expression of RhoC in the whole spectrum of breast tissues, ranging from normal breast, intra-ductal hyperplasia, ductal carcinoma *in situ*, invasive carcinomas, and breast cancer metastases. We found that a high level (4+) of RhoC protein is present only in invasive carcinomas and not present in normal breast epithelium, hyperplasia, or ductal carcinoma *in situ*. RhoC protein expression increased steadily from normal breast, to fibrocystic changes, to DCIS, and invasive carcinomas. The strongest RhoC expression was observed in locally advanced breast cancer and in

Table 5. Association of RhoC expression with other clinical and pathologic features

Characteristic:	Fisher's exact <i>p</i> -value	Median RhoC Staining Intensity, <i>N</i> (%)			
		1	2	3	4
Tumor stage:	0.8520				
1		11 (33.3)	33 (35.1)	17 (23.9)	4 (30.8)
2		10 (30.3)	29 (30.9)	29 (40.9)	4 (30.8)
3		9 (27.3)	17 (18.1)	17 (23.9)	4 (30.8)
4		0	3 (3.2)	2 (2.8)	0
Tumor size (cm):	0.5792				
≤ 2		11 (33.3)	38 (40.4)	32 (45.1)	4 (30.8)
>2		19 (57.6)	51 (54.3)	32 (45.1)	7 (53.9)
Tumor grade:	0.0166				
I		8 (24.2)	13 (13.8)	3 (4.2)	0
II		14 (42.4)	43 (45.7)	31 (43.7)	4 (30.8)
III		9 (27.3)	29 (30.9)	30 (42.3)	9 (69.2)
Positive lymph nodes:	0.0026				
Zero		16 (48.5)	45 (47.9)	26 (36.6)	5 (38.5)
1–3		4 (12.1)	19 (20.2)	21 (29.6)	2 (15.4)
4+		9 (27.3)	10 (10.6)	16 (22.5)	4 (30.8)
Lymphovascular invasion:	0.6962				
Present		10 (30.3)	23 (24.5)	22 (31.0)	6 (46.2)
Absent		23 (69.7)	69 (73.4)	48 (67.6)	7 (53.9)
Estrogen receptor:	0.0336				
Positive		23 (69.7)	65 (69.2)	46 (64.8)	3 (23.1)
Negative		10 (30.3)	26 (27.7)	22 (31.0)	10 (76.9)
Progesterone receptor:	0.0043				
Positive		22 (66.7)	55 (58.5)	35 (49.3)	1 (7.7)
Negative		11 (33.3)	35 (37.2)	34 (47.9)	12 (92.3)
Her2/Neu expression:	0.6965				
Positive		4 (12.1)	15 (15.9)	15 (21.1)	2 (15.4)
Negative		29 (87.9)	73 (77.6)	52 (73.2)	11 (84.6)

metastatic breast cancer. These findings suggest that accumulation of RhoC protein is an early and progressive event in the development of breast cancer, thereby justifying efforts aimed at developing novel therapeutic interventions that may prevent the increase in RhoC protein expression.

In the group of patients with invasive carcinomas, very high RhoC expression occurred in a small subset (13 of 211, 6.2%). However, those patients with high levels of RhoC protein in the tumor cells had uniformly a worse outcome than patients with low RhoC expression, despite of aggressive multimodality treatment. Consistently, high RhoC expression was associated with positive lymph nodes, higher histologic grade, and with negative ER and PR protein expression, all known markers of more aggressive disease. Patients with high RhoC expression had a 5- and 10-year overall survival of 57.5% and 23%, respectively, in contrast to patients with low RhoC expression, who had a 5- and 10-year overall survival of 70.5% and 53%, respectively (log rank test, $p = 0.002$). In the multivariable Cox regression analysis, patients with high RhoC levels had 100% increase in the risk of

death as compared to patients with low RhoC levels (hazard ratio of 2, 95% CI of 1–4.1, $p = 0.067$). This suggests that RhoC overexpression is a specific alteration that occurs infrequently in early breast cancer, but when present, it signals a biologically aggressive tumor phenotype with high likelihood of recurrence and poor survival despite different treatment interventions. We suggest that this finding is clinically highly relevant and, if further validated, it may be the basis of a new clinically applicable test.

Notably, when we analyzed the predictive value of RhoC in a group of breast cancer patients treated uniformly with a combination regimen of doxorubicin and cyclophosphamide, high RhoC levels were independently associated with overall survival after chemotherapy. Although the number of patients with high RhoC expression is low overall, our data suggest that RhoC may identify a small group of patients who have a poor survival despite doxorubicin-based chemotherapy. This is clinically relevant because, if further validated in a larger cohort of uniformly treated patients, it may identify patients who might benefit from other chemotherapeutic agents or alternative molecular

Table 6. Univariate analysis of overall survival

Characteristic	5-year		10-year		Log-rank <i>p</i> -value
	Estimate	95% CI	Estimate	95% CI	
Tumor stage					<0.0001
1	83.5	73.5–93.5	71.8	59.0–84.6	
2	78.2	68.0–88.4	53.2	40.0–66.4	
3 or 4	47.5	33.3–61.5	33.3	19.0–47.8	
Estrogen receptor					0.0078
Positive	75.0	66.9–83.0	55.8	45.9–65.7	
Negative	57.0	44.7–62.3	39.4	26.6–52.2	
Progesterone					0.0001
Positive	80.1	71.9–88.3	62.4	51.7–73.0	
Negative	57.0	46.3–67.7	37.4	26.2–48.5	
Lymphovascular invasion					0.0080
Absent	74.1	66.2–82.0	59.4	50.1–68.8	
Present	59.9	47.4–72.3	34.7	21.6–47.9	
Tumor grade					0.0245
I/II	78.1	69.9–86.4	58.8	48.2–69.3	
III	60.2	48.9–71.5	42.0	30.1–54.0	
Positive lymph nodes					0.0010
Zero	82.4	73.9–90.9	66.5	55.3–77.7	
1–3	78.1	65.3–90.8	56.3	39.7–72.9	
4+	53.7	37.3–70.0	37.4	19.8–54.9	
Tamoxifen use					0.0447
Yes	83.4	75.4–91.5	61.1	49.4–72.7	
No	62.0	52.1–71.9	45.1	34.5–55.8	
Median RhoC expression					0.0209
1	80.8	65.1–96.5	58.0	35.9–80.1	
2	69.3	59.6–79.1	48.5	37.4–59.7	
3	67.6	55.8–79.5	56.9	43.7–70.1	
Low (1, 2, or 3)	70.5	63.7–77.3	52.9	44.9–60.9	
High (4)	57.5	28.9–86.1	23.0	0.0–50.2	

therapies. More research is needed in this direction to further define the prognostic utility of RhoC.

The clinical significance of elevated RhoC protein in breast cancer is linked to and completely consistent with its biological functions. RhoC is a ras homology gene, with highly conserved motifs and shares a high degree of homology to RhoA, another member of the family [16–18]. Rho proteins in general, and RhoC and RhoA in particular, are involved in cytoskeletal reorganization, specifically in the formation of actin stress fibers and focal adhesion contacts [16–18]. When immortalized human mammary epithelial cells are transfected with RhoC, they undergo a striking change in the cytoplasmic shape and they become motile and invasive [9]. In our laboratory, we discovered the strong link between RhoC overexpression and inflammatory breast cancer, the most aggressive form of locally advanced breast cancer known [7–9,19]. Thus, it is not surprising that RhoC overexpression occurs in a small group of biologically aggressive non-IBC tumors with high propensity to recur and metastasize and which respond poorly to doxorubicin-based adjuvant treatment.

Recently, Rho proteins have been implicated in breast tubulogenesis and differentiation, probably through reg-

ulation of cell contractility [20]. Our descriptive observations support this notion since RhoC protein levels increased with decreasing differentiation of the invasive carcinomas. For example, well-differentiated invasive carcinomas with prominent tubule formation, monotonous appearing cells, and rare mitoses expressed little or no RhoC protein whereas poorly differentiated carcinomas that grew in disorganized sheets of pleomorphic malignant cells and exhibited a brisk mitotic activity expressed high levels of RhoC protein.

Since our initial reports of RhoC overexpression in breast cancer our findings have been supported by other investigations. RhoC overexpression has been found in malignancies derived from different cell lineages including non-small cell lung carcinoma, hepatocellular carcinoma, ovarian carcinoma, melanoma, pancreatic carcinoma, and gastric carcinoma [7,10,21–29]. In these malignancies, RhoC has been implicated in neoplastic transformation, progression, invasion, and metastases. Taken together, these data suggest that RhoC may be involved in a global, rather than a tissue type specific mechanism of tumor progression.

Rho proteins are prenylated in order to exert their functions and to localize appropriately to the sub

Table 7. Univariate analysis of disease free survival

Characteristic	5-year		10-year		Log-rank <i>p</i> -value
	Estimate	95% CI	Estimate	95% CI	
Tumor stage					< 0.0001
1	96.1	90.8–100	90.6	81.8–100	
2	85.7	77.0–94.4	67.3	54.0–80.5	
3 or 4	59.4	44.3–74.4	48.2	31.5–64.9	
Tumor size (cm)					0.0500
≤ 2	90.0	83.2–96.7	81.1	71.5–90.7	
> 2	74.3	64.3–84.3	66.5	55.0–78.1	
Tumor grade					0.0500
I/II	90.6	84.7–96.6	77.8	68.1–87.5	
III	69.3	58.3–80.3	59.5	47.2–71.9	
Positive lymph nodes					< 0.0001
Zero	93.5	87.9–99.0	86.0	77.3–94.7	
1–3	82.3	70.4–94.3	67.8	51.5–84.2	
4+	62.0	45.4–78.6	46.5	26.9–66.1	
Estrogen receptor					0.0041
Positive	86.6	80.1–93.0	74.5	65.4–83.7	
Negative	64.9	52.4–77.3	54.4	40.4–68.6	
Progesterone					0.0003
Positive	92.4	86.9–97.9	79.4	69.8–89.1	
Negative	65.1	54.3–75.8	55.2	43.1–67.4	
Lymphovascular invasion					< 0.0001
Absent	87.0	80.8–93.3	79.3	71.0–87.5	
Present	64.4	51.8–76.9	47.3	32.8–61.8	
Tamoxifen use					0.0121
Yes	87.8	80.7–95.0	80.9	71.6–90.2	
No	74.9	65.8–84.1	60.2	48.9–71.6	
Median RhoC expression					0.0736
1	92.1	83.1–100	72.7	51.4–94.0	
2	80.2	71.4–89.0	72.8	62.2–83.4	
3	78.7	68.3–89.1	68.6	55.7–81.6	
Low (1, 2, or 3)	81.5	75.5–87.4	71.6	63.9–79.2	
High (4)	64.7	36.2–93.2	32.4	0.0–67.1	

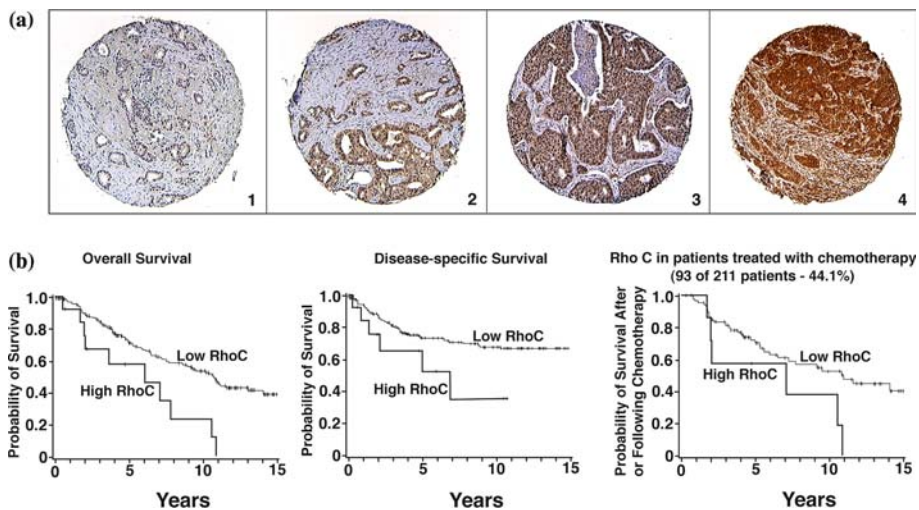


Figure 2. RhoC protein expression is associated with survival in patients with breast cancer. (a) Tissue microarray elements containing representative invasive carcinomas with negative (1), weak (2), moderate (3), and strong (4) RhoC staining intensities. Original magnification 40 \times . (b) High RhoC expression in invasive carcinomas is associated with worse overall, disease-free, and survival following doxorubicin and cyclophosphamide treatment.

Table 8. Best multivariate model predicting overall survival

Patient/tumor characteristic	HR	95% CI	p-Value
Tumor stage			
1	1.0		
2	2.2	1.2–4.0	0.0119
3 or 4	5.6	2.7–11.5	<0.0001
Lymphovascular invasion			
Absent	1.0		
Present	1.7	0.1–2.7	0.0274
Progesterone receptor			
Positive	1.0		
Negative	1.9	1.2–3.1	0.0059
Median RhoC			
Low expression	1.0		
High expression	2.0	1.0–4.1	0.0670
Radiotherapy			
No	1.0		
Yes	0.6	0.4–1.0	0.0543
Chemotherapy			
No	1.0		
Yes	0.3	0.2–0.6	0.0001
Tamoxifen			
No	1.0		
Yes	0.5	0.3–0.8	0.0030

Table 9. Best multivariate model predicting overall survival for patients receiving chemotherapy

Patient/tumor characteristic	HR	95% CI	p-value
Tumor stage			
1	1.0		
2	1.2	0.3–4.3	0.8114
3 or 4	4.2	1.3–13.9	0.0194
Median RhoC			
Low expression	1.0		
High expression	3.1	1.2–7.7	0.0176
Tamoxifen			
No	1.0		
Yes	0.4	0.2–0.9	0.0374

cytoplasmic membrane space [30–34]. Prenylation can be inhibited by farnesyl transferase inhibitors (FTIs) and FTIs are effective in modulating tumor growth in ras-transformed tumor cells [35–39]. Our group has previously found that FTIs were able to reverse of the RhoC-induced phenotype (even though RhoC is not itself farnesylated), manifested by a significant decrease in anchorage-independent growth, motility, and invasion [39]. Thus, we suggested that FTIs may be useful therapeutic compounds in RhoC overexpressing tumors. Another potentially useful strategy against RhoC phenotypes is represented by the HMGCoA (3-hydroxy-3-methylglutaryl-CoA) reductase inhibitors (statins). In particular, atorvastatin has been clearly shown to inhibit RhoC driven phenotypes in melanoma cells [40].

In summary, we discovered that RhoC expression increases with breast cancer progression and that it is associated with markers of aggressive disease and poor survival. Importantly, we found that RhoC overexpression is a negative predictor of response to doxorubicin and cyclophosphamide. This work supports that RhoC may have a role in the genesis of a highly aggressive doxorubicin resistant breast cancer phenotype. Our finding that RhoC overexpression is an infrequent and specific marker of aggressive breast cancer with poor outcome despite treatment may have important clinical implications. Specifically, RhoC detection at the time of primary tumor diagnosis may, in the future, aid clinicians in guiding treatment and paves the way to the development of targeted treatments. While our results are promising, RhoC expression needs to be validated in relationship to outcome in the context of cohorts treated in controlled clinical trials where all patients are treated uniformly. If confirmed, application of RhoC immunohistochemical analysis would be technically straightforward and feasible.

Acknowledgements

Supported in part by Army grants DAMD17-02-1-0490 (CGK), DAMD17-02-1-491 (CGK), DAMD-17-00-1-0345 (SDM), NIH grants K08 CA 090876 (CGK), RO1CA10746 (CGK), RO1CA77612 (SDM), 1 P50-CADE97258 (SDM), and a grant from the John Suzanne Munn Endowed Research Fund of the University of Michigan Comprehensive Cancer Center (CGK), and NIH grant 5 P30 CA46592 (University of Michigan Cancer Center Support Grant).

References

- Jemal A, Murray T, Samuels A, Ghafoor A, Ward E, Thun MJ: Cancer statistics CA Cancer J Clin 53: 5–26, 2003
- Ellis M, Hayes D, Lippman M: Treatment of metastatic disease. In: Harris J, Lippman ME, Morrow M (eds) Diseases of the Breast. Lippincott-Raven, Philadelphia 2000, pp. 749–798
- Hayes DF, Isaacs C, Stearns V: Prognostic factors in breast cancer: current and new predictors of metastasis J Mammary Gland Biol Neoplasia 6: 375–392, 2001
- Hayes DF, Trock B, Harris AL: Assessing the clinical impact of prognostic factors: when is “statistically significant” clinically useful? Breast Cancer Res Treat 52: 305–319, 1998
- Clark GM: Prognostic and predictive factors. In: Harris LM, J, Morrow M, Hellman S (eds) , Diseases of the Breast. Lippincott-Raven Publishers, Philadelphia 1996, pp. 461–485
- Hayes : Do we need prognostic factors in nodal-negative breast cancer? Arbieter Eur J Cancer 36: 302–306, 2000
- Golen KLvan, Davies S, Wu ZF, Wang Y, Bucana CD, Root H, Chandrasekharappa S, Strawderman M, Ethier SP, Merajver SD: A novel putative low-affinity insulin-like growth factor-binding protein, LIBC (lost in inflammatory breast cancer), and RhoC GTPase correlate with the inflammatory breast cancer phenotype Clin Cancer Res 5: 2511–2519, 1999

8. Golen KLvan, Wu ZF, Qiao XT, Bao L, Merajver SD: RhoC GTPase overexpression modulates induction of angiogenic factors in breast cells *Neoplasia* 2: 418–425, 2000
9. Golen KLvan, Wu ZF, Qiao XT, Bao LW, Merajver SD: RhoC GTPase, a novel transforming oncogene for human mammary epithelial cells that partially recapitulates the inflammatory breast cancer phenotype *Cancer Res* 60: 5832–5838, 2000
10. Kleer CG, Golen KLvan, Zhang Y, Wu ZF, Rubin MA, Merajver SD: Characterization of RhoC expression in benign and malignant breast disease: a potential new marker for small breast carcinomas with metastatic ability *Am J Pathol* 160: 579–584, 2002
11. Kleer CG, Cao Q, Varambally S, Shen R, Ota I, Tomlins SA, Ghosh D, Sewalt RG, Otte AP, Hayes DF, Sabel MS, Livant D, Weiss SJ, Rubin MA, Chinnaiyan AM: EZH2 is a marker of aggressive breast cancer and promotes neoplastic transformation of breast epithelial cells *Proc Natl Acad Sci USA* 100: 11606–11611, 2003
12. Perrone EE, Theoharis C, Mucci NR, Hayasaka S, Taylor JM, Cooney KA, Rubin MA: Tissue microarray assessment of prostate cancer tumor proliferation in African-American and white men *J Natl Cancer Inst* 92: 937–939, 2000
13. Elston EW, Ellis IO: Method for grading breast cancer *J Clin Pathol* 46: 189–190, 1993
14. Manley S, Mucci NR, Marzo AMDe, Rubin MA: Relational database structure to manage high-density tissue microarray data and images for pathology studies focusing on clinical outcome: the prostate specialized program of research excellence model *Am J Pathol* 159: 837–843, 2001
15. Rhodes DR, Sanda MG, Otte AP, Chinnaiyan AM, Rubin MA: Multiplex biomarker approach for determining risk of prostate-specific antigen-defined recurrence of prostate cancer *J Natl Cancer Inst* 95: 661–668, 2003
16. Nobes CD, Hall A: Rho, rac, and cdc42 GTPases regulate the assembly of multimolecular focal complexes associated with actin stress fibers, lamellipodia, and filopodia *Cell* 81: 53–62, 1995
17. Hall A, Nobes CD: Rho GTPases molecular switches that control the organization and dynamics of the actin cytoskeleton *Philos Trans R Soc Lond B Biol Sci* 355: 965–970, 2000
18. Leung T, Chen XQ, Manser E, Lim L: The p160 RhoA-binding kinase ROK alpha is a member of a kinase family and is involved in the reorganization of the cytoskeleton *Mol Cell Biol* 16: 5313–5327, 1996
19. Kleer CG, Zhang Y, Pan Q, Gallagher G, Wu M, Wu ZF, Merajver SD: WISP3 and RhoC guanosine triphosphatase cooperate in the development of inflammatory breast cancer *Breast Cancer Res* 6: R110–R115, 2004
20. Wozniak MA, Desai R, Solski PA, CJDer, Keely PJ: ROCK-generated contractility regulates breast epithelial cell differentiation in response to the physical properties of a three-dimensional collagen matrix *J Cell Biol* 163: 583–595, 2003
21. Suwa H, Ohshio G, Imamura T, Watanabe G, Arai S, Imamura M, Narumiya S, Hiai H, Fukumoto M: Overexpression of the RhoC gene correlates with progression of ductal adenocarcinoma of the pancreas *Br J Cancer* 77: 147–152, 1998
22. Horiuchi A, Imai T, Wang C, Ohira S, Feng Y, Nikaido T, Konishi I: Up-regulation of small GTPases, RhoA and RhoC, is associated with tumor progression in ovarian carcinoma *Lab Invest* 83: 861–870, 2003
23. Kamai T, Tsujii T, Arai K, Takagi K, Asami H, Ito Y, Oshima H: Significant association of Rho/ROCK pathway with invasion and metastasis of bladder cancer *Clin Cancer Res* 9: 2632–2641, 2003
24. Kondo T, Sentani K, Oue N, Yoshida K, Nakayama H, Yasui W: Expression of RHOC is associated with metastasis of gastric carcinomas *Pathobiology* 71: 19–25, 2004
25. Shikada Y, Yoshino I, Okamoto T, Fukuyama S, Kameyama T, Maehara Y: Higher expression of RhoC is related to invasiveness in non-small cell lung carcinoma *Clin Cancer Res* 9: 5282–5286, 2003
26. Wang W, Yang LY, Yang ZL, Huang GW, Lu WQ: Expression and significance of RhoC gene in hepatocellular carcinoma *World J Gastroenterol* 9: 1950–1953, 2003
27. Ikoma T, Takahashi T, Nagano S, Li YM, Ohno Y, Ando K, Fujiwara T, Fujiwara H, Kosai K: A definitive role of RhoC in metastasis of orthotopic lung cancer in mice *Clin Cancer Res* 10: 1192–1200, 2004
28. Clark EA, Golub TR, Lander ES, Hynes RO: Genomic analysis of metastasis reveals an essential role for RhoC *Nature* 406: 532–535, 2000
29. Carr KM, Bittner M, Trent JM: Gene-expression profiling in human cutaneous melanoma *Oncogene* 22: 3076–3080, 2003.
30. Seabra MC: Membrane association and targeting of prenylated Ras-like GTPases *Cell Signal* 10: 167–172, 1998
31. Kirschmeier PT, Whyte D, Wilson O, Bishop WR, Pai JK: *In vivo* prenylation analysis of Ras and Rho proteins *Methods Enzymol* 332: 115–127, 2001
32. Adamson P, Marshall CJ, Hall A, Tilbrook PA: Post-translational modifications of p21rho proteins *J Biol Chem* 267: 20033–20038, 1992
33. Sinensky M: Recent advances in the study of prenylated proteins *Biochim Biophys Acta* 1484: 93–106, 2000
34. Bishop AL, Hall A: Rho GTPases and their effector proteins *Biochem J* 348 (Pt2): 241–255 2000
35. Omer CA, Chen Z, Diehl RE, Conner MW, Chen HY, Trumbauer ME, Gopal-Truter S, Seeburger G, Bhimnathwala H, Abrams MT, Davide JP, Ellis MS, Gibbs JB, Greenberg I, Koblan KS, Kral AM, Liu D, Lobell RB, Miller PJ, Mosser SD, O'Neill TJ, Rands E, Schaber MD, Senderak ET, Oliff A, Kohl NE: Mouse mammary tumor virus-Ki-rasB transgenic mice develop mammary carcinomas that can be growth-inhibited by a farnesyl:protein transferase inhibitor *Cancer Res* 60: 2680–2688, 2000
36. Prendergast GC, Khosravi-Far R, Solski PA, Kurzawa H, Lebowitz PF, CJDer: Critical role of Rho in cell transformation by oncogenic Ras *Oncogene* 10: 2289–2296, 1995
37. Prendergast GC, Davide JP, deSolms SJ, Giuliani EA, Graham SL, Gibbs JB, Oliff A, Kohl NE: Farnesyltransferase inhibition causes morphological reversion of ras-transformed cells by a complex mechanism that involves regulation of the actin cytoskeleton *Mol Cell Biol* 14: 4193–4202, 1994
38. Lebowitz PF, Casey PJ, Prendergast GC, Thissen JA: Farnesyltransferase inhibitors alter the prenylation and growth-stimulating function of RhoB *J Biol Chem* 272: 15591–15594, 1997
39. van Golen KL, Bao L, DiVito MM, Wu Z, Prendergast GC, Merajver SD: Reversion of RhoC GTPase-induced inflammatory breast cancer phenotype by treatment with a farnesyl transferase inhibitor *Mol Cancer Ther* 1: 575–583, 2002
40. Collisson EA, Kleer C, Wu M, De A, Gambhir SS, Merajver SD, Kolodney MS: Atorvastatin prevents RhoC isoprenylation, invasion, and metastasis in human melanoma cells *Mol Cancer Ther* 2: 941–948, 2003

Address for offprints and correspondence: C.G. Kleer, 2G332 University Hospital, 1500 E. Medical Center Dr., Ann Arbor, MI 48109-0054; *Tel.:* +1-734-936-6775; *Fax:* +1-734-615-3441; *E-mail:* Kleer@umich.edu

Research article

Open Access

Inhibition of CCN6 (WISP3) expression promotes neoplastic progression and enhances the effects of insulin-like growth factor-1 on breast epithelial cellsYanhong Zhang¹, Quintin Pan^{2,3}, Hui Zhong¹, Sofia D Merajver^{2,3} and Celina G Kleer^{1,3}¹Department of Pathology, University of Michigan Medical Center, 1150 W Medical Center Drive, Ann Arbor, MI 48109, USA²Department of Internal Medicine, Division of Hematology/Oncology, University of Michigan Medical Center, 1500 E. Medical Center Dr., Ann Arbor, MI 48109, USA³Comprehensive Cancer and Geriatrics Center, University of Michigan Medical Center, 1500 E. Medical Center Dr. Ann Arbor, MI 48109, USACorresponding author: Celina G Kleer, kleer@umich.edu

Received: 29 Aug 2005 Revisions requested: 15 Sep 2005 Revisions received: 3 Oct 2005 Accepted: 13 Oct 2005 Published: 8 Nov 2005

Breast Cancer Research 2005, **7**:R1080-R1089 (DOI 10.1186/bcr1351)This article is online at: <http://breast-cancer-research.com/content/7/6/R1080>© 2005 Zhang *et al.*; licensee BioMed Central Ltd.This is an open access article distributed under the terms of the Creative Commons Attribution License (<http://creativecommons.org/licenses/by/2.0>), which permits unrestricted use, distribution, and reproduction in any medium, provided the original work is properly cited.**Abstract**

Introduction CCN6/WISP3 belongs to the CCN (Cyr61, CTGF, Nov) family of genes that contains a conserved insulin-like growth factor (IGF) binding protein motif. CCN6 is a secreted protein lost in 80% of the aggressive inflammatory breast cancers, and can decrease mammary tumor growth *in vitro* and *in vivo*. We hypothesized that inhibition of CCN6 might result in the loss of a growth regulatory function that protects mammary epithelial cells from the tumorigenic effects of growth factors, particularly IGF-1.

Method We treated human mammary epithelial (HME) cells with a CCN6 hairpin short interfering RNA.

Results CCN6-deficient cells showed increased motility and invasiveness, and developed features of epithelial-mesenchymal transition (EMT). Inhibition of CCN6 expression promoted anchorage-independent growth of HME cells and rendered them more responsive to the growth effects of IGF-1, which was coupled with the increased phosphorylation of IGF-1 receptor and insulin receptor substrate-1 (IRS-1).

Conclusion Specific stable inhibition of CCN6 expression in HME cells induces EMT, promotes anchorage-independent growth, motility and invasiveness, and sensitizes mammary epithelial cells to the growth effects of IGF-1.

Introduction

Wnt-1-induced secreted protein 3 (CCN6/WISP3) is a cysteine-rich protein that belongs to the CCN (Cyr61, CTGF, Nov) family of genes, which also contains five other members: CC1 (connective tissue growth factor or CTGF), CCN2 (Cyr61), CCN3 (Nov), CCN4 (WISP1) and CCN5 (WISP2) [1-3]. CCN4, the first cloned member of the WISP proteins was discovered because it was upregulated in the mouse mammary epithelial cell line C57MG transformed by Wnt-1 [2]. CCN6 shares high sequence homology to CCN4, although there is no evidence that CCN6 is induced by Wnt-1 signaling [2]. CCN growth factors are mostly secreted and extracellular matrix-associated proteins that regulate important functions including cellular differentiation and development, cell proliferation, survival, angiogenesis, cell migration and

adhesion [2-6]. CCN proteins interact with key signaling molecules such as cell surface integrins, NOTCH1, fibulin C, S100A4, and ion channels [7-12].

CCN proteins contain an N-terminal secretory signal, followed by four distinct motifs with homology to insulin-like growth factor (IGF)-binding protein; von Willebrand factor type C; thrombospondin 1 (TSP1); and a C-terminal region with heparin-binding motifs and sequence similarities to the C termini of von Willebrand factor and mucins, the latter also being present in other growth factors such as transforming growth factor- β , platelet-derived growth factor, and nerve growth factor [1,2,9]. It is becoming increasingly evident that CCN proteins function in a cell-type-specific and tissue-type-specific manner. For example, increased expression of CCN3 (Nov) was correlated

bp = base pair; EGF = epidermal growth factor; EMT = epithelial-mesenchymal transition; FBS = fetal bovine serum; HME = human mammary epithelial; IGF = insulin-like growth factor; IGF-1R = insulin-like growth factor-1 receptor; MTT = 3-(4,5-dimethylthiazol-2-yl)-2,5-diphenyl-2H-tetrazolium bromide; RT-PCR = reverse transcriptase-mediated polymerase chain reaction; siRNA = short interfering RNA.

with reduced tumorigenicity in glioma, choriocarcinoma, and Ewing's sarcoma cell lines [13-16]. However, increased expression of CCN3 was associated with enhanced tumor growth in renal cell carcinomas [17]. CCN2 (Cyr61) stimulates the growth of breast and gastric adenocarcinomas [18,19], whereas its expression is downregulated in non-small cell lung cancer, in which CCN2 suppressed the growth of NSCLC cells by triggering a signal transduction pathway through β -catenin [20,21]. These data suggest that two members of the CCN family, CCN2 and CCN3, behave under certain circumstances as oncogenes or tumor suppressor genes in different tissue types (reviewed in [12,22]).

CCN6 maps to chromosome 6q21-22, a locus that displays high rates of loss of heterozygosity in breast cancer [23,24]. We have previously reported that CCN6 is lost in the majority of inflammatory breast cancers, a highly aggressive and metastatic form of breast cancer [25]. Restoration of CCN6 expression in inflammatory breast cancer cells results in growth inhibition *in vitro* and *in vivo* [6,26]. After synthesis, CCN6 protein is secreted and is able to modulate the effects of IGF-1 on IGF-1 receptor (IGF-1R) activation and its signaling pathways [27]. Here we investigate the function of CCN6 in the normal breast epithelium. We show that inhibition of CCN6 expression in human mammary epithelial cells strongly induces epithelial-mesenchymal transition (EMT) and leads to a highly motile and invasive phenotype. CCN6 loss promotes anchorage-independent growth in breast epithelial cells and increases cell proliferation, which is mechanistically driven, at least in part, by enhancement of the growth effects of IGF-1 and the activation of IGF-1R signaling pathways.

Materials and methods

Cell culture

Human mammary epithelial (HME) cells were immortalized with human papilloma virus E6/E7 and were characterized as being positive for keratin 19 [6,28]. Cells were cultured in Ham's F-12 medium supplemented with 5% fetal bovine serum (FBS), hydrocortisone (1 μ g/ml), insulin (5 μ g/ml), epidermal growth factor (EGF; 10 ng/ml), cholera toxin (100 μ g/ml), fungizone (2.5 μ g/ml) and gentamycin (5 μ g/ml), at 37°C under 10% CO₂.

Generation of stable hairpin short interfering RNA-CCN6 HME cells

Hairpin short interfering RNA (siRNA) 5'-GATCCCGCCAGGGGAAATCTGCAATGTTCAAGAGACATTGCAGATTTCCCTGGTTTTTGGAAA-3' and the complementary strand 5'-

AGCTTTTCCAAAAACCAGGGGAAATCTGCAATGTCTCTTGAACATTGCAGATTTCCCCTGGCGG-3' were synthesized (Invitrogen, Carlsbad, CA, USA), and annealed hairpin siRNA-CCN6 inserts were cloned into pSilencer2.1-U6 hygro expression vector (Ambion, Austin, TX, USA). The sequence of siRNA-CCN6 (insert in) expression vector was confirmed by

sequencing (University of Michigan DNA Sequencing Core). HME cells were transfected with pSilencer2.1-U6 negative control (siRNA-control; Ambion) or siRNA-CCN6 plasmids by using FuGene 6 transfection reagent (Roche-Boehringer Mannheim, Mannheim, Germany). Stable transfectants were established by culturing transfected cells in the described medium supplemented with 100 μ g/ml hygromycin (Invitrogen) for 4 weeks.

RT-PCR analysis

Total RNA was isolated from HME cells and siRNA HME clones with a Trizol kit (Life Technologies, Inc., Gaithersburg, MD, USA). First-strand cDNA synthesis was performed by using 1 μ g of total RNA with AMV reverse transcriptase (Promega, Madison, WI, USA) and oligo(dT) as a primer. A 2 μ l portion of the reaction mixture was used for amplification by PCR. The following primers were used: CCN6 forward primer 5'-ATGCAGGGGCTCCTCTTCTCC-3' and CCN6 reverse primer 5'-CTTGAGCTCAGAAAATATATC-3' to amplify a 1,050 bp product; E-cadherin forward primer 5'-CCTTCCTCCAAATACATCTCCC-3' and E-cadherin reverse primer 5'-TCTCCGCCTCCTTCTTCATC-3' to amplify a 600 bp product. PCR was performed under the following conditions: denaturing for 1 minute at 94°C, annealing for 1 minute at 58°C for CCN6 and at 65°C for E-cadherin, and elongation for 1 minute at 72°C, for 35 cycles.

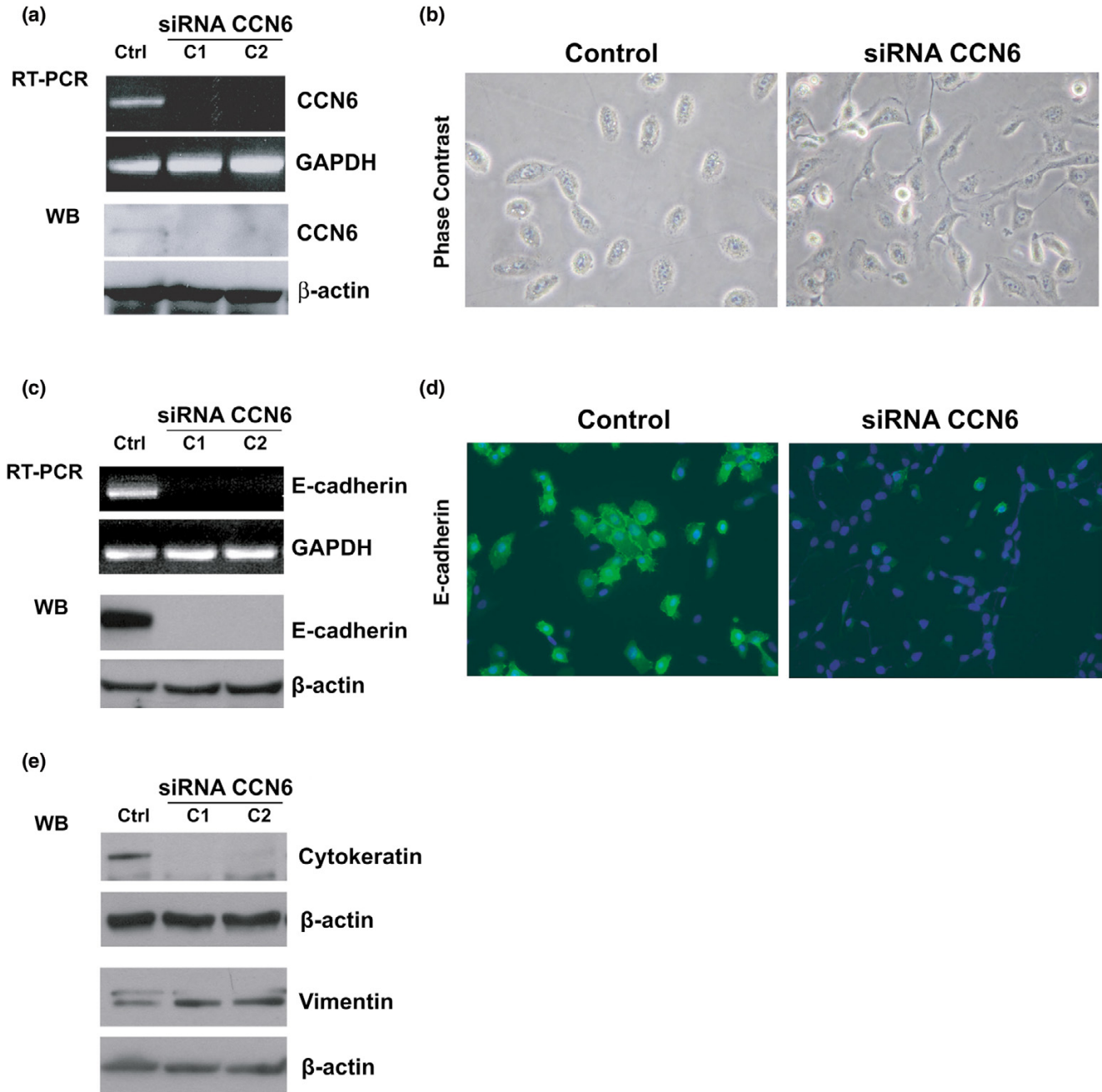
Immunofluorescence

Cells were grown on glass coverslips, fixed with methanol for 5 minutes at -20°C and then permeabilized with 0.2% Triton X-100 for 15 minutes at room temperature 25°C. The coverslips were then saturated for 30 minutes with 2% bovine serum albumin in PBS. After being washed in PBS, cells were incubated for 1 hour with a monoclonal antibody against E-cadherin (dilution 1:50, BD Transduction Laboratories, San Jose, CA, USA). Cells were exposed for 1 hour to Alexa Fluor anti-mouse Ig G (Molecular Probes, Eugene, OR, USA). After being washed with PBS three times, the coverslips were then mounted with prolong Gold anti-fade reagent with 4',6-diamidino-2-phenylindole and the borders were sealed with transparent nail polish.

Anchorage-independent growth

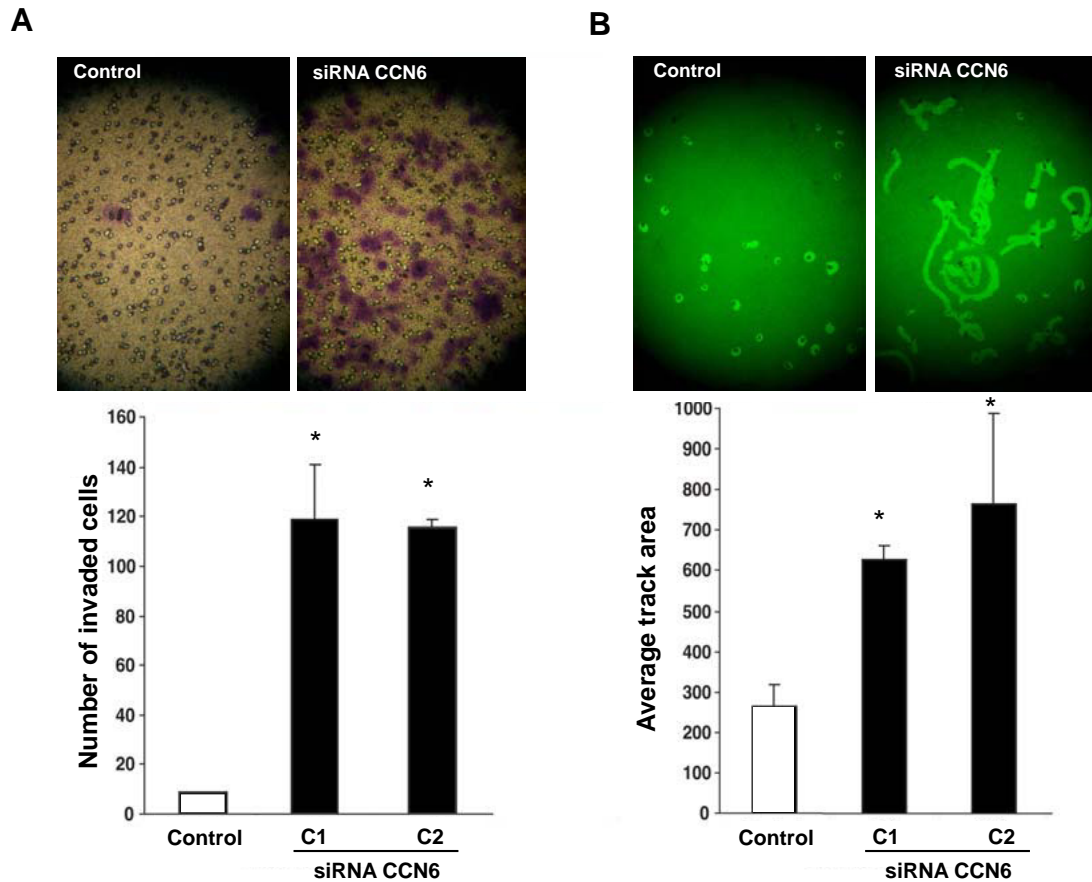
For studies of anchorage-independent growth we performed soft agar assays on stable clones of HME/CCN6 siRNA and on HME control cells. Each well of a six-well plate was first layered with 0.6% agar diluted with 5% FBS-supplemented Ham's F-12 medium complete with growth factors. The cell layer was then prepared by diluting agarose to concentrations of 0.3% with 5 \times 10³ cells in 2.5% FBS-supplemented Ham's F-12 (1.5 ml per well). Plates were maintained for 3 weeks at 37°C under 10% CO₂. Colonies were counted under a microscope with a grid. The experiment was performed three times independently.

Figure 1



Effect of CCN6 inhibition on the phenotype of mammary epithelial cells. **(a)** Human mammary epithelial (HME) cells were stably transfected with pSilencer2.1-U6 hygro expression vector expressing CCN6 hairpin siRNA. The suppression of CCN6 was confirmed by reverse transcriptase PCR and Western immunoblotting (WB). HME control cells express low levels of CCN6 protein. C1 and C2 (two stable HME CCN6 siRNA clones) show almost complete inhibition of CCN6. **(b)** Stable inhibition of CCN6 on HME cells results in a change from compact and oval-shaped cells to irregularly shaped cells with many protruding processes. **(c)** E-cadherin protein and mRNA were decreased in CCN6-deficient cells. **(d)** By immunofluorescence CCN6-deficient cells show a drastic decrease of membrane-associated E-cadherin protein. **(e)** Western immunoblots show that CCN6 inhibition results in a decrease in cytokeatin and an increase in vimentin proteins. GAPDH, glyceraldehyde-3-phosphate dehydrogenase.

Figure 2



Effect of CCN6 inhibition on random motility and invasion. **(a)** A reconstituted basement membrane invasion chamber assay was used to investigate the effects of CCN6 inhibition on the invasion abilities of HME cells. Representative fields of invaded and stained cells are shown. *t* test **p* < 0.04 vs. control. **(b)** Cell motility on a field of microscopic fluorescent beads. Representative photomicrographs show the clearing in the fluorescent bead field corresponding to phagokinetic cell tracks. **p* < 0.005 vs. control. Experiments were performed independently three times. C1 and C2 are two stable CCN6 deficient clones.

Basement membrane matrix invasion

HME/CCN6 siRNA and HME controls were trypsinized and 300 µl of 10⁶ cells/ml in serum-free medium were seeded at equal numbers onto the extracellular matrix layer (ECM; Chemicon, Temecula, CA, USA). Subsequently, we added 500 µl of medium containing 5% FBS to the lower chamber. After incubation for 24 hours, the non-invading cells and ECM gel from the interior of the insert were removed gently with a cotton swab. The invasive cells on the lower surface of membrane were stained, air dried, and photographed. The invaded cells were counted under the microscope. The experiment was performed three times independently.

Random motility

Random cell motility was determined as described in the motility assay kit (Cellomics Inc., Pittsburg, PA, USA). Cells were harvested and 500 cells per well were suspended in 2.5% FBS medium and plated on top of a field of microscopic fluorescent beads in a 96-well plate. After incubation for 16 hours, cells were fixed and areas of clearing in the fluorescent bead field corresponding to phagokinetic cell tracks were quantified with an NIH ScionImager. The experiment was performed three times independently.

Immunoprecipitation

HME cells and HME/CCN6 siRNA cells were serum-starved for 24 hours and subsequently stimulated for 15 minutes with 25 ng/ml IGF-1. Proteins were obtained by lysing the cells in

a buffer composed of 50 mM Tris-HCl, pH 7.4, 150 mM NaCl, 1% Nonidet P40, 1 mM Na_3VO_4 , 1 mM phenylmethylsulphonyl fluoride, 1 $\mu\text{g}/\text{ml}$ leupeptin, and 10 $\mu\text{g}/\text{ml}$ aprotinin. The IGF-1R was immunoprecipitated overnight from 500 μg of cell (protein) lysate with anti-IGF-1R monoclonal antibody (Oncogene, San Diego, CA, USA) at 4°C. After isolation with protein A/G PLUS-Agarose (Santa Cruz Biotechnology, Santa Cruz, CA, USA), the immunocomplexes were separated by 7.5% SDS-PAGE. The proteins were transferred to a poly(vinylidene difluoride) membrane and subsequently detected by immunoblotting with anti-IGF-1R β subunit polyclonal antibody (Santa Cruz Biotechnology). Tyrosine phosphorylation of immunoprecipitated IGF-1R was assessed with anti-phosphotyrosine monoclonal antibody PY20 (Transduction Laboratories, Lexington, KY, USA).

Western blot analysis

Cells were lysed in lysis buffer (50 mM Tris-HCl, pH 7.4, 150 mM NaCl, 1% Nonidet P40, 1 mM Na_3VO_4 , 1 mM phenylmethylsulphonyl fluoride, 1 $\mu\text{g}/\text{ml}$ leupeptin, and 10 $\mu\text{g}/\text{ml}$ aprotinin). Cell lysates (50 μg of protein) were fractionated by SDS-PAGE and transferred to Immobilon-P membrane (Millipore, Billerica, MA, USA). The membranes were blocked for 1 hour with Tris-buffered saline containing 5% non-fat milk and 0.1% Tween 20. Immobilized proteins were probed with antibodies specific for phosphorylated and total insulin receptor substrate-1 (IRS-1; Upstate Biotechnology), E-cadherin and vimentin monoclonal antibodies (BD Transduction Laboratories) and antibodies against cytokeratin 18 (c-04, ab668, Abcam Inc, Cambridge MA, USA) CCN6 was detected with a polyclonal anti-CCN6 antibody developed against an immunogenic peptide Ac-PEGRPGEVSDAPQRKQ-CONH₂ corresponding to amino acids 31 to 46 of human CCN6 with the assistance of Covance.

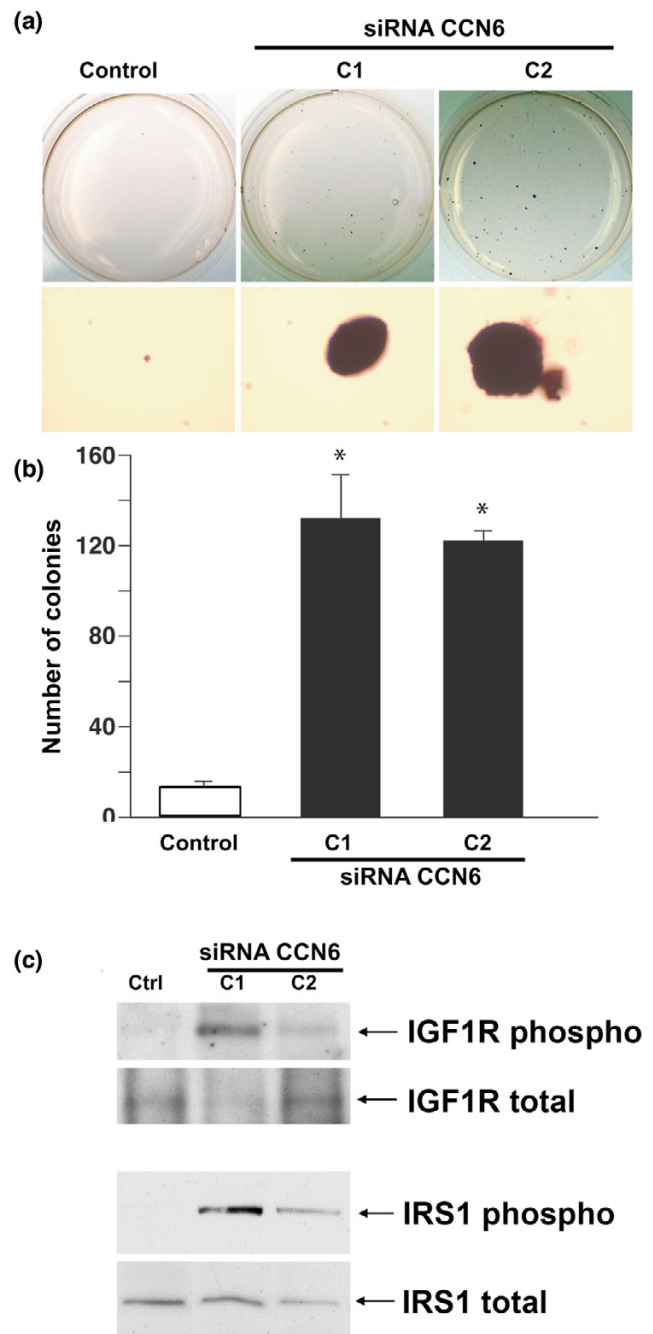
IGF-1 growth assay

HME/CCN6 siRNA and HME control cells were plated in 96-well plates at a concentration of 5×10^4 cells/ml and serum-starved for 24 hours. Subsequently, 25 ng/ml human recombinant IGF-1 (Upstate Biotechnology) was added. 3-(4,5-Dimethylthiazol-2-yl)-2,5-diphenyl-2*H*-tetrazolium bromide (MTT) reagents were added 24 hours later in accordance with the manufacturer's protocol, and the plate was read at a wavelength of 595 nm. The experiment was performed with triplicate samples.

S-phase analysis

HME/CCN6 siRNA and HME control cells were plated at a concentration of 5×10^4 cells/ml and serum-starved for 24 hours. Subsequently, 25 ng/ml human recombinant IGF-1 (Upstate Biotechnology) was added. Serum-starved and IGF-1-treated HME control cells and HME/CCN6 siRNA cells were pulsed for 2 hours with 10 μM bromodeoxyuridine (BrdU; Roche, Indianapolis, IN, USA), harvested with trypsin-EDTA, and fixed with 70% ethanol at -20°C for at least 1 hour.

Figure 3



CCN6-deficient cells acquire anchorage-independent growth abilities. **(a)** Anchorage-independent growth of human mammary epithelial stable cell lines in soft agar. The upper panels show an assay in soft agar; the lower panels show the colony size under a $\times 100$ magnification of the same wells after 3 weeks in culture. Three independent experiments yielded similar results. **(b)** Bar graph summarizing the results of three independent experiments in soft agar. **(c)** CCN6 inhibition induced an increase in phosphorylation of insulin-like growth factor-1 receptor (IGF-1R) and insulin receptor substrate-1 (IRS-1). C1 and C2 are two stable CCN6 deficient clones.

Cells were resuspended in 2 M HCl for 20 minutes at room temperature. After centrifugation, the cell pellets were resuspended in borax (pH 8.5) to neutralize any residual acid. After brief centrifugation the pellets were washed in 1 ml PBS and resuspended for 1 hour in fluorescein isothiocyanate-labeled anti-BrdU antibody (catalogue no. 347583; Becton Dickinson San Jose, CA, USA) in the dark. Cells were washed in PBS, resuspended in PBS containing propidium iodide, and analyzed for propidium iodide and BrdU staining on a Becton-Dickinson flow cytometer with the use of Cellquest software. The experiment was performed three times independently.

Results

Expression of CCN6 in immortalized human mammary epithelial cells

A CCN6-specific receptor has not yet been cloned; blockade of the receptor is therefore not yet feasible as a means of inhibiting CCN6 function. Thus, to investigate the role of CCN6 in the mammary epithelium and in breast tumorigenesis, HME cells were treated with a CCN6 hairpin siRNA. siRNAs silence gene expression in a sequence-specific post-translational way; they therefore constitute a useful strategy for identifying gene function [29].

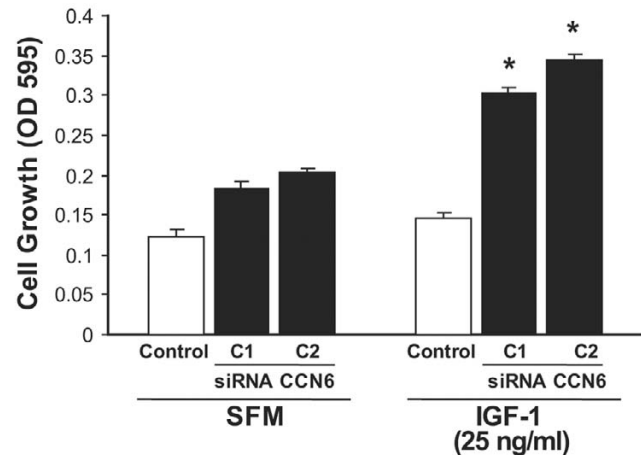
The expression of CCN6 transcript and protein in HME cells and HME cells stably transfected with CCN6 siRNA were studied by RT-PCR and Western immunoblotting, respectively (Fig. 1a). For subsequent experiments, two clones with CCN6 protein downregulation were selected to study the functional consequences of CCN6 inhibition. The hairpin inhibition of CCN6 protein levels was stable and remained stable 5 months after transfection, as tested by Western blotting.

CCN6 inhibition is a potent inducer of EMT and triggers motile and invasive properties on mammary epithelial cells

While the parental HME cells were compact, thick, and ovoid, with rare extended processes, CCN6 inhibition led to cells that were thin, spreading, with stellate shape and numerous cytoplasmic extended processes reminiscent of an epithelial to mesenchymal transition (EMT) (Fig 1b). Consistently, CCN6-deficient cells had loss of the epithelial markers E-cadherin and cytokeratin, whereas they exhibited increased vimentin protein, a characteristic marker for mesenchymal cells (Fig. 1c,d and 1e).

Because E-cadherin is crucial for epithelial cell-cell adhesion and its downregulation has been shown to enhance cellular motility and invasion, we tracked the movement of CCN6-deficient cells and their ability to invade a basement membrane. As shown in Fig. 2, CCN6 deficient cells were much more motile and invasive *in vitro* than the controls.

Figure 4



CCN6 inhibition increases the growth of human mammary epithelial cells in response to insulin-like growth factor-1 (IGF-1). Cells were serum starved for 24 hours, and subsequently stimulated with 25 ng/ml of IGF-1. MTT (3-(4,5-dimethylthiazol-2-yl)-2,5-diphenyl-2H-tetrazolium bromide) reagents were added 24 hours later and the plate was read at a wavelength of 595 nm. Results are expressed as means \pm SD for three independent experiments. Asterisks indicate statistical significance (*t* test); $p < 0.005$ for short interfering RNA (siRNA)/CCN6 after treatment with IGF-1 compared with serum free medium (SFM). C1 and C2 are two stable CCN6 deficient clones.

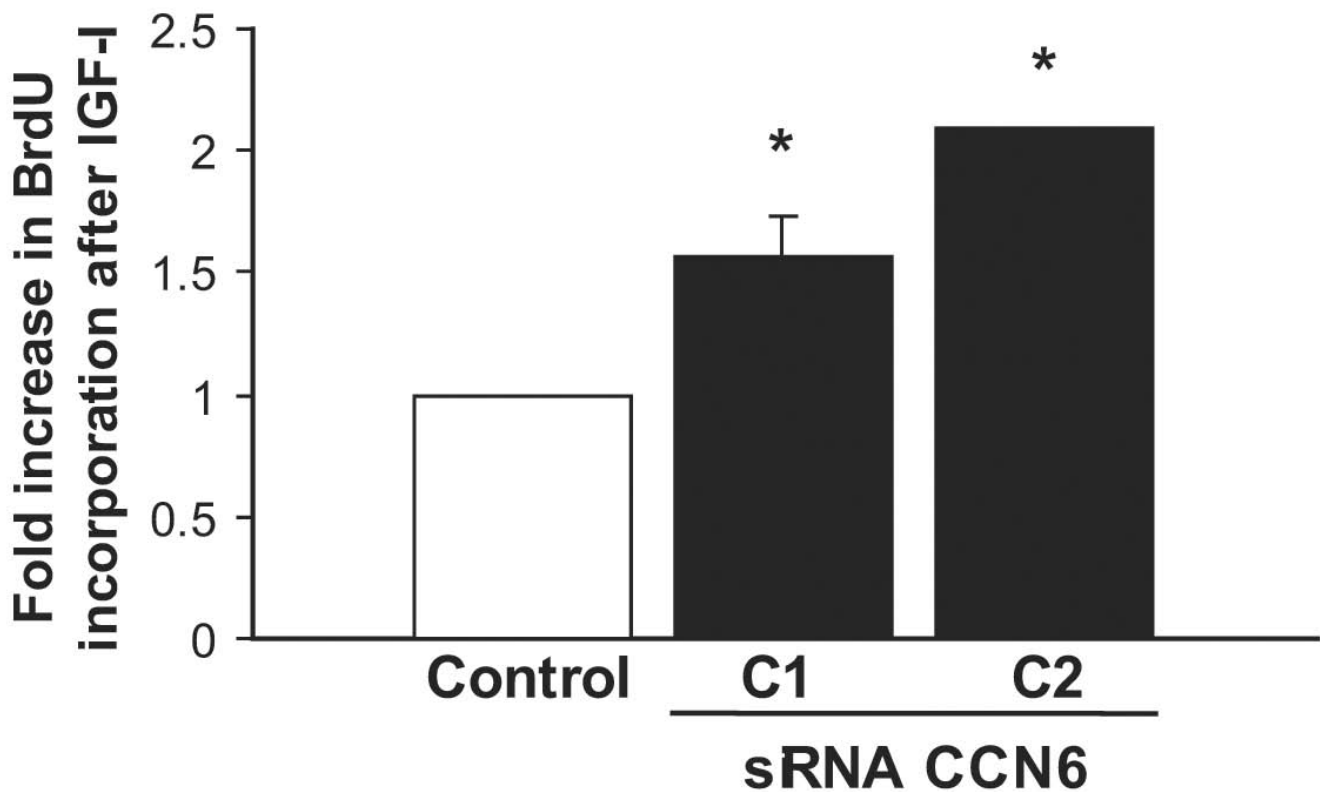
CCN6 inhibition promotes anchorage-independent growth, increases IGF-1R phosphorylation and potentiates the mitogenic effects of IGF-1

Stable inhibition of CCN6 by hairpin siRNA strongly promoted the growth of HME cells in soft agar (Fig. 3). CCN6-deficient cells were able to form colonies in medium supplemented with only 2.5% FBS, whereas HME control cells did not significantly form colonies under these conditions. CCN6-deficient cells formed about 10-fold more colonies than the control cells after 21 days. Furthermore, the colonies formed by the CCN6-deficient cells were much larger than the colonies formed by the control cells.

Our observation of the ability of CCN6-deficient cells to form colonies in soft agar in the presence of limiting serum suggested that these lines might have increased activation of growth receptor tyrosine kinase signaling pathways. This is a well-known mechanism for transformation that allows the cells to grow in the absence, or with minimal amounts, of growth factors [30,31]. Because CCN6 contains an IGFBP motif and once secreted it is able to modulate IGF signaling pathways [27], it was logical to begin our analysis by investigating whether inhibition of CCN6 might directly or indirectly induce the activation of IGF-1R. Stable CCN6 inhibition by hairpin siRNA led to an increase in the phosphorylation of IGF-1R and IRS-1 (Fig. 3c).

Next, we assayed CCN6-deficient cells and controls for their growth ability in serum free medium and in the presence of

Figure 5



CCN6 inhibition enhances the proliferative effects of insulin-like growth factor-1 (IGF-1) on mammary epithelial cells. The bar graph shows that CCN6-deficient cells exhibited a significant increase in bromodeoxyuridine (BrdU) incorporation in response to treatment with IGF-1 (*t* test, $p < 0.03$ for both clones). The human mammary epithelial (HME) control cells did not exhibit differences in the S-phase fraction after the addition of IGF-1. The experiment was performed three times independently. Results are expressed as means \pm SD for three independent experiments. C1 and C2 are two stable CCN6 deficient clones.

IGF-1 in the condition media. In the complete absence of serum, CCN6-deficient cells were able to survive and were metabolically active when compared to controls (Fig. 4). Upon addition of IGF-1 we observed that inhibition of CCN6 enhanced the growth effects of IGF-1. Inhibition of CCN6 stimulated the growth of HME cells in serum free medium, however, when 25 ng of IGF-1 was added, we noted a 2.5-fold increase in cell growth, which did not increase significantly with increasing concentrations of recombinant IGF-1 in the medium.

While IGF-1 stimulation did not affect the proliferative activity of the control cells, CCN6-deficient cells exhibited a significant increase in the S-phase fraction (Fig. 5). Taken together these data support the hypothesis that loss of CCN6 in HME cells results in loss of a growth regulatory mechanism which enhances the proliferative and growth response to IGF-1.

Discussion

In this study we characterize the function of CCN6, a recently identified gene that is lost in inflammatory breast cancer, the most lethal form of breast cancer [6,25]. Here we show that

inhibition of CCN6 expression induces the EMT of mammary epithelial cells and results in a highly motile and invasive phenotype. CCN6-deficient cells acquire anchorage-independent growth abilities and exhibit increased growth and proliferative response to IGF-1 through enhanced IGF-1R signaling.

To characterize the function of CCN6 in the breast epithelium, we first analyzed the phenotypic effects of stable inhibition of CCN6 expression by hairpin siRNA. Inhibition of CCN6 profoundly altered the phenotype of human mammary epithelial cells, leading to the acquisition of features of EMT. EMT involves the phenotypic alteration of epithelial cells to fibroblastoid, spindle, migratory, and more malignant cells, which show a mesenchymal gene expression program [32,33], and represents an important *in vitro* correlate of tumor progression [32,33]. Several proteins have been implicated in this process, which involves a dominant transcriptional repression that leads to a downregulation of E-cadherin expression and an increase in the expression of mesenchymal markers. The detailed mechanisms of EMT in breast epithelial cells remain elusive.

On the basis of our studies, inhibition of CCN6 results in a morphologic change towards a mesenchymal phenotype, which is accompanied by a marked downregulation of E-cadherin and cytokeratin, and an increase in vimentin, a mesenchymal marker. Functionally, CCN6 inhibition led to a pronounced increase in cell motility and invasion. The mechanism of E-cadherin downregulation brought about by the loss of CCN6 is intriguing. E-cadherin transcript expression was also inhibited in CCN6-deficient cells, suggesting that this effect is probably exerted at the transcriptional level, by epigenetic mechanisms such as hypermethylation and transcriptional silencing. These results were also obtained when CCN6 was knocked down in MCF10A cells (data not shown). It is possible that the loss of CCN6 might lead to increased methylation of the E-cadherin promoter, which has been shown to be correlated with a loss of E-cadherin expression in breast cancer cell lines and primary invasive ductal and lobular carcinomas of the breast [34,35]. It is also possible that CCN6 loss results in transcriptional silencing of E-cadherin, perhaps by the induction of transcriptional repressors, such as Snail [36,37] and SIP1/ZEB2 [36,37], known to inactivate the E-cadherin promoter. Supporting evidence has recently been reported by Sen and colleagues [38] showing that CCN6 is able to activate the SOX transcription factors by a similar mechanism.

CCN6 inhibition led to the acquisition of anchorage-independent growth abilities even under extremely low serum conditions. We therefore reasoned that loss of CCN6 might impair a central growth regulatory mechanism, rendering the cells more sensitive to the effect of even minimal amounts of growth factors such as EGF and IGF. Although CCN6 inhibition had no effect on the phosphorylation of the EGF receptor (data not shown), it markedly enhanced the growth effects of IGF-1, a potent mitogen for breast epithelial cells [39]. CCN6 inhibition led to an increase in the phosphorylation of IGF-1 and its main downstream target molecule IRS-1. This was coupled with an increase in the metabolic activity of mammary epithelial cells and also in cell proliferation. These data support a role for CCN6 a modulator of the growth effects of IGF-1 on the breast epithelium, and may have clinical implications, as CCN6 loss may mark an epithelium at increased risk of malignant transformation and might constitute a target for breast cancer prevention.

The IGF family of growth factors is crucial in the development and progression of breast cancer. Studies *in vitro* and *in vivo* have shown that IGFs promote the proliferation, survival, and metastatic ability of cancer cells [40-43]. The role of IGF-1R in promoting the proliferation of breast cancer cells is well established [39,44,45]. A role for IGF-1R in breast cancer metastases has been shown recently [40]. Compelling epidemiological and clinical data show that high concentrations of IGF-1 in serum are associated with increased mammographic density (one of the strongest predictors of breast

cancer risk), and also reliably predict increased breast cancer risk specifically in premenopausal women [46]. High expression of IGF-1R has been demonstrated in most primary human breast cancers when compared with normal or benign breast tissue, and hyperactivation of IGF-1R in breast cancer has been linked with increased radioresistance and cancer recurrence at the primary site [39,44,45]. High levels of IRS-1, a major signaling molecule downstream of the IGF-1R, are correlated with tumor size and shorter disease-free survival in estrogen receptor-positive breast cancer patients [47,48].

The effect of CCN6 inhibition on the phosphorylation of the IGF-1R and IRS-1 is consistent with a growth regulatory effect on the mammary epithelium. The relationship between the IGF family and CCN6 emerges from our previous investigations as well as from another laboratory [14,27,38]. CCN6-rich medium induces a decrease in IGF-1-stimulated IGF-1R phosphorylation in breast cancer cells, and then results in an inhibition of cellular proliferation [27]. In another system, Sen and colleagues [38] reported that anti-IGF-1 neutralizing antibody partly blocks the CCN6-mediated upregulation of COL2A1 mRNA in immortalized chondrocyte cell lines. In view of these data, we postulate that CCN6 may modulate the availability of IGF-1 to the IGF-1R, conceivably by binding and sequestering IGF-1, and/or by interfering with other regulators of the IGF signaling pathway.

Conclusion

We propose a model whereby CCN6 serves as an important growth regulatory protein of the mammary epithelium and controls the cellular responses to the growth stimulatory effects of IGF-1. Loss of CCN6 expression alters the phenotype of the breast epithelium and promotes motility and invasion. The CCN6-deficient cells are extremely sensitive to the growth stimulatory effects of IGF-1. The uncontrolled growth may in turn predispose to neoplasia. It is possible that pharmacological restoration of the CCN6 autocrine regulatory loop could be targeted to prevent malignant transformation of mammary epithelial cells.

Competing interests

The authors declare that they have no competing interests.

Authors' contributions

YZ carried out the cell culture, transfections, western blotting, RT-PCR, functional assays, and IGF-1 assays. She drafted the manuscript. QP assisted with the optimization of techniques, and was involved in the overall planning of experiments. HZ contributed her knowledge on flow cytometry and performed the BrdU incorporation assays. She assisted with the planning and interpretation of IGF-1 experiments, and manuscript writing. SDM conceived some ideas on the study, and contributed to the experimental plan, especially on the IGF-1 connection. She assisted in trouble shooting experiments. She helped planning the figures and edited the manuscript. CGK contrib-

uted ideas for the study and participated in the design and coordination of the study. She wrote and edited the manuscript significantly. She was involved and directed all the aspects of the study. SDM and CGK share senior authorship. All authors read and approved the final manuscript.

Acknowledgements

We thank members of the Kleer and Merajver laboratories for critical reading and constructive suggestions throughout the execution of this project, and Karilynn Schneider and Robin Kunkel for artwork. We thank Dr Bernard Perbal (Université de Paris 7 – Denis Diderot) for helpful discussions. This work was supported in part by NIH grants K08CA090876 and R01CA107469 (CGK), R01CA77612 (SDM), Department of Defense grants DAMD17-01-1-490 (CGK) and DAMD17-01-1-491 (CGK), a grant from the Breast Cancer Foundation and the Burroughs Wellcome fund (SDM).

References

- Hurvitz JR, Suwairi WM, Van Hul W, El-Shanti H, Superti-Furga A, Roudier J, Holderbaum D, Pauli RM, Herd JK, Van Hul EV, et al.: **Mutations in the CCN gene family member WISP3 cause progressive pseudorheumatoid dysplasia.** *Nat Genet* 1999, **23**:94-98.
- Pennica D, Swanson TA, Welsh JW, Roy MA, Lawrence DA, Lee J, Brush J, Taneyhill LA, Deuel B, Lew M, et al.: **WISP genes are members of the connective tissue growth factor family that are up-regulated in wnt-1-transformed cells and aberrantly expressed in human colon tumors.** *Proc Natl Acad Sci USA* 1998, **95**:14717-14722.
- Perbal B: **NOV (nephroblastoma overexpressed) and the CCN family of genes: structural and functional issues.** *Mol Pathol* 2001, **54**:57-79.
- Thorstensen L, Holm R, Lothe RA, Trope C, Carvalho B, Sobrinho-Simoes M, Seruca R: **WNT-inducible signaling pathway protein 3, WISP-3, is mutated in microsatellite unstable gastrointestinal carcinomas but not in endometrial carcinomas.** *Gastroenterology* 2003, **124**:270-271.
- Thorstensen L, Diep CB, Meling GI, Aagesen TH, Ahrens CH, Rognum TO, Lothe RA: **WNT1 inducible signaling pathway protein 3, WISP-3, a novel target gene in colorectal carcinomas with microsatellite instability.** *Gastroenterology* 2001, **121**:1275-1280.
- Kleer CG, Zhang Y, Pan Q, van Golen KL, Wu ZF, Livant D, Merajver SD: **WISP3 is a novel tumor suppressor gene of inflammatory breast cancer.** *Oncogene* 2002, **21**:3172-3180.
- Lin CG, Leu SJ, Chen N, Tebeau CM, Lin SX, Yeung CY, Lau LF: **CCN3 (NOV) is a novel angiogenic regulator of the CCN protein family.** *J Biol Chem* 2003, **278**:24200-24208.
- Sakamoto K, Yamaguchi S, Ando R, Miyawaki A, Kabasawa Y, Takagi M, Li CL, Perbal B, Katsube K: **The nephroblastoma overexpressed gene (NOV/ccn3) protein associates with Notch1 extracellular domain and inhibits myoblast differentiation via Notch signaling pathway.** *J Biol Chem* 2002, **277**:29399-29405.
- Perbal B, Martinerie C, Sainson R, Werner M, He B, Roizman B: **The C-terminal domain of the regulatory protein NOVH is sufficient to promote interaction with fibulin 1C: a clue for a role of NOVH in cell-adhesion signaling.** *Proc Natl Acad Sci USA* 1999, **96**:869-874.
- Li CL, Martinez V, He B, Lombet A, Perbal B: **A role for CCN3 (NOV) in calcium signalling.** *Mol Pathol* 2002, **55**:250-261.
- Wahab NA, Weston BS, Mason RM: **Connective tissue growth factor CCN2 interacts with and activates the tyrosine kinase receptor TrkA.** *J Am Soc Nephrol* 2005, **16**:340-351.
- Brigstock D, Lau L, Perbal B: **CCN workshop.** *J Clin Pathol* 2005, **58**:463-465.
- Gupta N, Wang H, McLeod TL, Naus CC, Kyurkchiev S, Advani S, Yu J, Perbal B, Weichselbaum RR: **Inhibition of glioma cell growth and tumorigenic potential by CCN3 (NOV).** *Mol Pathol* 2001, **54**:293-299.
- Benini S, Perbal B, Zambelli D, Colombo MP, Manara MC, Serra M, Parenza M, Martinez V, Picci P, Scotlandi K: **In Ewing's sarcoma CCN3(NOV) inhibits proliferation while promoting migration and invasion of the same cell type.** *Oncogene* 2005, **24**:4349-61.
- Fu CT, Bechberger JF, Ozog MA, Perbal B, Naus CC: **CCN3 (NOV) interacts with connexin43 in C6 glioma cells: possible mechanism of connexin-mediated growth suppression.** *J Biol Chem* 2004, **279**:36943-36950.
- Gellhaus A, Dong X, Propson S, Maass K, Klein-Hitpass L, Kibschull M, Traub O, Willecke K, Perbal B, Lye SJ, et al.: **Connexin43 interacts with NOV: a possible mechanism for negative regulation of cell growth in choriocarcinoma cells.** *J Biol Chem* 2004, **279**:36931-36942.
- Glukhova L, Angevin E, Lavielle C, Cadot B, Terrier-Lacombe MJ, Perbal B, Bernheim A, Goguel AF: **Patterns of specific genomic alterations associated with poor prognosis in high-grade renal cell carcinomas.** *Cancer Genet Cytogenet* 2001, **130**:105-110.
- Tsai MS, Hornby AE, Lakins J, Lupu R: **Expression and function of CYR61, an angiogenic factor, in breast cancer cell lines and tumor biopsies.** *Cancer Res* 2000, **60**:5603-5607.
- Babic AM, Kireeva ML, Kolesnikova TV, Lau LF: **CYR61, a product of a growth factor-inducible immediate early gene, promotes angiogenesis and tumor growth.** *Proc Natl Acad Sci USA* 1998, **95**:6355-6360.
- Tong X, O'Kelly J, Xie D, Mori A, Lemp N, McKenna R, Miller CW, Koeffler HP: **Cyr61 suppresses the growth of non-small-cell lung cancer cells via the beta-catenin-c-myc-p53 pathway.** *Oncogene* 2004, **23**:4847-4855.
- Tong X, Xie D, O'Kelly J, Miller CW, Muller-Tidow C, Koeffler HP: **Cyr61, a member of CCN family, is a tumor suppressor in non-small cell lung cancer.** *J Biol Chem* 2001, **276**:47709-47714.
- Bleau AM, Planque N, Perbal B: **CCN proteins and cancer: two to tango.** *Front Biosci* 2005, **10**:998-1009.
- Nessling M, Richter K, Schwaenen C, Roerig P, Wrobel G, Wessendorf S, Fritz B, Bentz M, Sinn HP, Radwimmer B, et al.: **Candidate genes in breast cancer revealed by microarray-based comparative genomic hybridization of archived tissue.** *Cancer Res* 2005, **65**:439-447.
- Chappell SA, Walsh T, Walker RA, Shaw JA: **Loss of heterozygosity at chromosome 6q in preinvasive and early invasive breast carcinomas.** *Br J Cancer* 1997, **75**:1324-1329.
- van Golen KL, Davies S, Wu ZF, Wang Y, Bucana CD, Root H, Chandrasekharappa S, Strawderman M, Ethier SP, Merajver SD: **A novel putative low-affinity insulin-like growth factor-binding protein, LIBC (lost in inflammatory breast cancer), and RhoC GTPase correlate with the inflammatory breast cancer phenotype.** *Clin Cancer Res* 1999, **5**:2511-2519.
- Kleer CG, Zhang Y, Pan Q, Gallagher G, Wu M, Wu ZF, Merajver SD: **WISP3 and RhoC guanosine triphosphatase cooperate in the development of inflammatory breast cancer.** *Breast Cancer Res* 2004, **6**:R110-R115.
- Kleer CG, Zhang Y, Pan Q, Merajver SD: **WISP3 (CCN6) is a secreted tumor-suppressor protein that modulates IGF signaling in inflammatory breast cancer.** *Neoplasia* 2004, **6**:179-185.
- Ethier SP, Mahacek ML, Gullick WJ, Frank TS, Weber BL: **Differential isolation of normal luminal mammary epithelial cells and breast cancer cells from primary and metastatic sites using selective media.** *Cancer Res* 1993, **53**:627-635.
- Elbashir SM, Harborth J, Lendeckel W, Yalcin A, Weber K, Tuschl T: **Duplexes of 21-nucleotide RNAs mediate RNA interference in cultured mammalian cells.** *Nature* 2001, **411**:494-498.
- Di Fiore PP, Pierce JH, Kraus MH, Segatto O, King CR, Aaronson SA: **erbB-2 is a potent oncogene when overexpressed in NIH/3T3 cells.** *Science* 1987, **237**:178-182.
- Di Fiore PP, Pierce JH, Fleming TP, Hazan R, Ullrich A, King CR, Schlessinger J, Aaronson SA: **Overexpression of the human EGF receptor confers an EGF-dependent transformed phenotype to NIH 3T3 cells.** *Cell* 1987, **51**:1063-1070.
- Zhou BP, Deng J, Xia W, Xu J, Li YM, Gunduz M, Hung MC: **Dual regulation of Snail by GSK-3 β -mediated phosphorylation in control of epithelial-mesenchymal transition.** *Nat Cell Biol* 2004, **6**:931-940.
- Huber MA, Azoitei N, Baumann B, Grunert S, Sommer A, Pehamberger H, Kraut N, Beug H, Wirth T: **NF- κ B is essential for epi-**

- thelial-mesenchymal transition and metastasis in a model of breast cancer progression. *J Clin Invest* 2004, **114**:569-581.
34. Nass SJ, Herman JG, Gabrielson E, Iversen PW, Parl FF, Davidson NE, Graff JR: **Aberrant methylation of the estrogen receptor and E-cadherin 5' CpG islands increases with malignant progression in human breast cancer.** *Cancer Res* 2000, **60**:4346-4348.
 35. Droufakou S, Deshmane V, Roylance R, Hanby A, Tomlinson I, Hart IR: **Multiple ways of silencing E-cadherin gene expression in lobular carcinoma of the breast.** *Int J Cancer* 2001, **92**:404-408.
 36. Batlle E, Sancho E, Franci C, Dominguez D, Monfar M, Baulida J, Garcia De Herreros A: **The transcription factor snail is a repressor of E-cadherin gene expression in epithelial tumour cells.** *Nat Cell Biol* 2000, **2**:84-89.
 37. Cano A, Perez-Moreno MA, Rodrigo I, Locascio A, Blanco MJ, del Barrio MG, Portillo F, Nieto MA: **The transcription factor snail controls epithelial-mesenchymal transitions by repressing E-cadherin expression.** *Nat Cell Biol* 2000, **2**:76-83.
 38. Sen M, Cheng YH, Goldring MB, Lotz MK, Carson DA: **WISP3-dependent regulation of type II collagen and aggrecan production in chondrocytes.** *Arthritis Rheum* 2004, **50**:488-497.
 39. Surmacz E: **Function of the IGF-I receptor in breast cancer.** *J Mammary Gland Biol Neoplasia* 2000, **5**:95-105.
 40. Sachdev D, Hartell JS, Lee AV, Zhang X, Yee D: **A dominant negative type I insulin-like growth factor receptor inhibits metastasis of human cancer cells.** *J Biol Chem* 2004, **279**:5017-5024.
 41. Yee D, Lee AV: **Crosstalk between the insulin-like growth factors and estrogens in breast cancer.** *J Mammary Gland Biol Neoplasia* 2000, **5**:107-115.
 42. Lee AV, Gooch JL, Oesterreich S, Guler RL, Yee D: **Insulin-like growth factor I-induced degradation of insulin receptor substrate 1 is mediated by the 26S proteasome and blocked by phosphatidylinositol 3'-kinase inhibition.** *Mol Cell Biol* 2000, **20**:1489-1496.
 43. Lee AV, Hilsenbeck SG, Yee D: **IGF system components as prognostic markers in breast cancer.** *Breast Cancer Res Treat* 1998, **47**:295-302.
 44. Resnik JL, Reichart DB, Huey K, Webster NJ, Seely BL: **Elevated insulin-like growth factor I receptor autophosphorylation and kinase activity in human breast cancer.** *Cancer Res* 1998, **58**:1159-1164.
 45. Turner BC, Haffty BG, Narayanan L, Yuan J, Havre PA, Gumbs AA, Kaplan L, Burgaud JL, Carter D, Baserga R, et al.: **Insulin-like growth factor-I receptor overexpression mediates cellular radioresistance and local breast cancer recurrence after lumpectomy and radiation.** *Cancer Res* 1997, **57**:3079-3083.
 46. Byrne C, Colditz GA, Willett WC, Speizer FE, Pollak M, Hankinson SE: **Plasma insulin-like growth factor (IGF) I, IGF-binding protein 3, and mammographic density.** *Cancer Res* 2000, **60**:3744-3748.
 47. Lee AV, Jackson JG, Gooch JL, Hilsenbeck SG, Coronado-Heinsohn E, Osborne CK, Yee D: **Enhancement of insulin-like growth factor signaling in human breast cancer: estrogen regulation of insulin receptor substrate-1 expression in vitro and in vivo.** *Mol Endocrinol* 1999, **13**:787-796.
 48. Rocha RL, Hilsenbeck SG, Jackson JG, VanDenBerg CL, Weng C, Lee AV, Yee D: **Insulin-like growth factor binding protein-3 and insulin receptor substrate-1 in breast cancer: correlation with clinical parameters and disease-free survival.** *Clin Cancer Res* 1997, **3**:103-109.

Identification of EZH2 as a Molecular Marker for a Precancerous State in Morphologically Normal Breast Tissues

Lei Ding,^{1,3} Christine Erdmann,^{3,4} Arul M. Chinnaiyan,^{1,3} Sofia D. Merajver,^{2,3} and Celina G. Kleer^{1,3}

Departments of ¹Pathology and ²Internal Medicine, ³the Comprehensive Cancer Center, University of Michigan Medical School; and ⁴Department of Epidemiology, University of Michigan School of Public Health, Ann Arbor, Michigan

Abstract

The discovery of molecular markers to detect the precancerous state would have profound implications in the prevention of breast cancer. We report that the expression of the Polycomb group protein EZH2 increases in histologically normal breast epithelium with higher risk of developing cancer. We identify EZH2 as a potential marker for detecting preneoplastic lesions of the breast *in vivo* and as a possible target for preventative intervention. (Cancer Res 2006; 66(8): 4095-9)

Introduction

To date, the earliest recognizable precursor of invasive carcinoma of the breast is atypical ductal hyperplasia (ADH), the diagnosis of which is based on pathologic criteria. Although ADH is cytologically atypical and architecturally more complex than usual ductal hyperplasia, it still does not have the features necessary for the diagnosis of ductal carcinoma *in situ* (DCIS; ref. 1). Emerging data support the hypothesis that histologically normal breast epithelial cells from healthy women already contain genetic and epigenetic alterations which render them more susceptible to malignant transformation (2, 3). However, molecular markers identifying a precancerous state from otherwise morphologically normal breast epithelial cells remain largely unknown.

We previously reported that EZH2 is an independent predictor of breast cancer recurrence and death (4). The increased EZH2 expression is consistently associated with the aggressive behavior of breast cancer including invasiveness and metastatic potential. EZH2 interfered with the ability of breast cells to repair DNA double-strand breaks, which is a cause of genomic instability and a mechanism of cancer development (5). We propose here that elevated EZH2 protein detects a precancerous state in morphologically normal breast epithelium.

Materials and Methods

Breast sample collection. Breast tissue samples were obtained from the Surgical Pathology files at the University of Michigan with Institutional Review Board approval, and an arbitrary number was assigned to each sample for de-identification purposes. One hundred and nineteen breast tissue samples comprising a wide range of normal, ADH, and DCIS were used (Table 1). Among the 50 histologically normal breast samples, 25 were from healthy women who underwent reduction mammoplasty, 13 derived from

women carrying a known BRCA1 heterozygous mutation who underwent a prophylactic mastectomy, and 12 were from women who underwent a biopsy which yielded benign breast parenchyma. BRCA1 mutation status and clinical information was obtained through the Breast and Ovarian Cancer Risk Evaluation Program at the University of Michigan Comprehensive Cancer Center (S.D. Merajver) and chart review, respectively.

Immunohistochemistry. Immunohistochemistry was done on tissue sections using standard biotin-avidin complex technique with a mouse monoclonal antibody against EZH2 (1:25, BD Biosciences, San Jose, CA) and a Ki-67 antibody (1:50; DAKO, Carpinteria, CA). DCIS samples were previously immunostained for estrogen receptor (ER) as part of the routine clinical evaluation using a monoclonal anti-ER antibody (clone 6F11, Ventana, Tucson, AZ). Once immunostained, the percentage of EZH2 and Ki-67-expressing epithelial cell nuclei was recorded independently by two observers (L. Ding and C.G. Kleer) in a blinded manner.

Statistical analyses. Statistical analyses were done by the epidemiologist in the study (C. Erdmann). The intensity of EZH2 staining in samples of normal peripheral tissue associated with ADH diagnosis, ADH diagnostic tissue, normal peripheral tissue associated with DCIS diagnosis, ADH peripheral tissue associated with DCIS diagnosis, and DCIS diagnostic tissue were compared with normal tissue obtained from normal individuals using the exact Wilcoxon test as the EZH2 distributions were not normally distributed. $P < 0.05$ was considered statistically significant. Among DCIS patients, the exact Wilcoxon test also was used to compare distributions of EZH2 staining intensities for nuclear grade, ER status, tumor size, and age. All statistical tests were two-sample and two-sided unless otherwise indicated. Spearman's rank correlation (ρ) was used to evaluate the correlation between EZH2, Ki-67, and DCIS grade. Spearman's ρ statistic also was used to determine the interrater reliability and the reproducibility of the scoring system.

Results and Discussion

To determine whether the expression level of EZH2 protein increases during the early phases of breast cancer development, we evaluated the expression of EZH2 protein in 119 breast tissue samples comprising a wide range of normal, ADH, and DCIS lesions (Table 1). When expressed, EZH2 was observed in the epithelial cells, mainly in the nucleus as described previously (refs. 4, 6, 7; Fig. 1). As compared with normal breast tissues from reduction mammoplasties that had little or no EZH2 expression (median, 0%), the EZH2 expression was elevated in ADH (median, 10%; Wilcoxon $P = 0.0009$), and was further elevated in DCIS (median, 45%; Wilcoxon $P < 0.0001$; Table 2). The highest percentage of cells expressing EZH2 was observed in high nuclear grade (grade 3) comedo type DCIS (median, 80%; Wilcoxon $P = 0.0005$), which is consistent with the clinical evolution of DCIS, as high nuclear grade DCIs is associated with higher rate of recurrence and shorter disease-free survival interval than low (grade 1) and intermediate (grade 2) nuclear grade lesions (ref. 1; Table 3). These findings suggest that the expression of EZH2 protein increases as breast cancer develops and progress.

Note: Supplementary data for this article are available at Cancer Research Online (<http://cancerres.aacrjournals.org/>).

Requests for reprints: Celina G. Kleer, Department of Pathology, University of Michigan, 3510C MSRB1, 1150 West, Medical Center Drive, Ann Arbor, MI 48109. Phone: 734-615-3448; Fax: 734-615-3441; E-mail: kleer@umich.edu.

©2006 American Association for Cancer Research.
doi:10.1158/0008-5472.CAN-05-4300

Table 1. Clinical and pathologic characteristics of patients in this study ($n = 119$)

Characteristics	
Diagnosis	
Normal/fibrocystic changes, no.	
Reductions	25
Biopsies	12
Prophylactic mastectomies (BRCA1)	13
ADH, no.	21
DCIS, no.	48
Median age, years (range)	59 (36-90)
Median size, cm (range)	1.1 (0.1-5.0)
Nuclear grade, no. (%)	
1	12 (25.00)
2	14 (29.17)
3	22 (45.83)
ER status	
Negative, no. (%)	13 (27.08)
Positive, no. (%)	30 (62.50)
Unknown, no. (%)	5 (10.42)

Histologically normal lobules adjacent to ADH and DCIS had a ~3-fold and ~15-fold increase in the percentage of cells expressing EZH2 (median, 3% and 15%, respectively), when compared with normal lobules from women without ADH or DCIS (median, 0%; Wilcoxon $P = 0.1005$ and $P < 0.0001$, respectively). Furthermore, EZH2 expression was higher in ADH associated with DCIS (median, 40%) when compared with ADH alone (median, 10%; Wilcoxon paired $P = 0.065$; Fig. 1; Table 2). It is possible that the observed up-regulation of EZH2 in normal epithelium in the vicinity of ADH and DCIS is due to a "field effect" resulting from the activation of signaling pathways triggered by adjacent atypical cells, as has been suggested previously (8, 9). Alternatively, in light of our previous

study (4) and present data showing that increased EZH2 expression is associated with progression in both early and late phases of breast cancer development, it is tempting to speculate that the expression of EZH2 in histologically normal epithelium may represent a molecular marker of a precancerous state that is associated with higher risk for the development of invasive breast cancer.

To test this hypothesis, we examined EZH2 expression in normal breast tissues from two populations of patients: BRCA1 mutation carriers and patients with benign lesions. It has been well documented that patients from these two groups have higher risk for breast cancer. First, we determined EZH2 expression in 38 histologically normal breast tissues derived from (a) 13 women carrying a known BRCA1 heterozygous mutation who underwent a prophylactic mastectomy, and (b) 25 patients who underwent a breast reduction and had no personal or family history of breast cancer (Supplementary Table S1). Women who inherit germ line mutations in the *BRCA1* gene have up to an 85% lifetime risk of developing breast cancer by the age of 70 (10). Using immunohistochemistry, we found that BRCA1 mutation carriers had a marked increase in the percentage of epithelial cells expressing EZH2 when compared with controls (median, 25% versus 0%; Wilcoxon $P < 0.0001$; Fig. 2A). Our data suggest that increased EZH2 expression may be associated with higher risk for breast cancer. The elucidation of the possible relationship between *EZH2* and *BRCA1* genes warrants further investigation.

Prospective and retrospective studies have shown that healthy women who undergo a breast biopsy for benign breast disease have a relative risk of breast cancer of 1.5 to 1.6 compared with women in the general population, and that this risk persists for at least 25 years after the initial biopsy (11–13). Despite advances in the understanding of the molecular mechanisms leading to breast cancer, the only risk factors identified to date for breast cancer after the diagnosis of benign breast disease include the histologic classification of a benign breast lesion and a positive family history of breast cancer (11). We next determined EZH2 expression levels in 12 benign breast

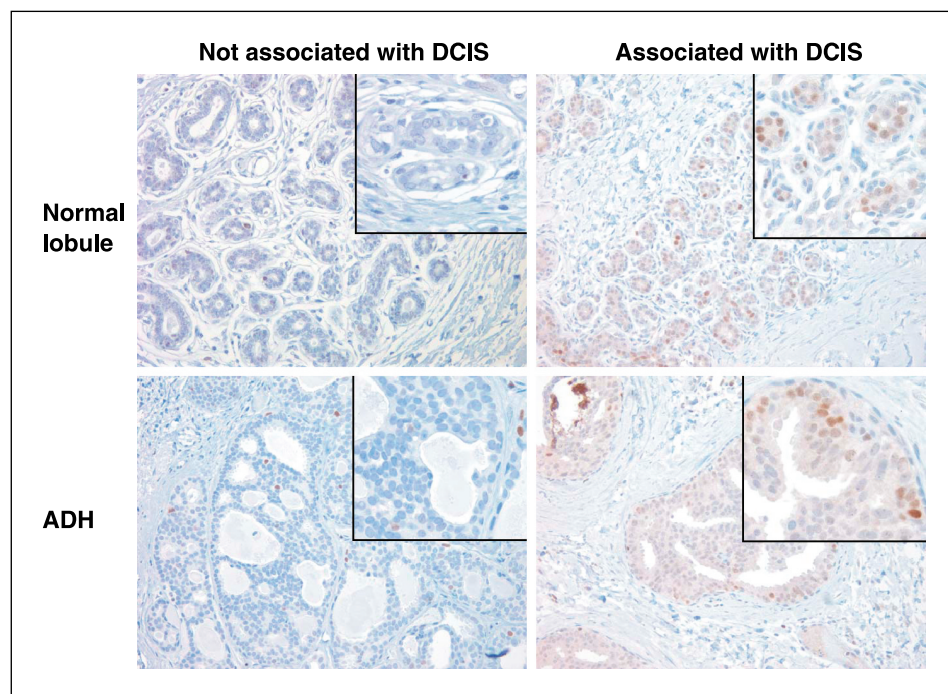


Figure 1. EZH2 expression is elevated in histologically normal breast epithelium and in ADH associated with DCIS (original magnification, $\times 200$).

Table 2. Comparison of EZH2 expression according to the pathologic diagnosis

Pathologic diagnosis	n	EZH2 median	EZH2 range	P*
Normal/fibrocystic changes	25	0.0	0-5	
Normal/fibrocystic changes associated with ADH	11	3.0	0-20	0.1005
ADH	21	10.0	0-50	0.0009
Normal/fibrocystic changes associated with DCIS	15	15.5	0-80	<0.0001
ADH associated with DCIS	11	40.0	10-80	<0.0001
DCIS	48	45.0	0-100	<0.0001

*Compared with normal/FCC group, Wilcoxon exact test.

tissue samples from women with no family history or personal history of breast cancer (Supplementary Table S1). Seven women developed cancer within the following 12 years, and five did not. Consistently, we found that the histologically normal breast tissues from patients who developed cancer had significant up-regulation of EZH2 (median, 20%) when compared with patients who did not develop cancer (median, 5%; Wilcoxon $P = 0.0088$; Fig. 2B). These results further support the hypothesis that increased EZH2 expression in normal tissues is correlated with higher risk of breast cancer. These data may have profound clinical implications as the increasing use of mammography has resulted in an increased number of benign breast biopsies. Furthermore, the discovery of markers of breast cancer risk is necessary for the development of strategies to prevent breast cancer progression. Our data support the theory that precursors to breast cancer exist in histologically normal breast tissues and offer a way to identify such precursors.

EZH2 expression has been linked with cellular proliferation in breast and other neoplasms (6, 7, 14–16). Consistent with this, we found that EZH2 was expressed in epithelial cells undergoing

mitosis (data not shown). Whereas EZH2 and the proliferative marker Ki-67 were nearly undetectable in normal breast samples from reductions, both were up-regulated in DCIS, and their levels increased with advancing histologic atypia (Spearman's $\rho = 0.77$; Fig. 3). Despite this positive correlation, the percentage of DCIS cells expressing EZH2 was higher than the percentage of Ki-67 positive cells suggesting that although EZH2 may be associated with the proliferative capacity of breast epithelial cells, it may have other nonproliferative functions in carcinogenesis. These data are in agreement with a previous study in bronchial carcinogenesis (16). Similar results were also observed in breast tissues from patients who underwent a benign biopsy (Fig. 2B). In this group of patients, even though EZH2 and Ki-67 (17) were elevated in women who later developed carcinoma compared with those who did not, EZH2 expression was higher than Ki-67. Notably, whereas EZH2 expression was higher in normal breast tissues from BRCA1 mutation carriers, Ki-67 remained low (Fig. 2A), further suggesting that EZH2 has nonproliferative functions during neoplastic transformation. Our data show that, EZH2 is a more sensitive marker than Ki-67 to predict breast cancer risk.

Table 3. Associations between EZH2 protein expression and clinical pathologic characteristics of patients with DCIS ($n = 48$)

Characteristic	n (%)	EZH2 (median)	EZH2 (range)	P*
Nuclear grade				
1	12 (25.00)	20.0	0-90	
2	14 (29.17)	30.0	0-100	0.5138
3	22 (45.83)	80.0	10-100	0.0005 [†]
ER				
Positive	30 (62.50)	40.0	0-100	
Negative	13 (27.08)	80.0	0-100	0.3657
Unknown	5 (10.42)			
Tumor size (cm)				
<2	35 (72.92)	40.0	0-100	
≥ 2	13 (27.08)	80.0	10-100	0.3455
Age				
<50	12 (25.00)	60.0	20-100	
≥ 50	32 (66.67)	30.0	0-100	0.0615
Unknown	4 (8.33)			

*Wilcoxon exact test.

[†] P values between tumor grades 1 and 3 is 0.0005, between tumor grades 2 and 3 is 0.0011.

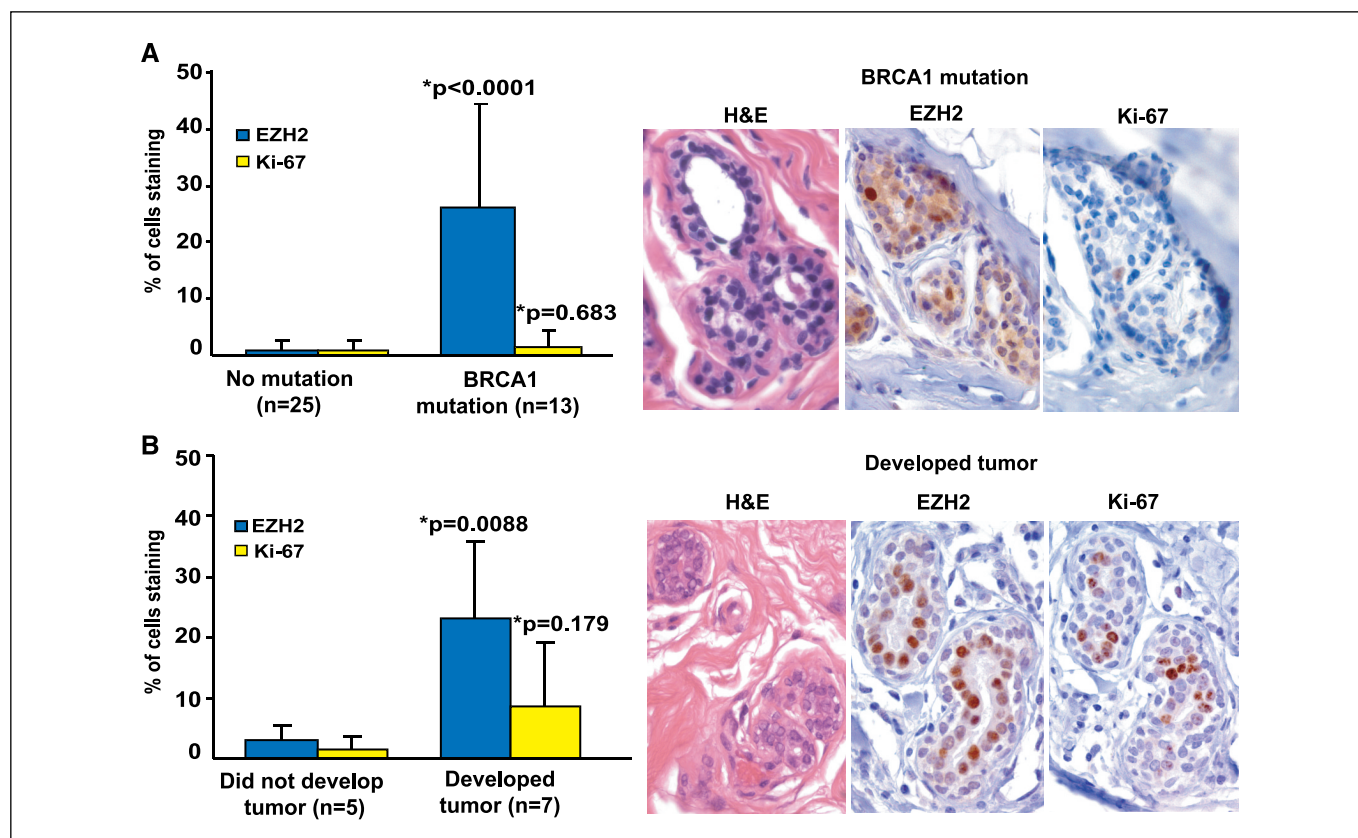


Figure 2. EZH2 expression as a marker of increased breast cancer risk in apparently normal breast tissues. **A**, EZH2 is elevated in histologically normal tissues from BRCA1 mutation carriers compared with normal tissues from women who underwent a breast reduction with no family or personal history of breast cancer. Note that Ki-67 is low in both groups. A representative picture of a histologically normal breast lobule from a BRCA1 mutation carrier is shown (original magnification, $\times 400$). **B**, EZH2 is elevated in benign breast tissues from patients who later developed breast cancer when compared with patients who did not develop breast cancer. A representative photomicrograph of a histologically normal lobule from a patient who developed breast cancer 5 years later is shown (original magnification, $\times 400$).

The advantage of using immunohistochemistry is that it is straightforward, widely available, and it allows for the evaluation of protein expression *in situ*, with direct visualization of the specific EZH2-expressing cells. We were able to achieve high interobserver reliability, as well as high reproducibility using our scoring method ($\rho = 0.96$, $P < 0.001$; and $\rho = 0.89$, $P < 0.0001$, respectively).

In conclusion, EZH2 detection in tissues by immunohistochemistry could potentially constitute the basis for a diagnostic test that distinguishes histologically normal breast tissues at higher risk for neoplastic progression. Finally, targeting EZH2 may provide a novel way to prevent breast cancer in women with increased risk at an earlier stage.

Acknowledgments

Received 12/1/2005; revised 2/3/2006; accepted 2/17/2006.

Grant support: National Cancer Institute grants K08CA090876 (C.G. Kleer) and R01CA107469 (C.G. Kleer); Department of Defense grant DAMD17-01-1-490 (C.G. Kleer); and the Histology and Immunohistochemistry Core at the University of Michigan Comprehensive Cancer Center through the University of Michigan's Cancer Center support grant (5 P30 CA46592).

The costs of publication of this article were defrayed in part by the payment of page charges. This article must therefore be hereby marked *advertisement* in accordance with 18 U.S.C. Section 1734 solely to indicate this fact.

We thank Dr. Yuan Zhu, Ph.D. (University of Michigan Department of Internal Medicine) for review of the manuscript and helpful critiques; Yanhong Zhang and Michael Zeidler for helpful suggestions during the execution of this project; and Kara Milliron, genetic counselor at the University of Michigan Comprehensive Cancer Center for providing information on the BRCA1 mutation status of the patients.

References

- Rosen PP. Rosen's Breast Pathology. In: PP, Rosen, editor. Rosen's breast pathology. vol. 1. Philadelphia (PA): Lippincott Williams & Wilkins; 2001.
- Li JJ, Weroha SJ, Lingle WL, Papa D, Salisbury JL, Li SA. Estrogen mediates Aurora-A overexpression, centrosome amplification, chromosomal instability, and breast cancer in female ACI rats. *Proc Natl Acad Sci U S A* 2004;101:18123-8.
- Crawford YG, Gauthier ML, Joubel A, et al. Histologically normal human mammary epithelia with silenced p16(INK4a) overexpress COX-2, promoting a premalignant program. *Cancer Cell* 2004;5:263-73.
- Kleer CG, Cao Q, Varambally S, et al. EZH2 is a marker of aggressive breast cancer and promotes neoplastic transformation of breast epithelial cells. *Proc Natl Acad Sci U S A* 2003;100:11606-11.
- Zeidler M, Varambally S, Cao Q, et al. The polycomb group protein EZH2 impairs DNA repair in human mammary epithelial cells. *Neoplasia* 2005;7:1011-9.
- Raaphorst FM, Meijer CJ, Fieret E, et al. Poorly differentiated breast carcinoma is associated with increased expression of the human polycomb group EZH2 gene. *Neoplasia* 2003;5:481-8.
- Bracken AP, Pasini D, Capra M, Prosperini E, Colli E, Helin K. EZH2 is downstream of the pRB-E2F pathway, essential for proliferation and amplified in cancer. *EMBO J* 2003;22:5323-35.
- Gauthier ML, Pickering CR, Miller CJ, et al. p38 regulates cyclooxygenase-2 in human mammary epithelial cells and is activated in premalignant tissue. *Cancer Res* 2005;65:1792-9.
- Cavalli LR, Singh B, Isaacs C, Dickson RB, Haddad BR. Loss of heterozygosity in normal breast epithelial tissue and benign breast lesions in BRCA1/2 carriers with breast cancer. *Cancer Genet Cytogenet* 2004;149:38-43.
- Rahman N, Stratton MR. The genetics of breast cancer susceptibility. *Annu Rev Genet* 1998;32:95-121.
- Hartmann LC, Sellers TA, Frost MH, et al. Benign breast disease and the risk of breast cancer. *N Engl J Med* 2005;353:229-37.
- Dupont WD, Page DL. Risk factors for breast cancer in women with proliferative breast disease. *N Engl J Med* 1985;312:146-51.

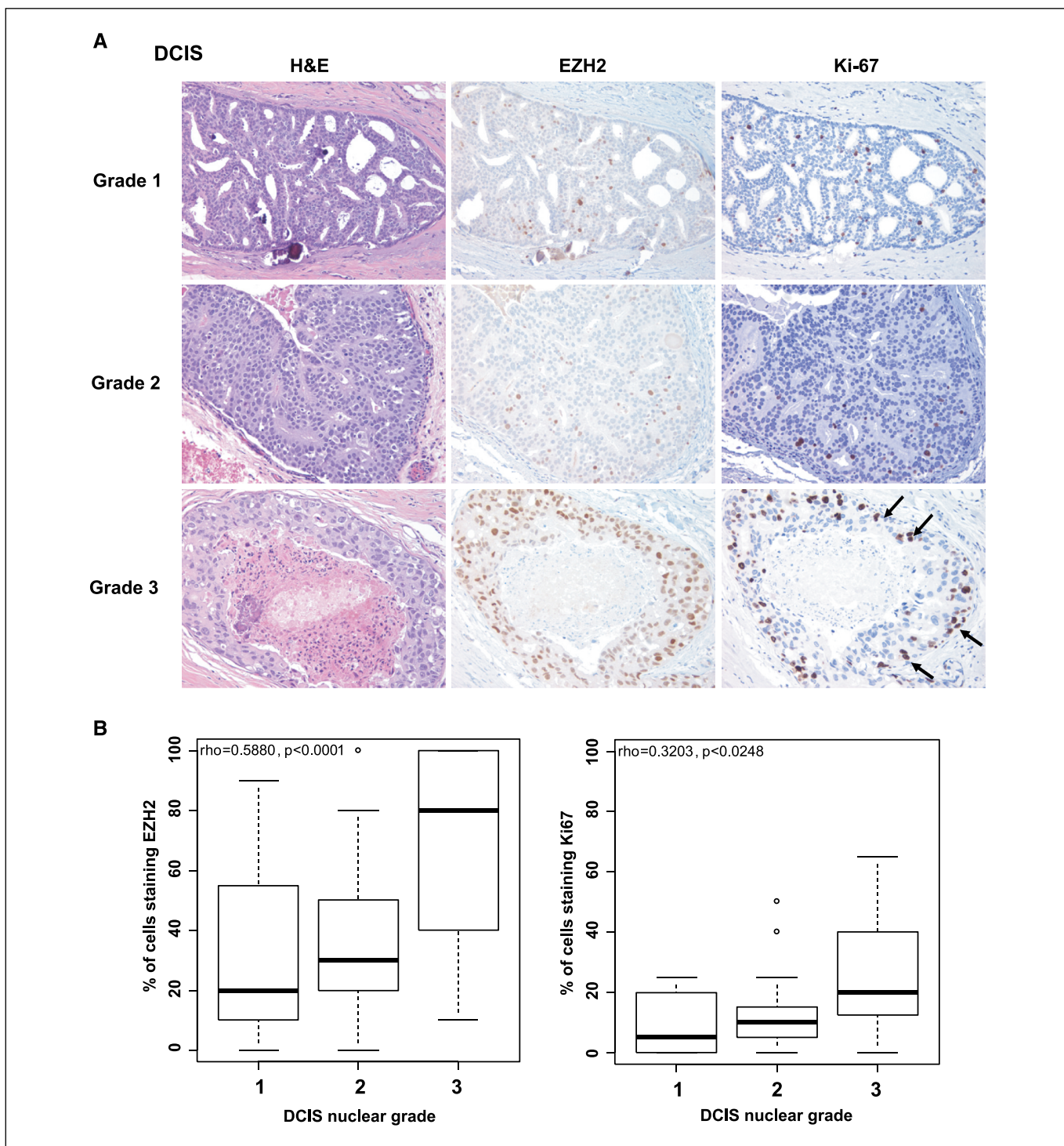


Figure 3. Expression of EZH2 and Ki-67 in DCIS. *A*, H&E staining of DCIS of nuclear grades 1, 2, and 3, and corresponding EZH2 and Ki-67 protein expression. EZH2 and Ki-67 proteins increase with advancing nuclear grade of the DCIS (original magnification, $\times 200$). *B*, box plots illustrating that EZH2 and Ki-67 proteins are significantly higher in high nuclear grade DCIS (grade 3) when compared with low and intermediate grades (1 and 2). Note that the magnitude of association between EZH2 and DCIS grade is stronger than that for Ki-67 and DCIS grade.

13. Wang J, Costantino JP, Tan-Chiu E, Wickerham DL, Paik S, Wolmark N. Lower-category benign breast disease and the risk of invasive breast cancer. *J Natl Cancer Inst* 2004;96:616-20.

14. Bachmann IM, Halvorsen OJ, Collett K, et al. EZH2 expression is associated with high proliferation rate and aggressive tumor subgroups in cutaneous melanoma

and cancers of the endometrium, prostate, and breast. *J Clin Oncol* 2005;24:1-6.

15. Varambally S, Dhanasekaran SM, Zhou M, et al. The polycomb group protein EZH2 is involved in progression of prostate cancer. *Nature* 2002;419:624-9.

16. Breuer RH, Snijders PJ, Smit EF, et al. Increased expression of the EZH2 polycomb group gene in BMI-1-

positive neoplastic cells during bronchial carcinogenesis. *Neoplasia* 2004;6:736-43.

17. Khan QJ, Kimler BF, Clark J, Metheny T, Zalles CM, Fabian CJ. Ki-67 expression in benign breast ductal cells obtained by random periareolar fine needle aspiration. *Cancer Epidemiol Biomarkers Prev* 2005;14:786-9.